ABSTRACT

Title of Document:	OXIDATIVE FUNCTIONALIZATION OF Pd^{II}-C BONDS USING HYDROGEN PEROXIDE: EXPLORING THE POTENTIAL OF THE Pd^{II} HYDROCARBYL – DPK SYSTEM
	Dave A. Jenkins Jr., Master of Science, 2013
Directed By:	Professor of Chemistry, Andrei Vedernikov, Department of Chemistry and Biochemistry

Previously the oxidation utilizing hydrogen peroxide and various monoarylpalladium(II) complexes supported by di-(2-pyridyl)-ketone was shown to proceed via palladium(IV) intermediates that undergo C-X reductive elimination to produce the corresponding phenols, chlorides, and bromides in protic solvents. However, the conversion of monoalkylpalladium(II) complexes using hydrogen peroxide to their monoalkylpalladium(IV) derivatives as well as the transform,ations of the latter to form C-X bonds (X = F, Br, Cl, and I) are yet to be established. Herein, we report palladium – mediated oxidative C(sp^3)-H functionalization of 8-methylquinoline, 4-amino-2-*tert*-butylpyridine and C(sp^2)-H functionalization of benzo[*h*]quinoline, with various nucleophilic sources (H$_2$O, MeOH, LiCl, LiBr, LiI, AgF etc) and hydrogen peroxide as an oxidizing agent. Our results demonstrate that oxidation of Pd(II) precursors with hydrogen peroxide affords new Pd(IV) complexes. The observation that Pd(IV) monoalkyl complexes can react with various

nucleophiles in solution opens up an opportunity to produce functionalized organic compounds containing various C−X bonds.

.

OXIDATIVE FUNCTIONALIZATION OF Pd^{II}-C BONDS USING HYDROGEN
PEROXIDE: EXPLORING THE POTENTIAL OF THE Pd^{II} HYDROCARBYL –
DPK SYSTEM

By

Dave A. Jenkins Jr.

Thesis submitted to the Faculty of the Graduate School of the
University of Maryland, College Park, in partial fulfillment
of the requirements for the degree of
Master of Science
2013

Advisory Committee:
Professor Andrei Vedernikov, Chair
Michael P. Doyle
Philip DeShong
Bryan Eichhorn

Table of Contents

Introduction

The selective oxidative C-H functionalization of organic compounds is an important problem in synthetic organic chemistry.[1,2] A number of reports on heteroatom-directed catalytic C-H functionalization have appeared recently.[1-9] The use of the Pd^{II} complexes in combination with hypervalent iodine, electrophilic fluorine compounds and other strong oxidants have proved not environmentally benign, cheap, and readily available.[10-32] In contrast, an alternative such as H_2O_2 or O_2 can be used in place of such oxidants to produce C-X (OH, OAc, Br, Cl, and I) bonds via PdIV intermediates in a stoichiometric and/or catalytic fashion.[33-36] Given the fact that facile oxidative functionalization of arylpalladium(II) complexes[37] can be promoted by di-(2-pyridyl)-ketone ligand (DPK) (Scheme 1), we were interested in finding out i) whether the reactivity of these arylpalladium(II) systems can be extended to other functional groups (F) and ii) whether dpk-supported Pd^{IV} monoalkyl complexes can be prepared and used in various C-X bond forming reactions (X = F, Cl, Br, I, OH). In the latter case the possible mechanisms of these reactions, an S_N2 with the inversion of the Pd^{IV} – bound carbon atom configuration and an intramolecular C-X reductive elimination with the retention of the configuration are also of great interest.
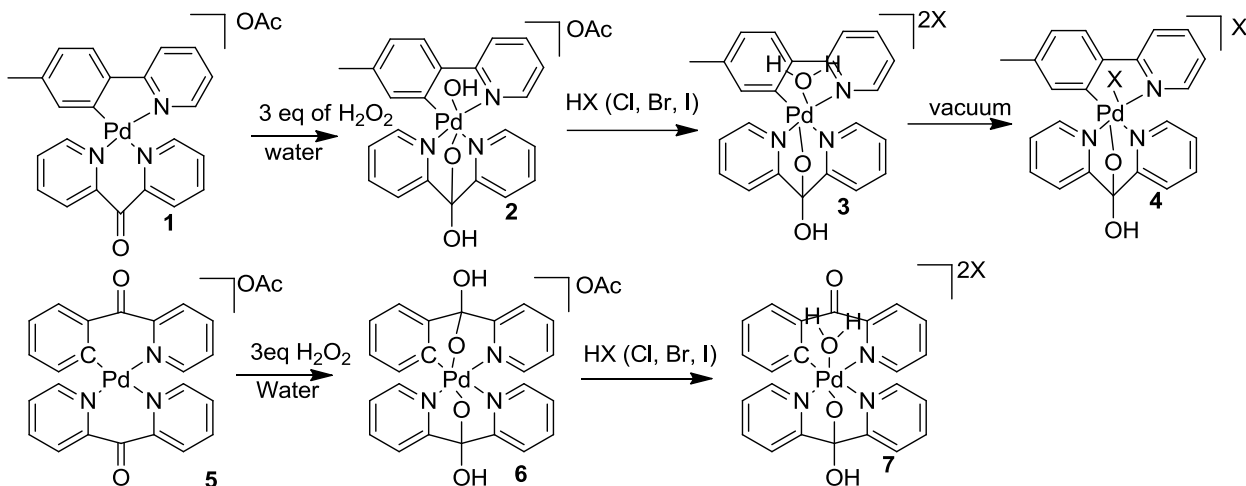
**Scheme 1.** Proposed pathway for the formation of Pd^{IV} monohydrocarbyl complexes.

A useful route to various organopalladium(II) complexes is *via* C-H activation and cyclopalladation of suitable organic substrates with "PdX$_2$" sources (X = OAc, Cl) in acetic acid and other solvents.[1-9] Palladacycles containing Pd-C(sp^2)[33] and Pd-C(sp^3)[34] bonds are typically unreactive toward hydrogen peroxide and dioxygen, but stronger oxidants were used successfully for their functionalization.[1-9] Electron-rich heterocycles can be predictably and regioselectively halogenated under catalysis with palladium, rhodium, iridium, copper, and nickel complexes.[1-9] Functionalization of directing-group-containing arenes has been extensively investigated.[1-9] However, for both kinetic and thermodynamic reasons, metal-catalyzed functionalization of unactivated C(sp^3)-H bonds is more difficult than that of C(sp^2)-H bonds. The activation of C(sp^2)-H bonds is favored by pre-coordination of the arene π system to the transition metal, greater C-H acidity as well as the formation of aryl-metal bond that is typically stronger than the corresponding alkyl-metal bond. In contrast, benzylic C(sp^3)-H bonds undergo functionalization relatively easily, presumably due to weakness of those C-H bonds.[1-7] Consequently, transition-metal-mediated

functionalization of activated C(sp^3)-H bonds is quite common and many examples have been described in literature.[8] On the other hand, catalytic functionalization of nonactivated, alkane C(sp^3)-H bonds is more rare. Most of the examples published so far report functionalization of C(sp^3)-H bonds adjacent to quarternary centers which is the easiest case due to impossibility of β-hydride elimination from the metallated intermediates.[9] Notable examples are provided in works by Jin-Quan Yu[38] and Daugulis[39] who demonstrated arylation, alkylation, and bromination of unactivated C($sp)^3$-H bonds via palladium(IV) intermediates, some of which could be characterized crystallographically, such as shown below (Scheme 2).
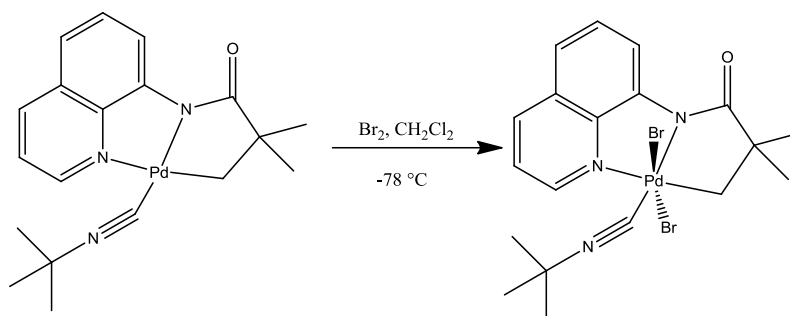

Scheme 2. Conversion of palladium(II) monohydrocarbyl complex to palladium(IV) dibromo species using bromine as an oxidant.

Chlorination of C(sp^3)-H bonds mediated by Pd^{IV} was also demonstrated by Vicente.[40] The reaction below shows the conversion of a palladium(II) chloride complex to a palladium(IV) monohydrocarbyl complex. However, the palladium (IV) complex below was only characterized by NMR; no crystallographic data was obtained (Scheme 2b).[40] Vicente also isolated palladium(IV) monoalkyl chloro, bromo, and iodo complexes in 2011.[41-42]
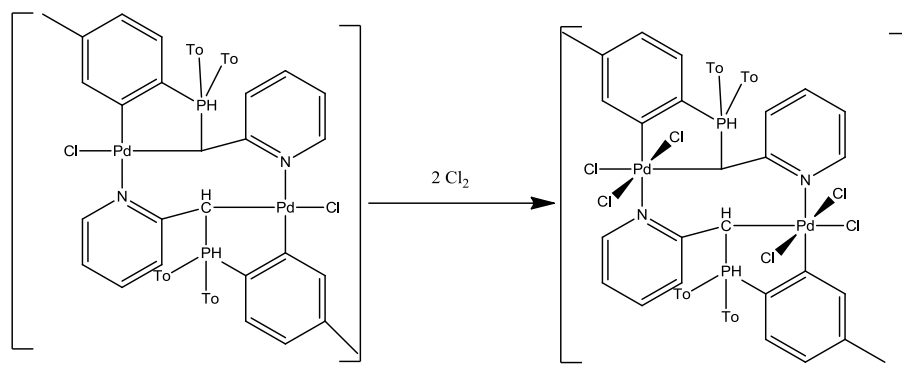
Scheme 2b. Conversion of palladium(II) monohydrocarbyl complex to palladium(IV) dichloro species using chlorine gas as an oxidant.

Molecules bearing a fluorine moiety in aromatic and aliphatic substrates have been extensively researched.[13] However, very few efficient approaches are known for the synthesis of these fluorinated molecules, and the use of transition metals are particularly rare.[13-32] Recently several groups have described methods for palladium catalyzed fluorination of aromatic and aliphatic compounds,[13] in which the generation of C-F bonds have been demonstrated *via* Pd [II/IV] intermediates. The reaction is initiated through oxidative addition of F^+ reagents to a Pd(II) hydrocarbyl(Scheme 3).[10,11] For instance, Ritter[10] has reported the use of Selectfluor® as an F^+ source in the hetero-atom directed fluorination of C-H bonds, and Sanford has explored the electrophilic fluorination of hydrocarbyl complexes with XeF_2 (Scheme 3 and 4).[11]
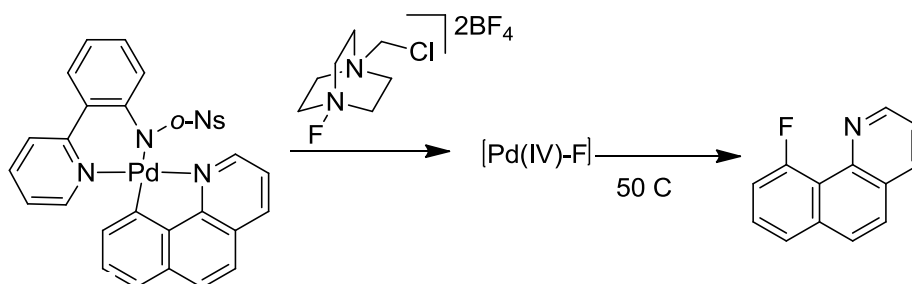
Scheme 3. The fluorination of cyclopalladated benzo[h]quinoline complex using

Selectfluor®.

Sanford has also verified that palladium(II) fluoride complexes can be oxidized and fluorinated using xenon difluoride, another expensive fluorination reagent (Scheme 4).[10]
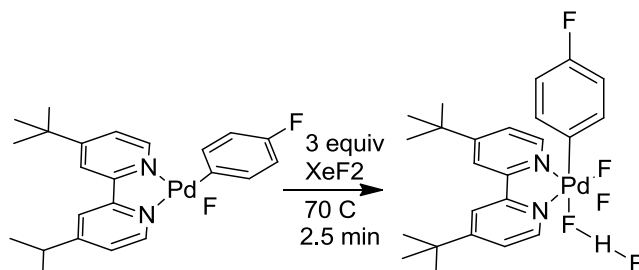

Scheme 4. Illustration of using XeF_2 to access palladium (IV) fluoro-complex.[11]

Meanwhile, similar $Pd^{II/IV}$ species have been successfully employed to accomplish palladium-catalyzed functionalization of aromatic and aliphatic compounds[17] such as trifluoromethylation,[13] of C-H bonds, difluorination,[18] and fluoroamination[19] of alkenes which provide versatile strategies to prepare organic substrates with fluorine containing groups. We envisioned that instead of F^+ reagents the use of F^- reagents (TBAF·$3H_2O$, CsF, AgF, CuF_2, Me_4NF etc.) in combination with hydrogen peroxide could achieve facile oxidative fluorination.

In this work, we report the oxidative functionalization of three model substrates, one donor of C(sp^2)-H bonds, benzo[h]quinoline, and two donors of C(sp^3)-H bonds, 8-methylquinoline with benzylic C-H bonds and 4-amino-2-(*tert*-butyl)pyridine having non-activated C(sp^3)-H bonds. In all the cases DPK supported palladium(IV) monohydrocarbyl complexes were generated using aqueous H_2O_2 and some of their C-X bond elimination reactions demonstrated leading to the corresponding phenol (Scheme 4a), 8-quinolylmethyl, and 2-pyridyl ethyl alcohols

and halides (Scheme 4a).
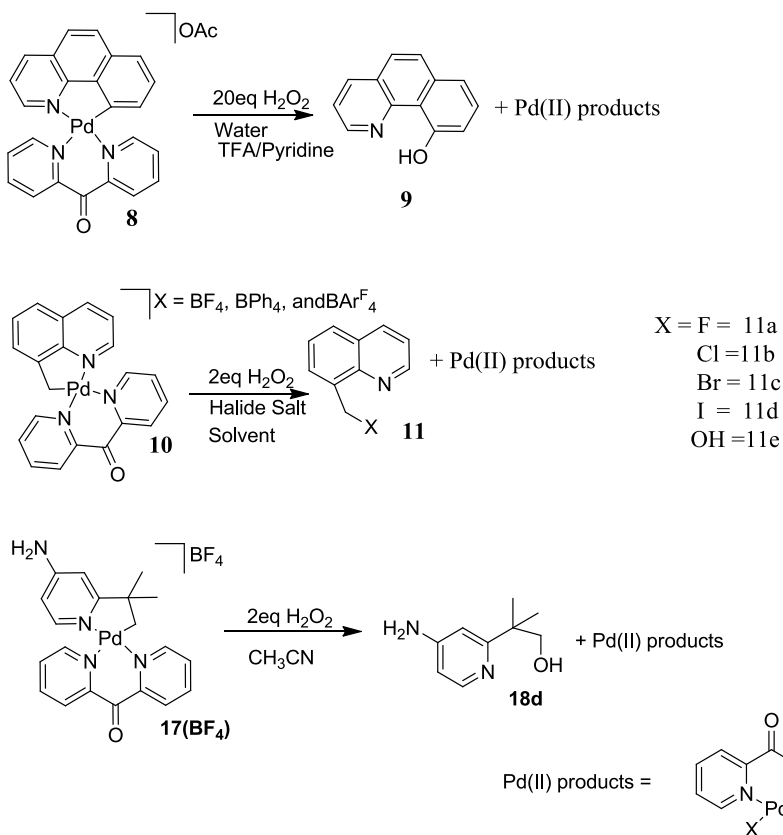
Scheme 4a. C-H functionalization of 8-methylquinoline, benzo[*h*]quinoline, and 2-(*tert*-butyl)pyridin-4-amine.

Results and Discussion

C(*sp*³)-H Functionalization of 8-methylquinoline and 4-amino-2-tertbutylpyridine

Compounds containing carbon-X (X = F, Br, Cl, I) bonds are of great importance in many areas of chemistry,[43] and, as a result, transition metal catalyzed approaches to C-X bond formation have been the subject of intense recent research.[43] Transition-metal-catalyzed carbon-fluorine coupling reactions are particularly rare and constitute powerful synthetic tools to complement more conventional methods. In

particular, efficient catalytic fluorination via either C-CF$_3$ cross-coupling[13] or C-H functionalization[14] allows to introduce fluorine –containing groups into biologically active molecules.[15-32] We and others have previously reported the Pd-mediated catalytic conversion of C-H bonds to C-X(OAc and OH) bonds using dioxygen and hydrogen peroxide as terminal oxidants.[43] These reactions are believed to proceed via monohydrocarbyl palladium(IV) intermediates such as that shown in Scheme 1, where C-X bond-forming reductive elimination from Pd^{IV}(R)(X) **4** serves as a key step.[37] Very few palladium(IV) monoalkyl complexes have been isolated and characterized so far;[39-42] their reactivity is poorly known and virtually unexplored. One can expect that highly electrophilic Pd^{IV} monoalkyl complexes will accept readily attacks at the alkyl carbon by various nucleophiles, include halide anions, leading to the formation of C-halogen bond. Hence, we set up to prepare a series of isolable Pd^{IV} monoalkyl complexes supported by the hydrated dpk ligand.

To begin, 8-methylquinoline was chosen as an organic substrate in the expectation of high reactivity of the resulting Pd^{IV} alkyl (benzyl) complexes towards various nucleophiles. Corresponding pallada(II)cycles can be prepared readily by reacting Pd(OAc)$_2$ and this substrate.[44] Reaction of the resulting palladacycle with dpk leads to the formation of the dpk-supported Pd^{II} precursor **10(OAc)** (Scheme 5)**.**
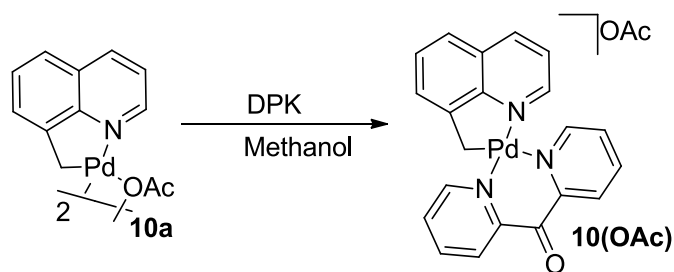
Scheme 5. Conversion of 8-methylquinolyl palladium(II) acetate salt to 8-

methylquinolyl palladium(II) DPK complex **10(OAc)**.

Complex **10(OAc)** was characterized by ^{1}H, ^{13}C NMR spectroscopy and ESI-MS. X-ray quality crystals of tetrafluoroborate analog **10(BF₄)** were obtained by slow diffusion of benzene into its solution in dichloromethane at 25°C. The crystal structure of **10(BF₄)** shows that palladacyclic fragment of the cyclometallated ligand is rigid and almost planar, whereas the dpk fragment is flexible and adopts a boat
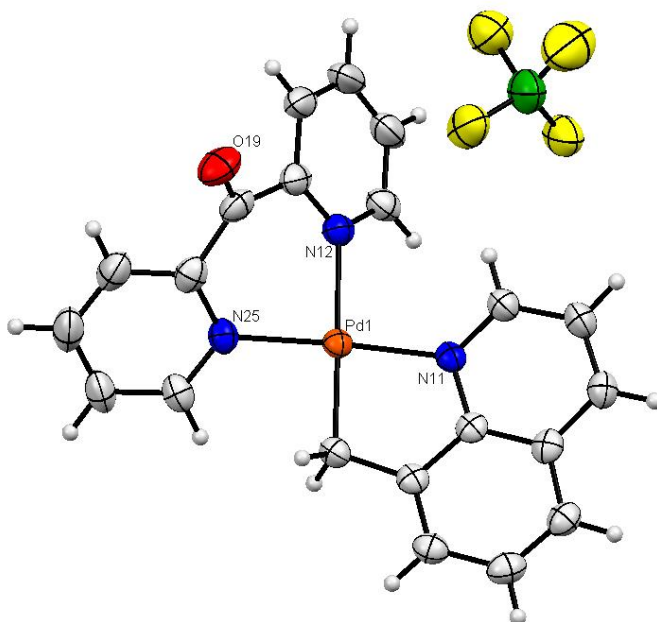

confirmation (Figure 1).

Figure 1. Ellipsoid representation of **10(BF₄)** (50% probability).

To probe the reactivity of the systems comprised of **10(OAc)** or **10(BF₄)** and H_2O_2 the oxidative halogenation of **10⁺** was performed in the presence of modest (Cl⁻) and good nucleophiles Br⁻, I⁻. The results are summarized in Table 1. Two solvents were used in these reactions, MeOH and MeCN, the first one being nucleophilic enough to compete with the halides. In all the cases the corresponding alkyl halides were produced in good or high yields after 1h of reaction. In the reaction in MeOH (entries

1-3), yields of 8-quinolylmethyl halides were lower compared to reactions in MeCN (entries 4-6). For example, under otherwise identical reaction conditions, oxidative chlorination of **10(BF₄)** afforded an 82% yield of 8-(chloromethyl)quinoline with hydrogen peroxide in acetonitrile(entry 4) and only a 75% yield in methanol (entry 1). This difference can be attributed to competition of Cl⁻ and methanol for the electrophilic Pd(IV) alkyl intermediate. In fact, in the reactions in methanol 8-quinolylmethyl ether and 8-quinolylmethanol were observed as the minor reaction products. In turn, the latter compound was the minor reaction product in MeCN solutions; water from the oxidant, 30% aqueous H_2O_2 was responsible for this reaction.

Table 1. Oxidative halogenation of 8-methylquinoline palladium complex with H_2O_2 / LiX.
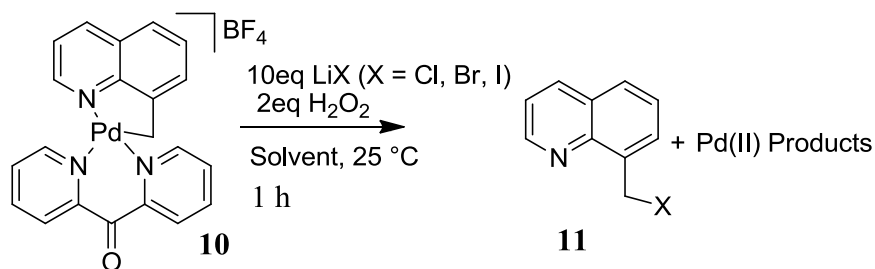
Entry	Solvent(1mL)	Temperature (°C)	Lithium Salt	Time (hrs)	NMR Yield (%)	Isolated Yields (%)
1	MeOH	25	LiCl	1	75	65
2	MeOH	25	LiBr	1	78	75
3	MeOH	25	LiI	1	78	73
4	CH₃CN	25	LiCl	1	82	80
5	CH₃CN	25	LiBr	1	84	82
6	CH₃CN	25	LiI	1	84	82

To get some evidence for the intermediacy of Pd^{IV} monoalkyl complexes in the reactions in Table 1 we monitored the reaction of **10(BF₄)** and 30% aqueous H_2O_2 in

MeCN solution using ^{1}H NMR spectroscopy. Analysis of the reaction mixture containing 1.5 equiv of hydrogen peroxide after regular intervals at room temperature showed the formation of two new species, each with two pairs of characteristic doublets with $J=$ 6 and 10 Hz in the range of 5-7 ppm(84%).
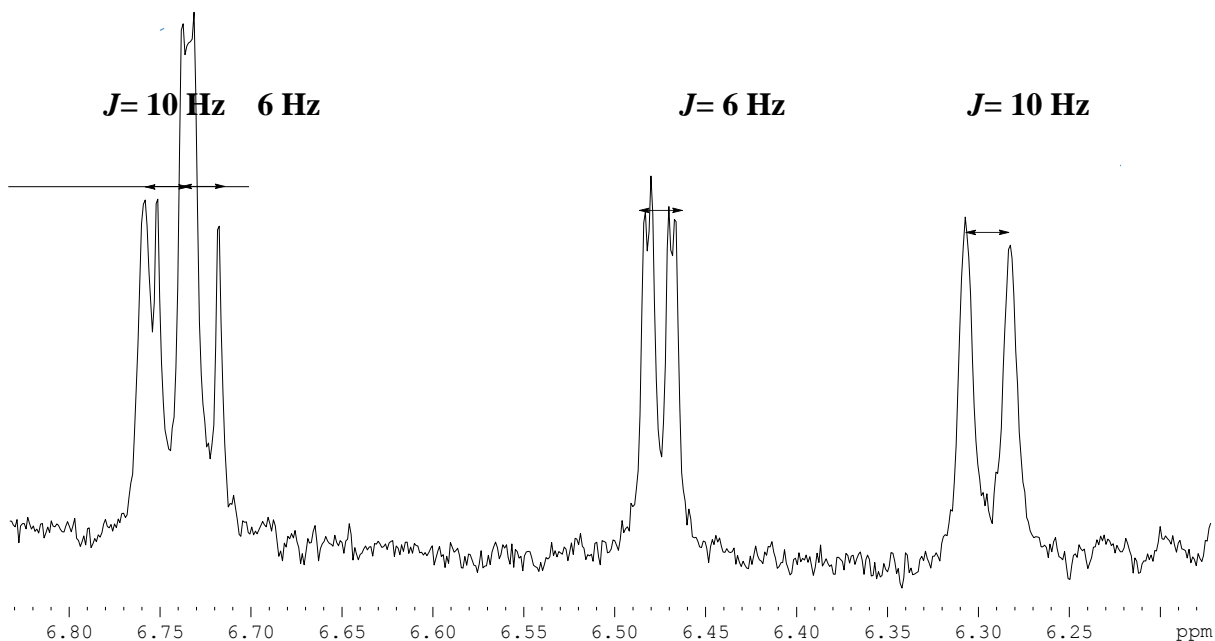

Figure 2. A fragment of an ^{1}H NMR spectrum showing signals originating from 8-methylquinolyl CH$_2$ group of the proposed palladium(IV) intermediates.

These signals were assigned to the diastereotopic hydrogen atoms of the Pd^{IV} – bound CH$_2$ group in the presumed Pd(IV) intermediate **12(BF$_4$)** and its isomer **12a(BF$_4$)** featuring the alkyl group *trans-* to the hydrated dpk oxygen atom. After 24hrs, the palladium(IV) species underwent C-O reductive elimination to form cleanly the 8-hydroxymethyl-quinoline – derived oxapalladacycle (75%) which, in part, reacted with water to produce the corresponding alcohol **11e** (25%).

To confirm the presence of electrophilic alkyl Pd^{IV} species in the solutions above we next probed the reactivity of the alkyl palladium(IV) intermediates toward

various lithium halides (X = Br, Cl, and I). Intriguingly, addition of 10 equiv of lithium chloride to t)he mixture of **10(BF₄)** and H_2O_2 in MeCN 2h after their mixing, as described above, afforded in less than 15 minutes **11b** in high yield (70%) (Scheme 6). Both Pd(IV) species **12(BF₄)** and **12a(BF₄)** are consumed.
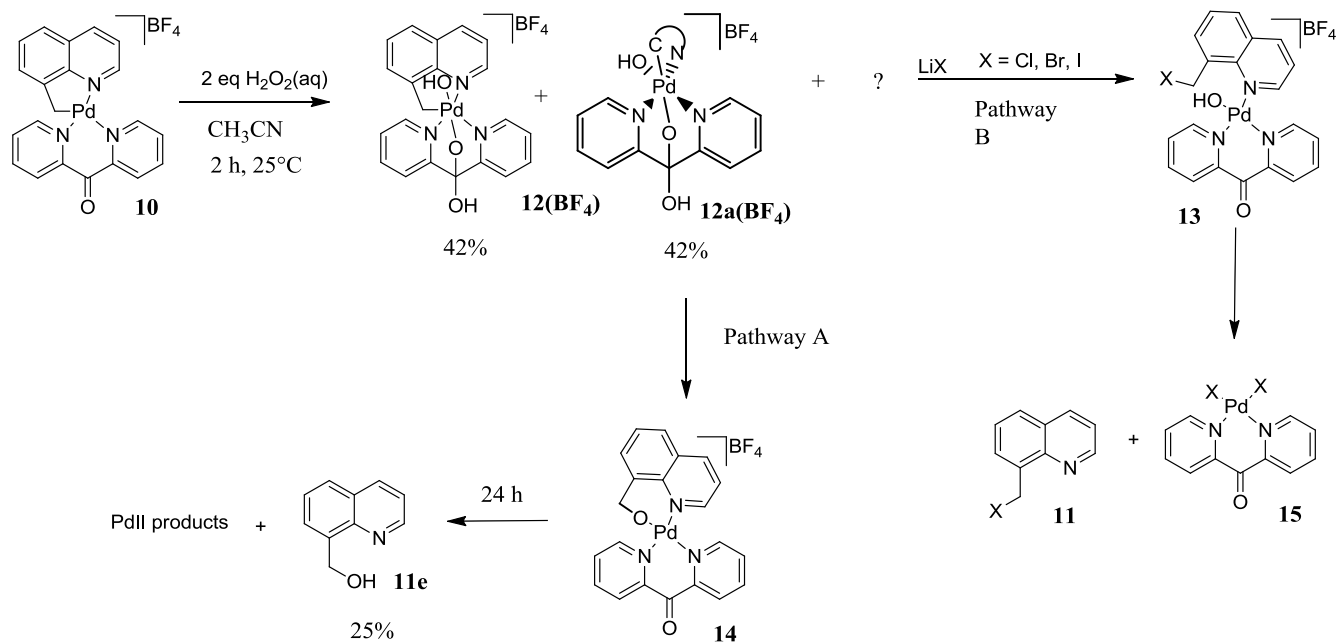
Scheme 6. Proposed mechanism of halogen substitution of Pd^{IV} intermediate.

We next sought to study the reactivity of the alkyl Pd^{IV} complexes **12(BF₄)** and **12a(BF₄)** toward O-nucleophiles. Addition of lithium hydroxide to the above solution of **12(BF₄)** and **12a(BF₄)** led to the immediate formation of 8-methylquinolylmethanol in 40% NMR yield. This result strongly suggests an outer-sphere mechanism of the C-O coupling that involves an S_N2 attack of a nucleophile on the Pd(IV)-bound alkyl carbon. On the basis of these preliminary observations, we hypothesized that the observed C-Pd^{II} functionalization reactions could proceed via the pathway depicted in Scheme 6. This involves three distinct steps: (1) oxidation of the dpk- supported Pd(II) alkyl species with hydrogen peroxide to form a mixture of

Pd(IV) derivatives, (2) attack of a nucleophile at the Pd(IV)-bound alkyl carbon, and (3) organic product release. Warming a solution of **12(BF₄)** and **12a(BF₄)** to 78°C in the absence of LiOH resulted in the C-O elimination to generate oxapalladacycle **14(BF₄)** in 80% yield.

The challenge for developing a palladium mediated alkyl halogenation reaction was to find reaction conditions that allowed all elementary steps — Pd(II)-to-Pd(IV) oxidation and C-X reductive elimination with the desired group X from the resulting Pd(IV) species — proceed in the same reaction vessel. In the systems above the heavier halides, Cl⁻, Br⁻ and I⁻, were nucleophilic enough to form the C-X elimination products in high yield. Ionic fluorides MF (M = Li, Na, K, *n*-Bu₄N) may be not reactive enough in the presence of methanol and water originating from aqueous H_2O_2; competition from water and the solvent may produce exclusively the corresponding C-O elimination products.

A conventional synthesis of 8-(fluoromethyl)quinoline using hydrogen peroxide and several fluoride sources was explored next. In particular, AgF was chosen as a promising fluoride source due to silver greater electronegativity and expected greater "covalent character" of its halides compared to alkali metal fluorides, which may help retain high nucleophilicity typical for a "naked" fluoride and known applications of AgF in a variety of fluorination reactions.[31] The higher the ionicity of the fluoride source the more strongly fluoride will be stabilized by water so diminishing its nucleophilicity and interfering with the fluorination process.

Next, complex **10(BF₄)** was subjected to oxidative fluorination with H_2O_2 / F⁻ under varied conditions (Table 2). In these experiments **10(BF₄)** was combined in a
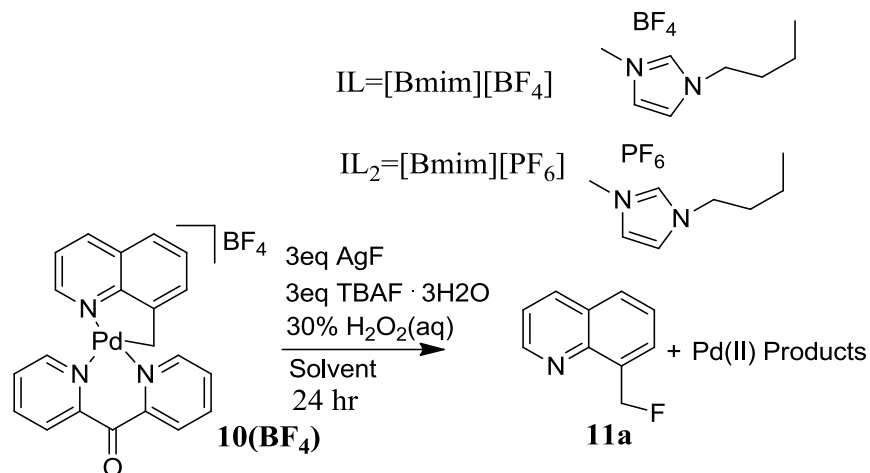
chosen solvent with 1.5 - 5 equivalent of H_2O_2(aq) at 25°C forming a dark orange solution. Additives of AgF, CuF_2, Me_4NF and tetra-*n*-butyl ammonium fluoride trihydrate (TBAF) were used as a source of F$^-$. The composition of reaction mixture was analyzed after 1-24h. As expected, no fluorination was observed in methanol because of the anticipated strong interaction of F- with this protic solvent resulting in diminished nucleophilicity of fluoride(entries 1-4). The C-O elimination products formed predominantly. Similar was the case of MeCN and DCM as solvents, though the reasons for the lack of the reactivity may be different (e.g., fluoride source issues) (entries 5-6). With AgF as Fluoride source, fluorinations conducted with both MeCN – dichloromethane mixtures provided improved solubility of AgF, albeit with no C-F formation(7-8). The use of MeCN – dichloromethane mixtures was more efficient and the target alkylfluoride **11a** was detected in ~5% yield, in the presence of TBAF (entries 9-10). When the amount of H_2O_2 was reduced to 2 equivalent the fluorinated product **11a** was produced in 15% yield, presumably because of the accompanying decrease in the water content in the system, which would affect the nucleophilicity of fluoride anion in the same way as MeOH solvent (entries 11-12). The use of a different source of nucleophilic fluoride, tetra-*n*-butyl ammonium bifluoride or tetrabutylammonium bifluoride/anhydrous CuF_2 in MeCN – dichloromethane mixtures also produce C-F coupling product **11a** with aqueous hydrogen peroxide albeit in the same low yield 5-15% (entries 13-14). With the exception of using only CuF_2 as a fluoride source (entry 15). The best outcome was obtained with AgF/CuF_2, which afforded **11a** in 54% yield (entry 16). In this case, anhydrous CuF_2 was thought to bind water (entry 17 – 19). The use of AgF, CuF_2, Me4NF and tetra-*n*-butylammonium fluoride

trihydrate and variations of the MeCN or THF: DCM ratio led to 20% or 15% yield of **11a** (entry 20 and 21). The same 20% yield of **11a** was achieved with AgF as the fluorinating agent in a mixture of acetonitrile with an ionic liquid 1-butyl-3-methylimidazolium tetrafluoroborate ([Bmim][BF4]-IL) (entry 22).Finally, the use of AgF with dichloromethane / the ionic liquid mixtures was also efficient enough allowing to produce **11a** in 40-44% yield (entries 23-24). Less efficient was the fluorination using a dichloromethane/acetonitrile mixture with AgF and anhydrous tetramethylammonium fluoride with anhydrous urea hydrogen peroxide adduct (anh)(entry 26).

Fluorination with AgF in DCM and MeCN listed in Table 2 turned out to be the best though slower compared to the halogenation of 8-methylquinoline derivative **12(BF₄)** using lithium halides due to the low solubility of AgF and low nucleophilicity of fluoride. Attempted oxidative fluorination of **10(BF₄)** using AgF or TBAF and a different solvent, solely ionic liquid and AgF or TBAF led to the corresponding alcohol (60%) and no **11a** (entries 27-31). Interestingly, mixtures containing AgF and tetra-*n*-butylammonium tetrafluoroborate (TBABF₄) or 1-butyl-3-methylimidazolium Hexafluorophosphate([Bmim][PF₆]-IL₂) produce 11-14% of **11a** (entries 25 and 32).

Purification of 8-fluromethyl-quinoline was not achieved due to the difficulty of extracting organic substrate from ionic liquid, however **11a** was clearly identified using ^{1}H NMR spectroscopy.

Table 2. Oxidative Fluorination of complex **10(BF₄)** under various conditions

IL=[Bmim][BF$_4$]

IL$_2$=[Bmim][PF$_6$]

3eq AgF
3eq TBAF · 3H2O
30% H$_2$O$_2$(aq)
Solvent
24 hr

10(BF$_4$) → 11a + Pd(II) Products

Entry	Solvent(1 mL)	Temperature (°C)	Fluoride Source (3eq)	H$_2$O$_2$ (eq)	Time (h)	NMR Yield of C-F (%)	Isolated Yields of C-F (%)
1	MeOH	25	AgF or TBAF	5	1 or 24	0	0
2	MeOH	25	AgF/TBAF	5	1	0	0
3	MeOH	60	AgF/TBAF	5	1	0	0
4	MeOH	80	AgF/TBAF	5	1	0	0
5	CH$_3$CN	25	AgF or TBAF	5	1 or 24	0	0
6	CH$_2$Cl$_2$	25	AgF or TBAF	5	1 or 24	0	0
7	CH$_3$CN(20% dcm)	25	AgF or TBAF	5	24	0	0
8	CH$_2$Cl$_2$(20% CH$_3$CN)	25	AgF or TBAF	5	24	0	0
9	CH$_3$CN(20% dcm)	25	AgF/TBAF	5	1	5	N/A
10	CH$_3$CN(20% dcm)	25	AgF/TBAF	5	24	5	N/A
11	CH$_3$CN(20% dcm)	25	Agf/TBAF	2	24	15	N/A
12	CH$_3$CN(20% dcm)	78	Agf/TBAF	2	24	15	N/A
13	CH$_3$CN(20% dcm)	25	CuF$_2$/TBAHF$_2$	2	24	5	N/A
14	CH$_3$CN(20% dcm)	25	TBAHF$_2$	2	24	10	N/A
15	CD$_2$Cl$_2$(20% CH$_3$CN)	25	CuF$_2$	2	24	0	0
16	CD$_2$Cl$_2$(20% CH$_3$CN)	25	6eq AgF/1eq CuF$_2$	2	24	48	32

17	CD$_2$Cl$_2$(20% CH$_3$CN)	25	4eq AgF/1eq CuF$_2$	2	24	54	45
18	CD$_2$Cl$_2$(20% CH$_3$CN)	25	3eq AgF/1eq CuF$_2$	2	24	32	15
19	CD$_2$Cl$_2$(20% CH$_3$CN)	25	1eq AgF/1eq CuF$_2$	2	24	28	9
20	CD$_2$Cl$_2$(20% CH$_3$CN)	25	AgF/TBAF	2	24	20	10
21	CD$_2$Cl$_2$(20% THF)	25	AgF/TBAF	2	24	15	N/A
22	CD$_3$CN(50% IL)	78	6eq AgF	2	24	20	15
23	CD$_2$Cl$_2$(50% IL)	25	6eq AgF	2	24	40	32
24	CD$_2$Cl$_2$(50% IL)	25	6eq AgF	1.5	24	44	35
25	CD$_2$Cl$_2$(50% IL$_2$)	25	6eq AgF	1 eq anh	24	14	N/A
26	CD$_2$Cl$_2$(20% CH$_3$CN)	25	AgF/NMe$_4$	2	24	5	0
27	IL$_2$	25	6eq AgF	2	24	0	0
28	IL	25	6eq AgF	1 eq anh	24	0	0
29	IL$_2$	25	6eq AgF	1 eq anh	24	0	0
30	CD$_2$Cl$_2$(20% CH$_3$CN)	25	TBAF	1 eq anh	24	0	0
31	CD$_2$Cl$_2$(20% CH$_3$CN)	25	TBAF/TBABF$_4$	1 eq anh	24	0	0
32	CD$_2$Cl$_2$(20% CH$_3$CN)	25	AgF/TBABF$_4$	2	24	11	N/A

While we have been successful with oxidative fluorination of **10(BF₄)**, the reactions in Table 2 suffer from the distinct disadvantage that water is present in the reaction mixture giving rise to the alcohol 8-quinolylmethanol **11e**, as a major product. We hypothesized that by reducing the amount of water in the system the Pd-mediated C-H fluorination would produce higher yields of fluorinated product. Thus, we also examined the use of anhydrous urea - hydrogen peroxide adduct to minimize the formation of the alcohol. In fact, when the urea - hydrogen peroxide is used, the highest yield of the **11a** obtained after 24 hrs (entry 25) was 14%. Notably, less than

50% of the hydroxylated product **11e** was observed when anhydrous CuF_2 - AgF combination was used (Scheme 6a, entry 17).
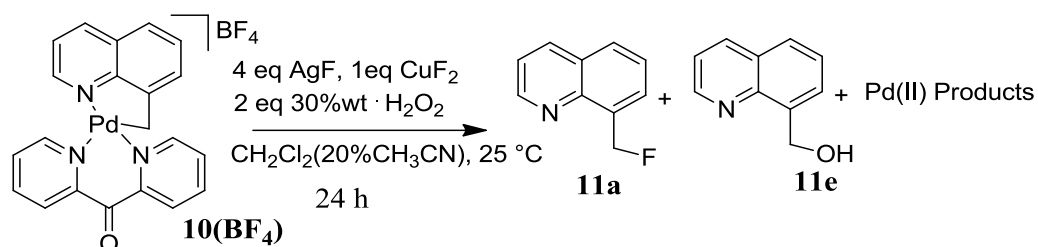
Scheme 6a. Oxidative fluorination of pallada(II)cycle **10(BF₄)** using aqueous hydrogen peroxide under optimized conditions.

In nucleophilic fluorination, as shown in Table 2, fluoride serves as the nucleophile and the alkyl reaction component serves as the electrophile.[31] In 2012, C-F bond formation by a complementary approach—using an electrophilic fluorination reagent—was reported by Sanford and co-workers.[32] In this case, the mechanism proposed involved reductive elimination of C-F from a palladium(IV) intermediate. However, an S_N2 mechanism can also be a plausible explanation of the formation of the C-F bond. Based on our findings, we propose a similar mechanism whereby the nucleophile is fluoride formed as a result of dissociation of the Pd(IV)-F bond. To elucidate the mechanism substrates containing stereogenic centers may be used. Inversion of stereochemistry is expected for an S_N2 mechanism and retention of configuration for reductive elimination.

The successful realization of the oxidative halogenation of the 8-methylquinoline derivative **10(BF₄)** containing reactive benzylic carbon – Pd bond led us to engage in a similar study of 4-amino-2-*tert*-butylpyridine as a substrate featuring non-activated (non-benzylic) $C(sp^3)$-H bonds. Corresponding Pd^{IV}

monoalkyl complexes are expected to be less reactive and, therefore, easier to isolate and characterized compared to 8-methylquinoline derivatives. In addition, such Pd^{IV} monoalkyls may be more prone to react via an intramolecular C-X coupling mechanism so helping avoid problems of low nucleophility and poor solubility some C-X coupling partners. Hence, we were very eager to explore Pd^{IV} chemistry of this new substrate. Few monoalkyl Pd^{IV} complexes have been isolated and characterize so far.[39-42]

Starting from the 4-amino-2-*tert*-butyl and palladium(II) acetate, chelation-assisted C-H activation leads to palladacycle **16** (56%) (Scheme 7). Reaction with acetonitrile forms **16a** (82%). The addition of DPK in methanol produces **17(OAc)** in moderate yield (75%).
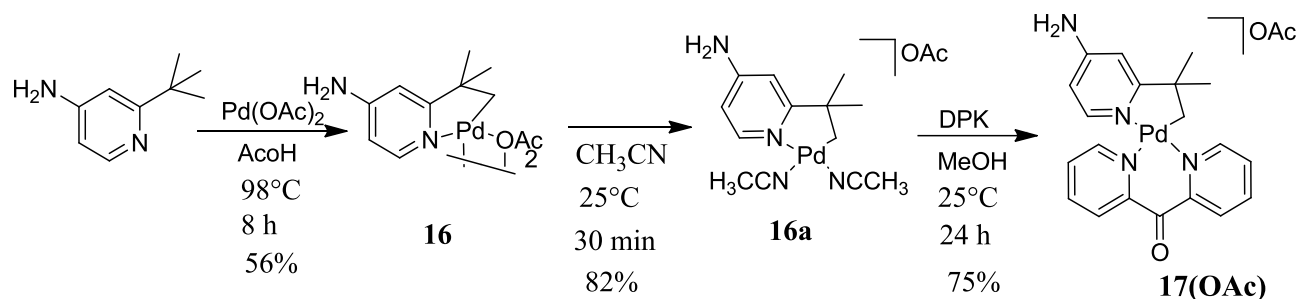
Scheme 7. 4-amino-2-*tert*-butylpyridine – derived dpk – supported palladacycle
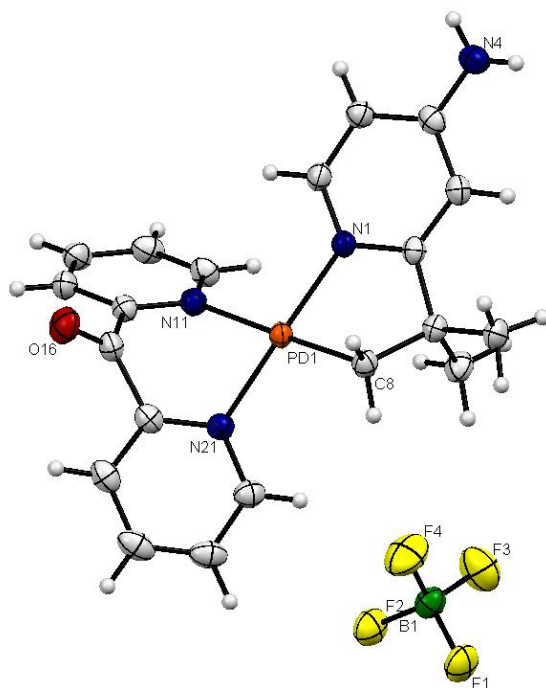
17(OAc).

Figure 3. Ellipsoid representation of **17(BF₄)** (50% probability).

The more lipophilic tetrafluoroborate analog of **17(OAc)**, **17(BF₄)**, was prepared by precipitation with NaBF₄ in water and characterized by means of ^{1}H, ^{13}C NMR spectroscopy and single crystal X-ray diffraction (Fig. 3). With **17(BF₄)** in hand, we focused our attention on the isolation and characterization of the Pd^{IV} derivative **18(BF₄)**. Acetonitrile was used as a solvent for oxidation of **17(BF₄)** with H₂O₂ to avoid undesirable reactions of **18(BF₄)** with nucleophilic solvents such as water or methanol (Scheme 8). **18(BF₄)** was isolated from MeCN solutions as a dark-orange crystalline solid within 15 minutes and was found to be stable for few hours at 25°C. When left for 30hrs at 25°C in MeCN solution **18(BF₄)** undergoes complete conversion to produce C-O reductive elimination products including the corresponding alcohol **18d** (17%) (Scheme 8). Another not yet identified reaction

product may be corresponding oxapalladacycle. The identity of **18(BF₄)** was proven by single crystal X-ray diffraction (Fig. 4).

Scheme 8. The formation of the Pd[IV] monoalkyl complex **18** and its C-O reductive elimination.
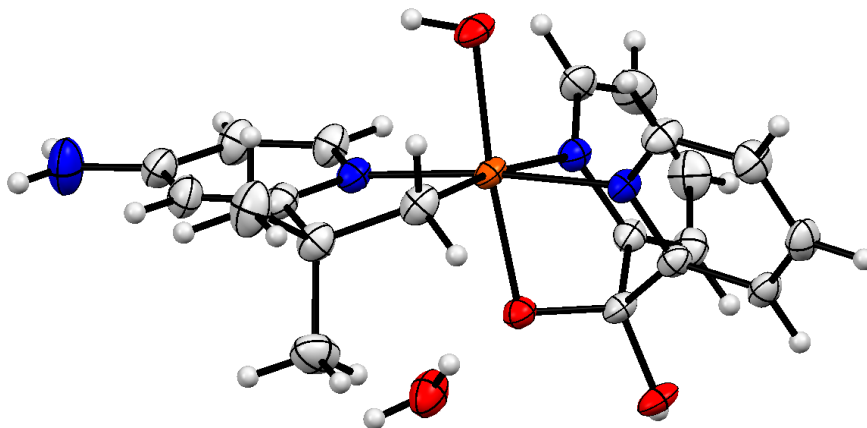
Figure 4. Ellipsoid representation of **18(BF₄)** (50% probability) with BF$_4$ anion not shown.

The structure of **18(BF₄)** in solution was analyzed using ^{1}H NMR, selective NOE and COSY NMR spectroscopy. Interestingly, ^{1}H NMR spectra of a freshly prepared **18(BF₄)** in MeCN show the presence of a second, minor species with a low intensity resonances of the Pd-CH$_2$ fragment at 4.62 ppm and 4.78 ppm.

The most important NOE interactions for **18(BF₄)** were observed between *ortho*-H in one of the rings of the dpk – derived ligand and the Pd-CH$_2$ group. These results argue strongly in favor of the structure **18⁺**.
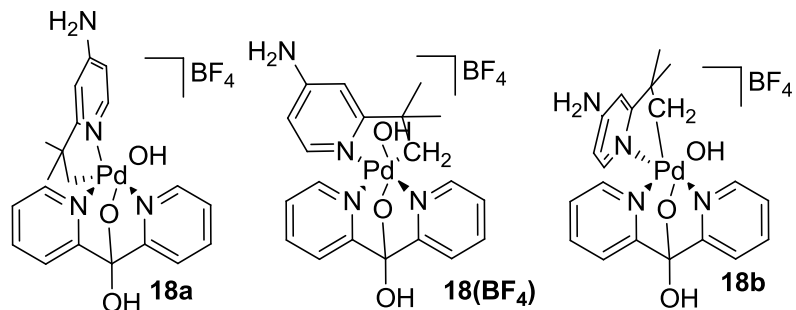
Figure 5. Isomers of **18⁺**.

The minor complex present along with 18**(BF₄)** may be one of its isomers. Possible isomers of **18(BF₄)** that might exist in its solutions are shown in Fig. 5.

To probe the reactivity of the new monoalkyl Pd^{IV} complex **18(BF₄)** we set up a test reaction of **18(BF₄)** with LiBr. To **18(BF₄)** in a solution of acetonitrile(wet) were added 10 equivalent of lithium bromide to produce modest yields of brominated product (50%) at room temperature after 1 hour. A significant amount of alcohol **18d** (45%) was produced as a second reaction product. To compare, complex **12(BF₄)** gave higher conversion to the corresponding C-Br product (84%) and lower level of impurities, presumably due to the greater reactivity of its C-Pd^{IV} bond towards external nucleophiles. Another possible reason for these differences is the realization of an additional mechanistic pathway, an intramolecular C-O coupling for **18(BF₄)**.

In support to this hypothesis, **18(BF₄)** featuring non-activated C(sp^3)-Pd^{IV} bond and **12(BF₄)** having a benzylic C(sp^3)-Pd^{IV} bond exhibit different rates of the C-O reductive elimination from the Pd^{IV} center in wet acetonitrile. After 24hrs the conversion of **18(BF₄)** is 70%(half life – 14h) vs. 100% conversion of **12(BF₄)**. Interestingly, the monoaryl palladium(IV) hydroxo complex **2(BF₄)** reported by Vedernikov and Oloo undergoes C-O reductive elimination with the half-life of about 6h under analogous conditions. Further testing of reactivity of **18(BF₄)** is required

21

that may involve the use of kinetics experiments and isotopic labeling with ^{18}O-labeled water as a potential nucleophile to distinguish between intra- and intermolecular C-O reductive elimination mechanisms of this compound.

Electrophilic halogenating reagents and formation of palladium(IV) intermediates.

The incorporation of a ligand X (e.g., halides) into the Pd(IV) coordination sphere is usually achieved by using an electrophilic halogen-containing terminal oxidant (e.g., Selectfluor, NCS, NBS).[10-32] The following section describes the results of application of conventional electrophilic halogenating agents for halogenation of dpk-supported Pd(II) alkyl complex **17(BF₄)** with the goal of isolation of the corresponding monohydrocarbyl palladium(IV) halides and characterization of their C-X bond forming reactivity.

17(BF₄) was chosen as a model complex in the expectation of a relative stability of the resulting Pd[IV] alkyl complexes towards reductive elimination that would allow for their detailed characterization, as we observed with the corresponding palladium(IV) hydroxo complex. To introduce a fluoro into the Pd(IV) coordination sphere to an acetonitrile solution containing complex **17(BF₄)** were added 5 equivalents of 1-fluoro-2,4,6-trimethylpyridinium tetrafluoroborate (NF) at 25°C and stirred for 5 minutes(Scheme 8). Complex **19(BF₄)** formed in 98% yield and was characterized using conventional ^{1}H NMR techniques and X-ray diffraction (Figure 6). Notably, monitoring **19(BF₄)** in DMSO for 72 hrs showed that the corresponding 4-amino-2-(2-fluoro-1,1-dimetylethyl)pyridine is produced in moderate yields (68%). Further studies will focus on performing kinetics of the C-F

reductive elimination of **19(BF₄)** with and without additives of F⁻ and analysis of possible C-F coupling mechanisms.
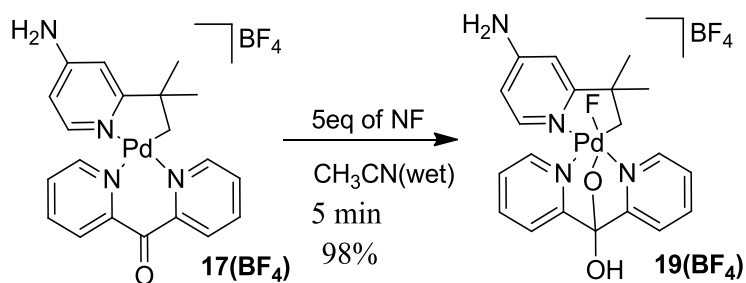
Scheme 8. The isolation of palladium(IV) monohydrocarbyl fluoro complex.

Furthermore, starting from 17(BF₄), the palladium(IV) fluoro complex could be easily detected by ^{19}F NMR which shows a prominent signal at -320.85 ppm (Pd-F).
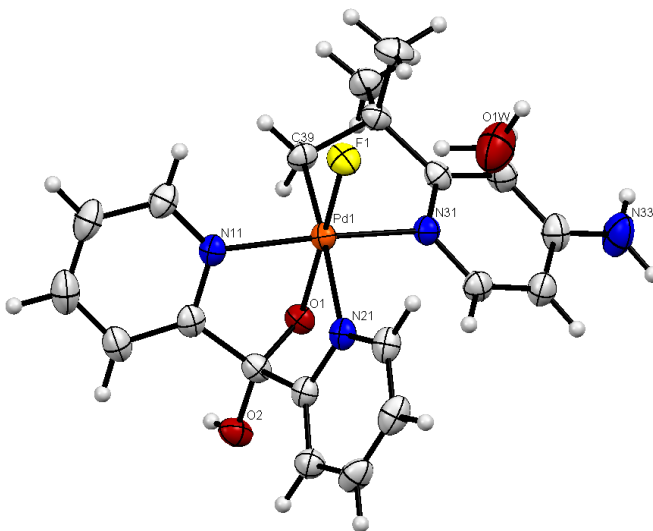
Figure 6. Palladium(IV) Fluoro monoalkyl complex with BF₄ anion and acetonitrile not shown.

The approach above is efficient for producing palladium(IV) and C-F bonds, but hydrogen peroxide as the oxidant in combination with a fluoride source to form C-F bonds through a palladium(IV) intermediate is more desirable due to reasons

stated in the introduction. Complex **19(BF4)** will be used as a model for constructing palladium(IV) fluoro intermediates, while exploring alternative reagents to enable the fluorination.

For comparison, N-Bromosuccinimide was also employed under identical conditions as an oxidant. When excess N-Bromosuccinimide (NBS) was reacted with **17(BF4)** under analogous conditions **21** (Scheme 9) was obtained after 24hrs (58%), followed by N=N bond formation and aromatic C-H bromination to yield **23** after 5 weeks (45%).
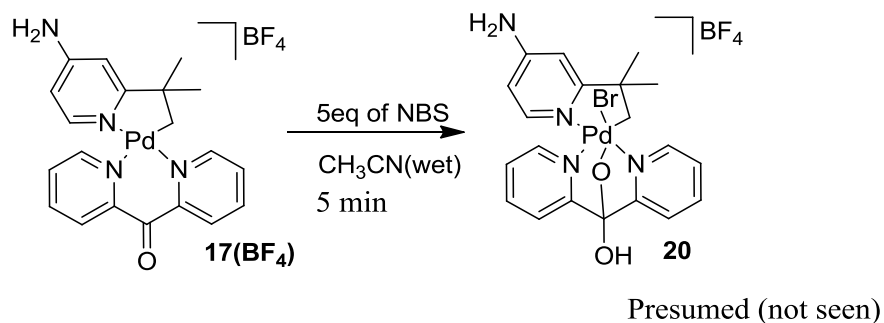
Scheme 9. Electrophilic bromination of **17(BF4)** using NBS.

Further indications of a second C-H activation were provided by single crystals obtained from the reaction mixture of **23** in acetonitrile at -15°C (Figure 7).
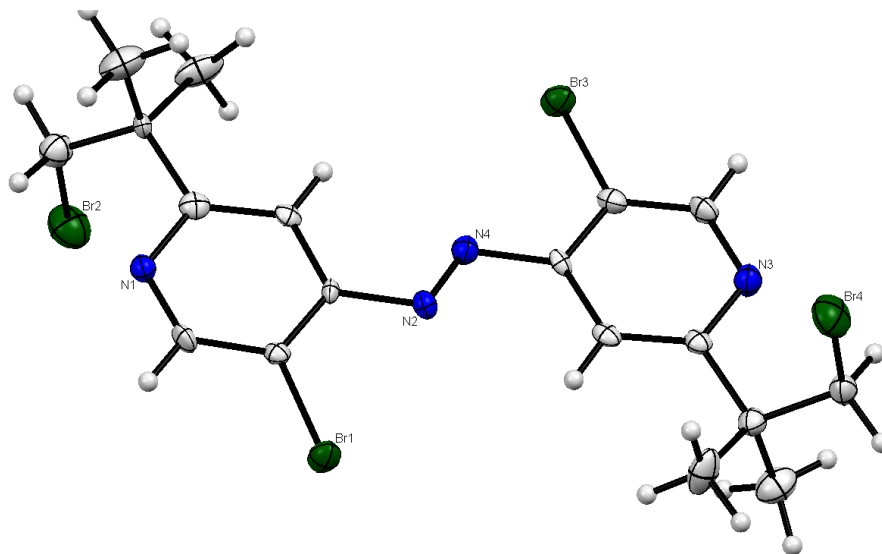
Figure 7. X-ray crystal structure of **23** (50% probability)

To rationalize this tandem process, we proposed a plausible mechanism (Scheme 10). Presumably, NBS oxidatively adds to complex **17(BF₄)**, which leads to the generation of cationic species **20**. The cationic species **20** then reductively eliminates to form **21**. Further oxidation of **21** with NBS produces an azopyridine which undergoes cyclopalladation, bromination and C(sp^2)-Br elimination to form **23** **(Figure 7).** Alternatively, **21** undergoes electrophilic bromination first and then N=N coupling. Future investigations will be focused on conducting detailed investigations of mechanism of these transformations. Reactions with stoichiometric amount of NBS should be performed, on the first place.
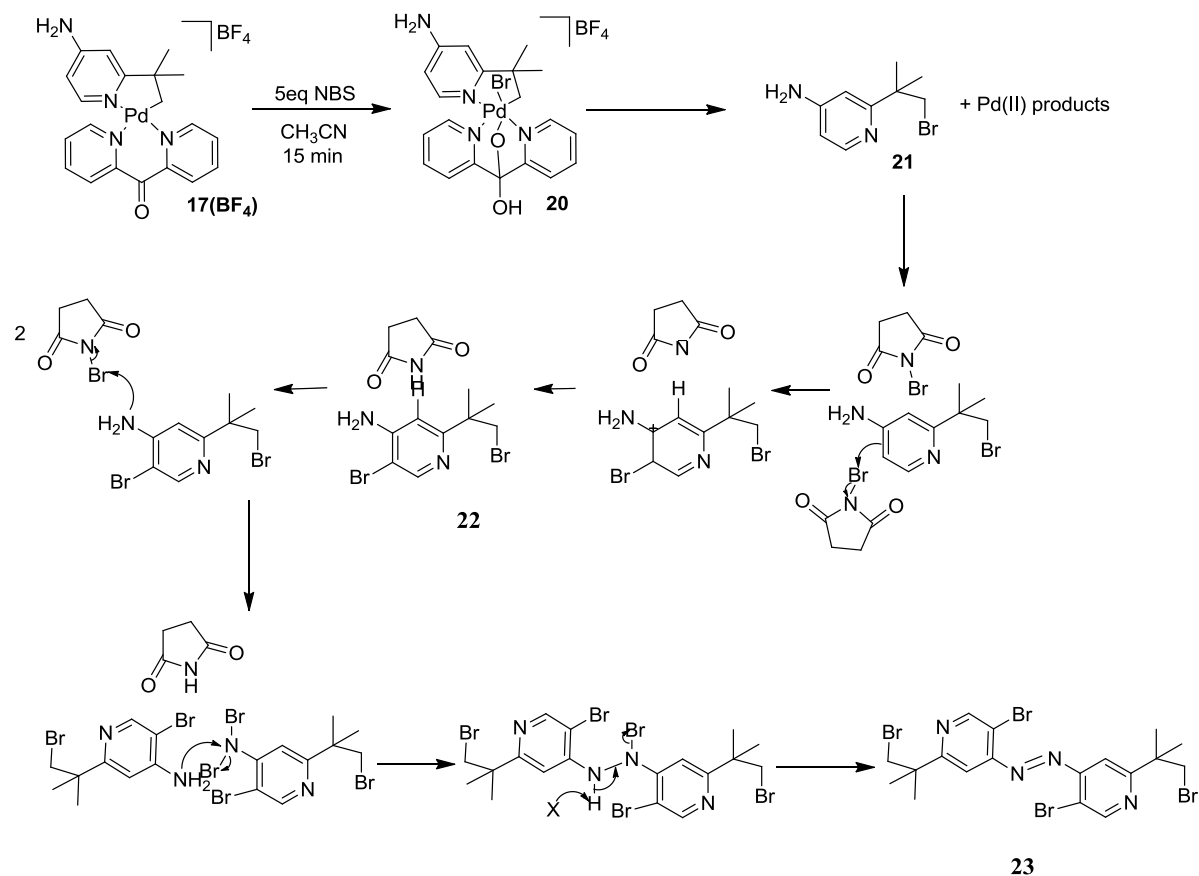
Scheme 10. Proposed mechanism for the multiple functionalization of 2-*tert*-butylpyridine derivative via Pd^{IV} intermediate.

It appears that a reaction between NBS and NH$_2$ group on the pyridine ring takes place resulting in the azo compound. A hydrazine intermediate species were also detected by ESI mass spectrometry.

Thus, overall, NBS proved to be less effective in forming a stable palladium(IV) intermediate in this benchmark reaction than NF. In stark contrast, the fluoropalladium(IV) complex 19 was detected and isolated by X-ray diffraction (Scheme 9). Instead, when excess NBS is used, a subsequent reaction takes place that consumes approximately 40% of 20 after 5 weeks. As a consequence, NCS will be tested for higher stability of the palladium(IV) intermediate.

Hydroxylation of Benzo[*h*]quinoline

uIn 2010, Vedernikov and Oloo reported that oxidation of the 2-(*p*-tolyl)pyridine – derived dpk –supported pallada(II)cycle **1(OAc)** reacted with hydrogen peroxide affords the corresponding monoaryl Pd(IV) hydroxo complex **2(OAc)** (Scheme 1).[37] The Pd(IV) intermediates were isolated and demonstrated to undergo facile reductive elimination yielding phenol already at 20°C. The formation of the reactive Pd(IV) complex **2(OAc)** and the preparation of a more robust Pd(IV) complex **6(OAc)** (Scheme 1) raised confidence regarding the generality of the proposed dpk –enabled oxidation of Pd(II) monohydrocarbyls to Pd(IV) derivatives. Notably, while the Pd(IV) complex **6(OAc)** having two facially chelating 1-hydroxo-1,1-diarylmethoxide ligands is kinetically stable up to 90ºC in aqueous solutions, complex **2(OAc)** having only one facially chelating 1-hydroxo-1,1-diarylmethoxide ligand decomposes at 20 ºC in the course of 36 hrs.[37] Importantly, Oloo has shown that **2(OAc)** and **6(OAc)** can reductively eliminate C-X (OH, OAc, Cl, and Br) bonds when the appropriate solvent or reagent is present. According to his observations, the stability of the Pd(IV) chloro- and bromo-analogs of **2**⁺ (X=Br, Cl) is not significantly different from that of the relatively unstable parent complex **2**⁺, so making characterization of their structure and reactivity challenging.[37] In order to prepare analogous but kinetically more stable Pd(IV) complexes and allow for their more convenient characterization a different substrate, benzo[*h*]quinoline, was chosen and a dpk-supported pallada(II)cycle **8(BF₄)** prepared (Scheme2). X-ray quality crystals of **8(BF₄)** were obtained by slow diffusion of benzene into a solution of **8(BF₄)** in dichloromethane at 25°C. The crystal structure of **8(BF₄)** shows that the

cyclometalated ligand is planar, whereas the bipyridyl unit adapts a boat conformation (Figure 8). The rigidity of the metallacycle is expected to increase the barrier of various C-X elimination reactions involving derived Pd^{IV} species.
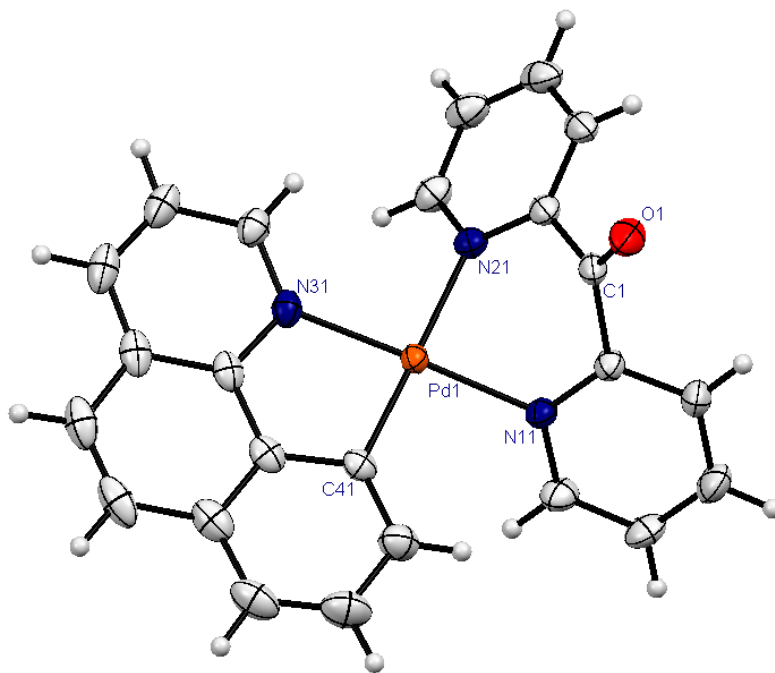
Figure 8. Ellipsoid representation of **8(BF₄)** (50% probability) with BF₄ anion not shown.

Our subsequent efforts were focused on accessing some benzo[*h*]quinoline derived Pd(IV) complexes. Scheme 9 shows a reaction sequence that we wanted to use to convert a Pd(II)-DPK complex **8(OAc)** into the corresponding Pd(IV) hydroxo derivative and phenol. We found that the oxidation of **8(OAc)** with H$_2$O$_2$ in aqueous solution at 20°C with subsequent heating the reaction mixture at 90°C for 2 hours and treatment with few equivalents of TFA/pyridine (4:1) to liberate organic products yields the corresponding phenol **24a** in 87% yield(Scheme 11).
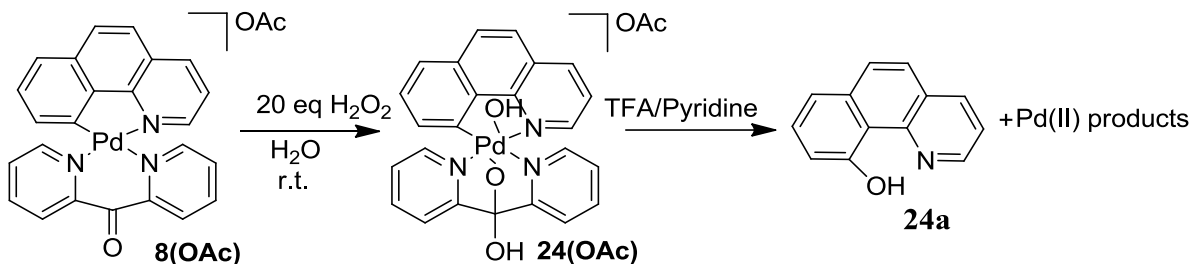
Scheme 11. The transformation of cyclopalladated benzo[h]quinoline derivative to corresponding palladium(IV) hydroxo complex and phenol.

To get an insight into the mechanism of the reaction above the reaction mixtures containing **8(OAc)** and 20 equiv. H_2O_2 in water were monitored using ^1H NMR at 20ºC. The results are presented in Fig. 9. The starting complex **8(OAc)** was completely consumed after ~10 min to produce one major species assigned as complex **24(OAc)**. The major species possesses two set of pyridine resonances, consistent with an asymmetric complex structure. **24(OAc)** is considerably more stable than **2(OAc)**.
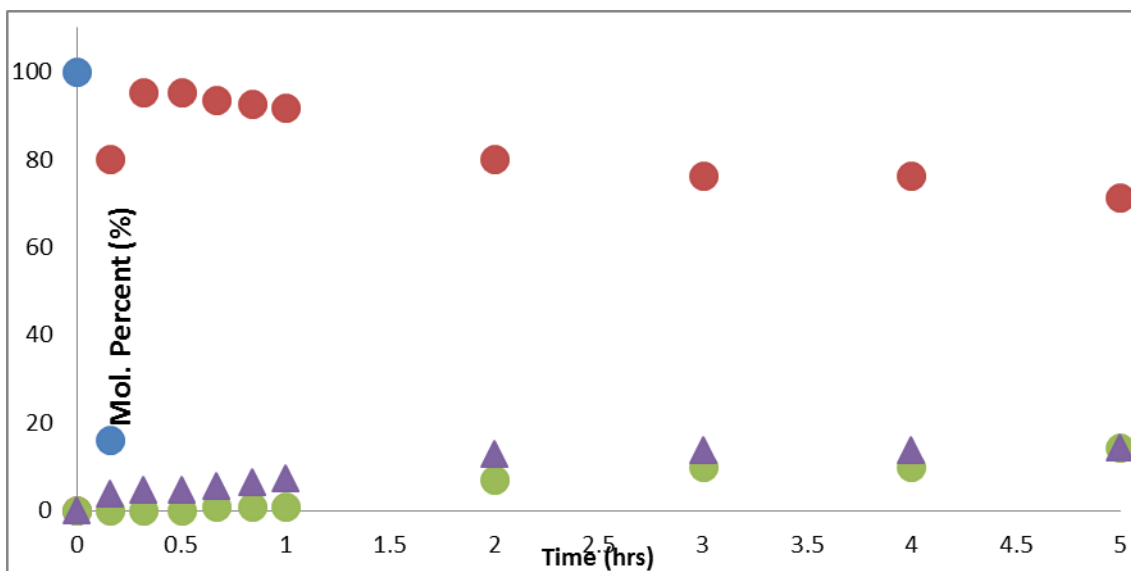
Figure 9. The oxidation of cyclopalladated benzo[h]quinoline palladium(II) complex **8(OAc)** with H_2O_2 in D_2O solution at 20ºC to form the hydroxopalladium(IV)

derivative **24(OAc)** and subsequent formation of the reductive eliminated products. The fractions of: **8$^+$** (blue circles), **24$^+$** (red circles), unknown #1 (violet triangles) and product of CO reductive elimination (unknown #2, green circles).

To confirm its identity, complex **24(PF$_6$)** was prepared in a solution of acetonitrile at -15 °C, isolated as **24(PF$_6$)** and characterized by single crystal X-ray diffraction (Fig. 10). The cation **24$^+$** adopts octahedral coordination geometry similar to **2$^+$** and **6$^+$** reported by Vedernikov and Oloo.[3]

The ^{1}H NMR spectrum of **24(OAc)** in DMSO-d_6 shows the signals of the PdOH and the ligand OH groups as two singlets at 9.30 and 8.70 ppm.
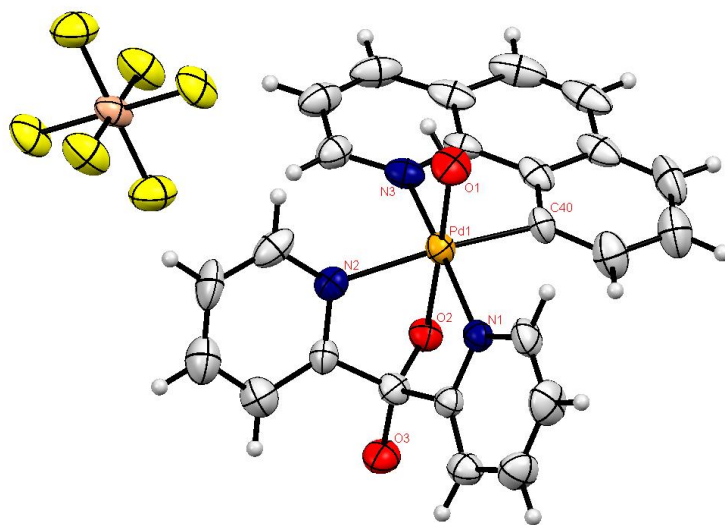
Figure 10. Ellipsoid representation of **24(PF$_6$)** (50% probability).

Besides **24$^+$** one more minor species forms in the experiment illustrated in Fig. 9 that was tentatively assigned to an isomeric complex **24$^+$**(Scheme 12), similar to oxidation of **2(OAc)**.[3]
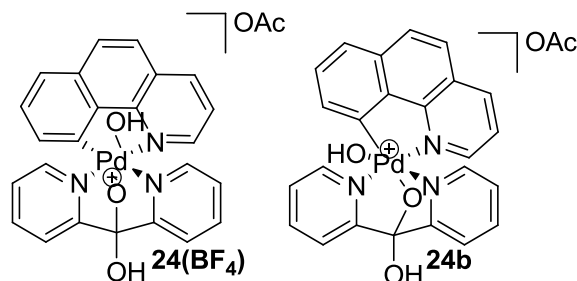
Scheme 12. Isomeric complexes **24(BF₄)** and **24b**.

An extended ^{1}H NMR monitoring of the reaction mixture in Fig. 9 containing palladium(IV) complexes **24⁺** and **24b⁺** shows a slow formation of the C-O reductive elimination product, oxopallada(II)cycle **25⁺**. The color of the reaction mixture changes to yellow after 24 hrs. After this time the NMR yield of **25⁺** is 72% (Scheme 13).
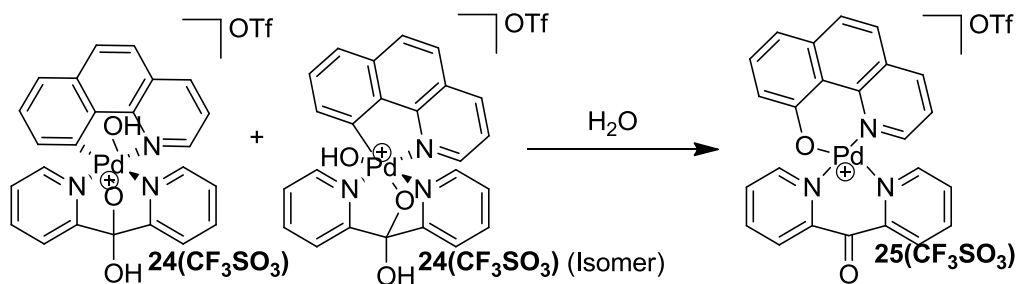
Scheme 13. The C-O reductive elimination of **24(CF₃SO₃)** in water at room temperature.

X-ray quality crystals of **25(CF₃SO₃)** were obtained by slow diffusion of pentanes into a solution of **25(CF₃SO₃)** in acetonitrile at 25°C. The identity of complex **25⁺** was also confirmed by single crystal X-ray diffraction (Figure 11) and ESI-MS with the corresponding $m/z = 484.03$ (calculated for $C_{24}H_{16}N_3O_2{}^{106}Pd = 484.03$), DPK was added as an internal standard.
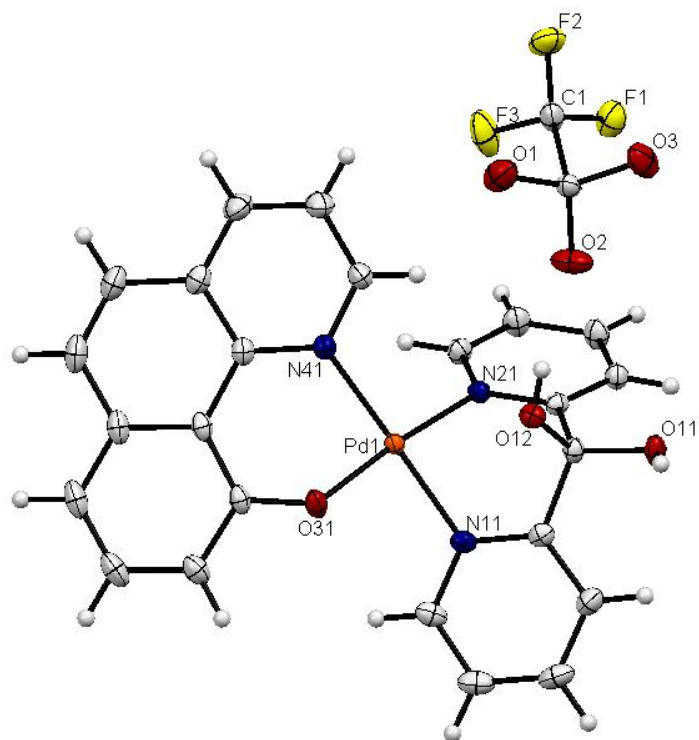
Figure 11. Ellipsoid representation of **25(CF$_3$SO$_3$)** (50% probability).

The reactions presented above have begun to address some of the unmet needs in organopalladium(IV) chemistry. Future research in palladium(IV) chemistry will need to focus on the development of more general and practical C-O forming reactions. A key feature of the investigated complex **24** is the semilabile tridentate DPK ligand. This ligand stabilizes octahedral cationic Pd^{IV} centers toward reductive elimination. However, coordinatively unsaturated species can be accessed readily via dissociation of the OH or pyridine arm of the ligand. This ligand dissociation is believed to promote the key ligand exchange and configurational isomerization steps. Ongoing investigations are focused on expanding this reactivity to other octahedral high valent palladium metal centers and to conducting detailed investigations of the factors governing site selectivity in these transformations.

Homocoupling of Benzo[*h*]quinoline

Iodine - mediated transformations are of great interest since iodine is an nontoxic, relatively inexpensive reagent.[63] The utility of iodine for C-C coupling, particularly organometallic chemistry, is more emphasized in the use of hypervalent iodine derivatives.[43-62] Efforts to use iodine in palladium catalyzed C-H activation for C-C bond formation is limited. Recently, C-H activation has become a hot topic because of its economic advantages and its ability to provides a direct method for carbon-carbon bond formations.[43-62] A wide range of transition-metal catalysts, such as Pd^{II},[44] Cu^{II},[45] Rh^{III},[46] and Co^{II} complexes have been applied in the direct carbon-carbon cross coupling via $C(sp^2)$-H and $C(sp^3)$-H functionalization.[47] While attempting the Pd-mediated conversion of benzo[h]quinoline to 10-iodobenzoquinoline, we discovered an unexpected C-C homocoupling of 10-benzo[h]quinolyl palladium(II) complex **8(BF₄)** in the presence of excess iodine followed by subsequent double C-H activation leading to C-N bond formation to yield **28(I₃)₂**.

To a solution in acetonitrile (20% aq) containing **8(BF₄)** were added 5 equivalent of I_2 to form **26** in 24hrs, followed by the formation of **28(I₃)₂** after 3 weeks. Cation **27⁺** has only been observed by ESI-MS within 2 weeks. After 3 weeks the dark brown solution was filtered through an alumina column to produce **28(I₃)₂** in 45% yield (Scheme 14). X-ray quality crystals of **28(I₃)₂** were obtained by slow diffusion of benzene into a solution of **28(I₃)₂** in dichloromethane at 25°C (Figure 12).
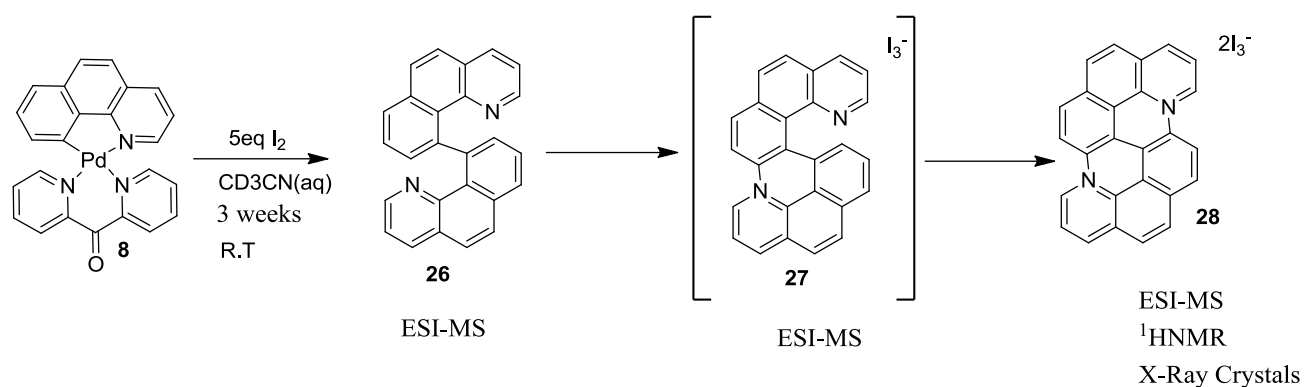
Scheme 14. The cyclization of 10-benzo[h]quinolyl palladium complex **8(BF₄)** to form the polycyclic dicationic product **28(I₃)₂**.
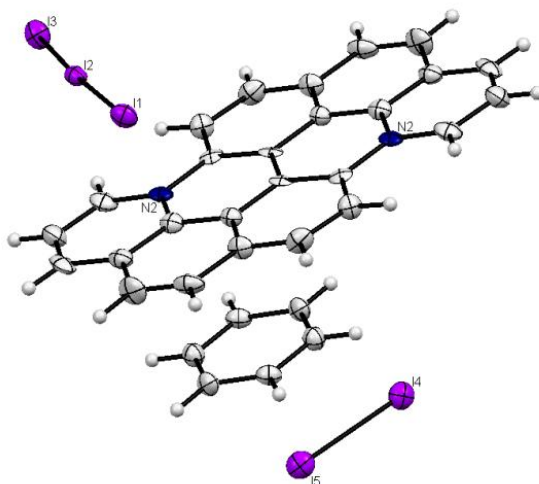
Figure 12. Ellipsoid representation of **28(I₃)₂** (50% probability).

A plausible mechanism of this reaction is given in Scheme 15. We presume that iodine oxidatively adds to complex 8^+ to form intermediate 29^+. The formation of 10-iodo-benzo[h]quinoline **30** triggers another oxidative addition of complex 8^+ and **31**, which leads to the generation of cationic species 32^+.[63] The cationic species 32^+ then reductively eliminates C-C bond to form **26**. The rest of the C-H activation / C-N coupling reactions may be Pd(II) − mediated.
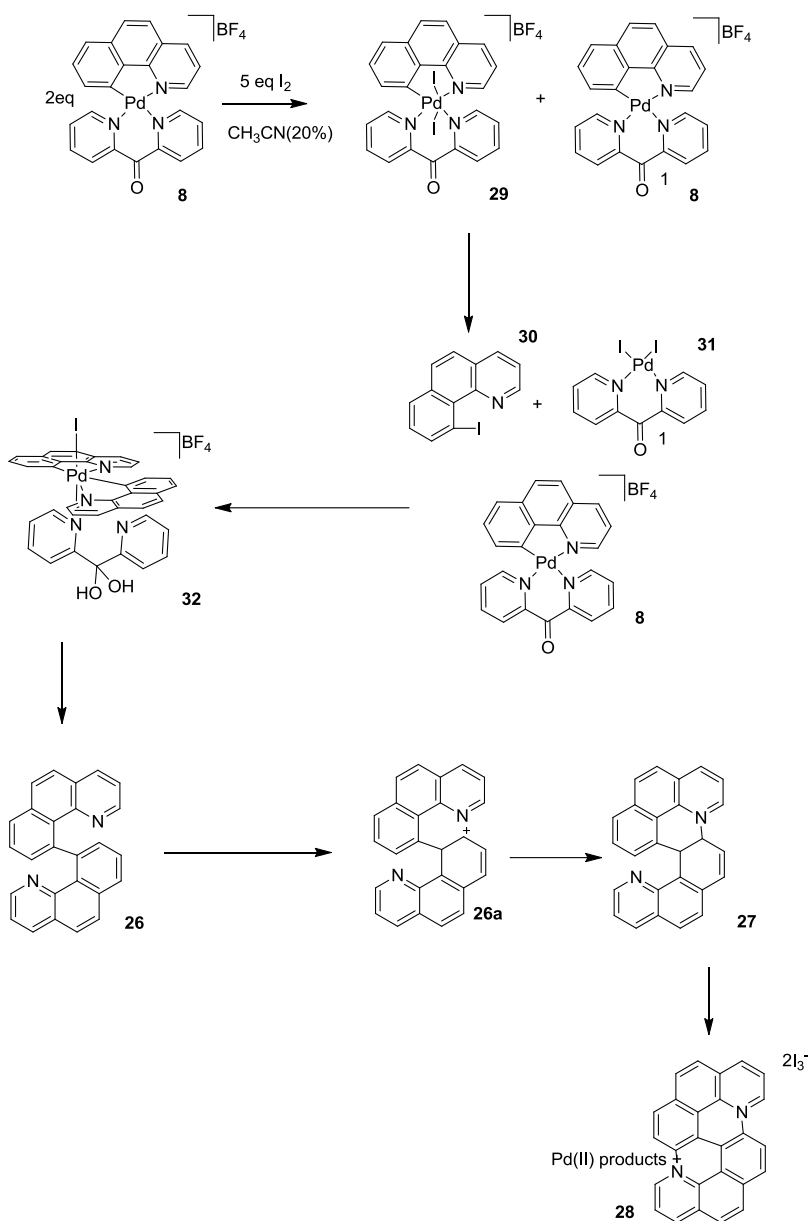
Scheme 15. Proposed mechanism of condensation of benzo[h]quinoline.

The mechanism of this remarkable reaction remains unclear. The C-N coupling might be palladium mediated. Further studies will investigate the role of excess of iodine on **8** as well as conduct experiments on similar substrates such as 2-*p*-(tolyl)-pyridine.

Attempted Fluorination of 2-(difluoro(phenyl)methyl)pyridine

In an attempt to generate a palladium(IV) fluoride intermediate **33** using the substrate benzylic CF$_3$ group as a source of nucleophilic fluorine (Scheme 17) we decided to use 2-(difluoro(phenyl)methyl)pyridine as a donor of C-H bond and fluorine atom at the same time. The new compound 2-(difluoro(phenyl)methyl)pyridine **35** (82%) was prepared by treatment of readily available benzoyl pyridine **34** (see the Supporting Information) with bis(2-methoxyethyl)amino]sulfur trifluoride (Deoxofluor®) at 90˚C (Scheme 16). **35** is a liquid stable under air, which does not hydrolyze readily upon addition of water.
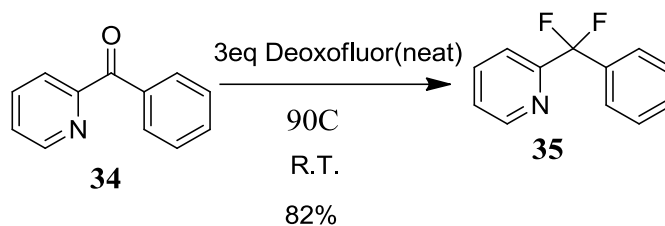
Scheme 16. Fluorination of 2-benzoylpyridine using Deoxofluor®.

We hypothesized that due to the proximity of benzylic fluorine to the five-coordinate palladium(IV) center generated upon oxidation of **36** with aqueous hydrogen peroxide water would displace fluoride with the assistance of the Pd(IV) center, converting into an intermediate **33**. To begin, an acetonitrile solution of **36** was combined with hydrogen peroxide at 25ºC. After 5 minutes reductive elimination occurred to form **38** (Scheme 17); no **39** was detected.
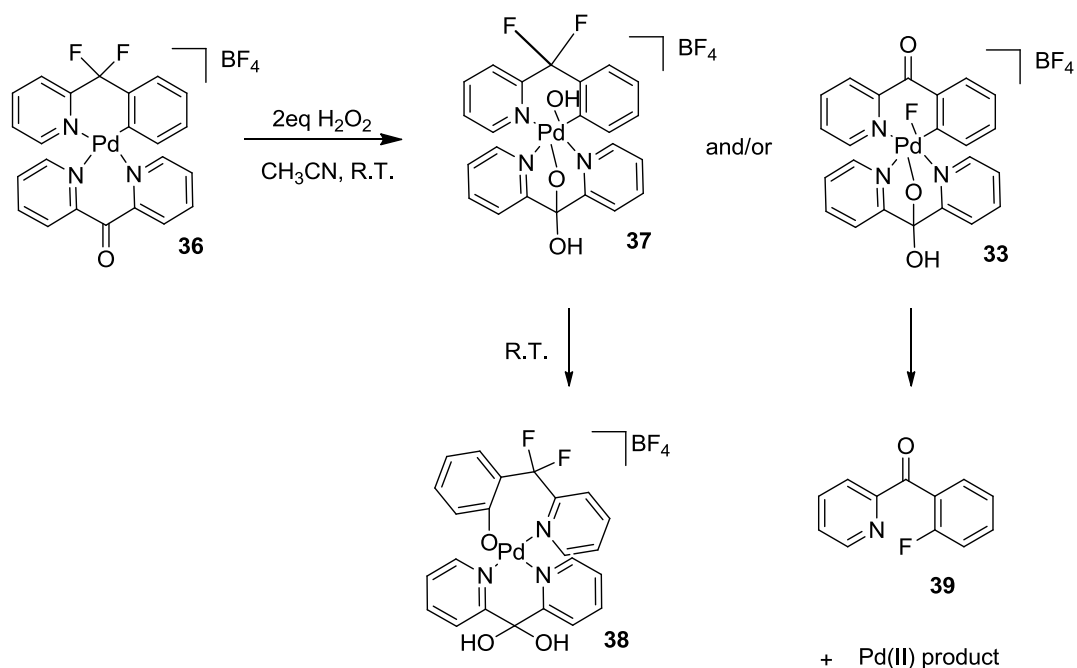
Scheme 17. The oxidative addition and reductive elimination of 2-(difluoro(phenyl)methyl)pyridine palladium complex **36**.

After an acidic work up only compound **39a** was isolated (70%) and characterized by ^{1}H NMR spectroscopy and ESI-MS (Scheme 18).
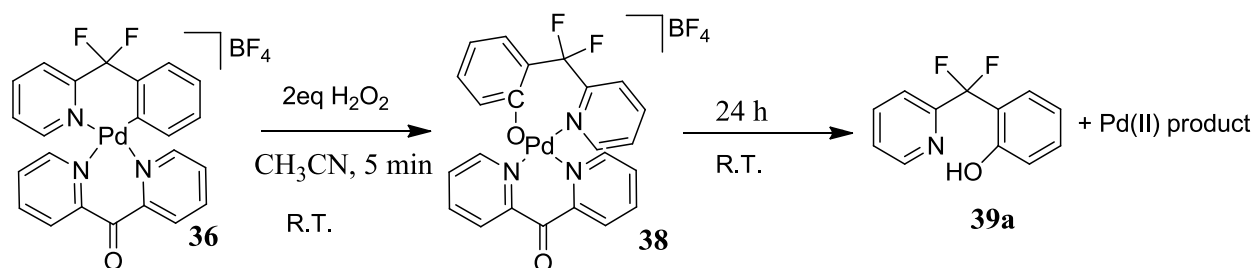
Scheme 18. Hydroxylation of difluromethylated complex **36**.

The involvement of Pd(IV) species during C−O bond formation is also suggested by the reaction of **36** with urea hydrogen peroxide, which gives almost stoichiometric amounts of C-O product **39a** suggesting an oxidative addition step followed by C-O elimination. The coordination versatility of F⁻(AgF and TBAF) is

currently being explored for C-F bond formation instead of water facilitating the reaction.

Oxidative C(sp^3)-H chlorination of 8-methylquinoline

In past years, transition-metal-catalyzed carbon-chlorine bond formation has attracted considerable attention for its broad applications in organic synthesis.[64] In general, transition metals[40-45] are often used to activate the inert C-H bonds. To determine suitable reaction conditions for the catalytic C-H functionalization of 8-methylquinoline, we investigated a model oxidative chlorination system similar to one developed by Vedernikov and coworkers.[45] Our goal here was to show that the original system can be modified to allow installation of functional groups different from the original OAc, such as Cl and then move on to the development of much more valuable catalytic aerobic C-H fluorination and/or iodination. Hence, we consider the chlorination system as a model one. The results are displayed in scheme 19 below.
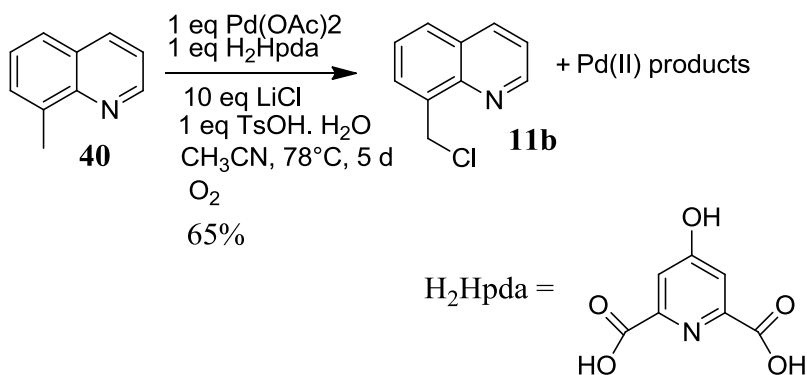
Scheme 19. The one pot synthesis of 8-chloromethylquinoline.

The stoichiometric palladium mediated conversion of 8-methylquinoline to 8-chloromethylquinoline using dioxygen as an oxidant was investigated. 8-

methylquinoline was treated with palladium acetate, dioxygen, 4-hydroxo-2,6-pyridinedicarboxylic acid (H₂hpda), lithium chloride, and *p*-toluenesulfonic acid in acetonitrile at 78 °C for 5 days (Scheme 19). NMR analysis of the reaction mixture revealed the formation of **11b** produced in 65% yield along with other reaction products identified as 8-quinolylmethanol and corresponding aldehyde. The yield of **11b** was only 25% in the absence of *p*-toluenesulfonic acid.

We propose that O_2 as an oxidant and H_2Hpda as supporting ligand enable formation and functionalization of Pd^{II}-C bond leading to 8-quinolylmethanol and, presumably, some 8-quinolylmethyl Pd^{IV} derivatives. Chloride anion then attacks the Pd^{IV}-C bond of the latter to produce **11b** (compare to Scheme 6). Another (major) pathway leading to **11b** may involve reaction of 8-quinolylmethanol and LiCl that requires the presence of a strong acid such as *p*-toluenesulfonic acid. The use of O_2 as an oxidant in combination with lithium chloride to produce chlorinated products has, as far as we can tell, not been previously reported.

Oxidative C(sp^3)-H fluorination of 8-methylquinoline

To an acetonitrile(wet) solution containing 8-methylquinoline were added 1 equivalent of palladium Tetrakis(acetonitrile)palladium(II) tetrafluoroborate (Pd(BF₄)) (See Supplemental), which was commercially available, followed by 6 equivalence of Deoxofluor® at 90°C and stirred for 24 hrs to form **11a**(5%). While HF is formed due to the presence of water, **11a** was characterized using Teflon coated NMR tubes and conventional ¹H NMR techniques. Notably, using 20 mol% of Pd(BF4) yields 11% of **11a** after 24 hrs. The results are displayed in scheme 20

below. The stoichiometric palladium mediated conversion of 8-methylquinoline to 8-(fluoromethyl)-quinoline using Deoxofluor® was investigated.

1 eq Pd(CH$_3$CN)$_4$(BF4)$_2$

6 eq Deoxofluor
1 mL of CH$_3$CN(wet)
90°C, 24hr, O$_2$ (1 atm)

11a
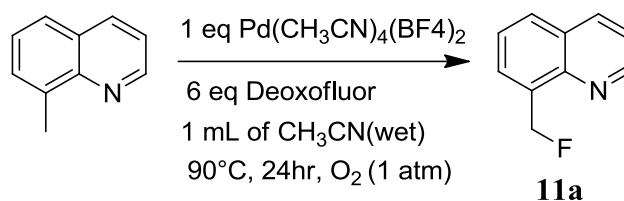
Scheme 20. The one pot synthesis of 8-chloromethylquinoline.

Nucleophilic, aliphatic fluorination via palladium(IV) intermediates has not yet been established, but metal catalysis based on palladium alkyl complexes with electrophilic fluorinating reagents can be used to make C-F bonds selectively.[31] Better prediction of the reactivity of well-defined transition metal complexes has supported the advances in nucleophilic aromatic fluorination. This work has proven that palladium-mediated C-F bond formation is also viable in the presence of a fluoride source such as AgF and benign oxidant (H$_2$O$_2$ or O$_2$), albeit in low to moderate yields (11-54%). Readily available fluorinating agents such as AgF, CuF$_2$, and Deoxofluor® are arguably among simple sources of nucleophilic fluorine that can be employed in this reaction. Still, whenever fluoride is used, its basicity and the basicity of the transition metal complexes derived from it are often problematic, because water and protic functional groups inhibit the desired reactivity. Future nucleophilic fluorination reactions may benefit from the availability of even less ionic/more covalent metal fluorides such as TlF and HgF$_2$. The combination of palladium(II) precursors, benign oxidant, and 4-*tert*-Butyl-2,6-dimethylphenylsulfur trifluoride will be also probed as a reagent for aerobic C-H fluorination.

Summary

In summary, this paper reports a detailed investigation of a di(2-pyridyl)ketone ligand − enabled Pd-mediated oxidative C(sp^3)−H functionalization using aqueous hydrogen peroxide, an environmentally benign reagent, as the oxidant. The substrates used involve 8-methylquinoline with reactive benzylic C(sp^3)-H bonds and 4-amino-2-*tert*-butylpyridine featuring non-activated C(sp^3)-H bonds. The reaction sequence involves (1) preparation of the dpk-supported Pd(II) hydrocarbyl species via C-H activation of a suitable substrate, (2) oxidation of the resulting dpk–supported Pd(II) complexes with hydrogen peroxide to form a mixture of Pd(IV) derivatives, (3) attack of a nucleophile at the Pd(IV)-bound alkyl carbon, and (4) organic product release. The feasibility of each of these steps is supported by separate experiments. In particular, the preparation and characterization of several new dpk-supported palladium(IV) aryl and alkyl monohydrocarbyl complexes is reported. The reactivity of the resulting C(sp^3)-Pd^{IV} bonds toward various nucleophiles (OH⁻, F⁻, Cl⁻, Br⁻, I⁻) is demonstrated.

A key feature of the investigated systems is the use of the semilabile tridentate 1-hydroxo-1,1-di(2-pyridyl)methoxide ligand derived from a hydrated di(2-pyridyl)ketone (dpk). The dpk ligand facilitates the Pd^{II} oxidation by H$_2$O$_2$ to form a stabilized octahedral Pd^{IV} species and, at the same time, allows for the subsequent facile C-X bond reductive elimination from the Pd^{IV} center facilitated.

The mild conditions necessary for this C-H functionalization sequence via palladium(IV) intermediates renders this process attractive for applications in catalytic C−H functionalization processes mediated by high oxidation state palladium.

Future investigations are focused on expanding this reactivity toward other nucleophiles and to conducting detailed investigations of the factors governing site selectivity in these transformations.

Future Directions

Halogenation of Oxazoline derivatives

Future studies will be directed toward the development of new Pd-coordinated tridentate facially chelating catalysts, We have reported NMR spectroscopic and X-ray diffraction evidence of the in situ formation of Pd(IV) monohydrocarbyl alkyl complexes of the composition (DPK)Pd(alkyl). These complexes were prepared by reacting dimeric cyclopalladated complexes with DPK in methanol. Inspired by the results of these groups, future studies are directed toward study of the reactions of involving oxazoline palladium(II) precursors under different conditions; the proposed scheme are presented below(Scheme 21)
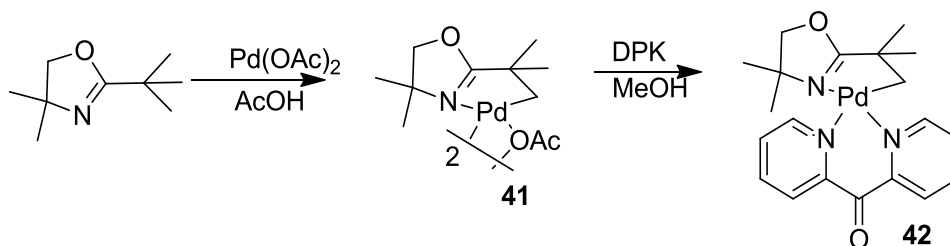
Scheme 21. Synthesis of Oxazoline palladacycle and palladium(II) DPK complex.

Reaction of the oxazoline palladacycle[62] **41** with a Commercial (Sigma-Aldrich Co.) source of DPK in methanol will be part of a study to elucidate the mechanism of C-H functionalization using benign oxidants in acetonitrile. In order to determine whether this transformation is applicable to other cyclopalladated C(sp^3)-X functionalization, **42**, will be subjected to the same reaction conditions as reported in the 4-amino-2-*tert*-butylpyridine system.

Homocoupling of 2-*p*-(tolyl)-pyridine

Transition metal mediated coupling–cyclization processes, of which many rely on palladium catalysis and involve in situ generation of palladium(IV) intermediates, have proven to be an efficient and versatile way of constructing carbocyclic and heterocyclic structures. Recently, cyclization of C–C triple bond with a wide variety of nucleophiles, including N, O, and S nucleophiles, has been studied extensively[45-60] and proved to be an efficient method for intramolecular cyclization. This approach is particularly attractive as it offers the advantage of further transformation of the iodide functional group of the resulting compound into other substituents that is not often feasible via organocatalyst tandem coupling–cyclization method in a single pot.

This has been well exemplified by the recent synthesis of a wide array of heterocycles. Notably, while studying the Pd-catalyzed conversion of benzo[*h*]quinoline to 10-Iodobenzoquinoline,[63] we discovered an unexpected homocoupling of benzo[*h*]quinoline followed by subsequent C-N formation to yield **28** after 3 weeks at room temperature. To a solution of acetonitrile(20% aq) containing **8(BF₄)** were added 5 equivalence of I_2 to form **26** in 24hrs, followed formation of **28** after 3 weeks. To understand the tandem process of these systems 2-*p*-(tolyl)-pyridine will be chosen to test similar reactivity. We envision that 2-*p*-(tolyl)-pyridine palladium(II) DPK complex **2(BF₄)** will undergo similar cyclization.

Oxidative Chlorination of 8-methylquinoline

The development of metal-catalyzed methods for converting C-(sp^3)-H bonds into C–Cl bonds using dioxygen as a terminal oxidant remains a grand challenge in organometallic chemistry. Methods for the selective aerobic oxygenation of unactivated primary C–H bonds in the presence of weaker benzylic, allylic, secondary, or tertiary C–H bonds remain particularly elusive. Over the past decade Pd-catalyzed ligand-directed C–H oxidation has emerged as a powerful approach to achieve C-(sp^3)-H acetoxylation, alkoxylation, and hydroxylation. However, the oxidants used in these transformations are most typically reagents such as PhI(OAc)$_2$, IOAc, or K$_2$S$_2$O$_8$, which have the significant disadvantages of have poor atom economy, high cost, the formation of stoichiometric byproducts, and/or moderate functional group tolerance.

Recent elegant studies by Vedernikov and coworkers have shown that it is possible to address this challenge through the selection of pyridine dicarboxylic acid derivatives. However, these successful examples of aerobic Pd-catalyzed ligand-directed C–H functionalization are far from a general solution, because they exhibit a narrow substrate scope. The Pd(OAc)$_2$-mediated C–H chlorination of 8-methylquinoline was selected as a test reaction, since we have reported it to proceed efficiently with oxidants like dioxygen. With dioxygen as an oxidant, this transformation provided moderate yields of C-Cl product **11b**(65%) as described in scheme 14. The following 8-methylquinoline derivatives will be chosen to probe the reactivity of electron withdrawing and donating substituents.

Fluorination of Benzo[*h*]quinoline and 4-amino-2-*tert*-butylpyridine

Based on our findings, the more "covalent character" of the fluoride source the less interference from water. Transition-metal-mediated cross coupling between an electrophile and a nucleophile may be a more general approach for C-F bond formation, because it does not require an electrophilic halogenating reagent. Fluoride sources such as HgF_2 and TlF will be used as possible fluorinating reagents. Based on the Hg electronegativity (1.50, Pauling scale), HgF_2 is expected to have a higher "covalent character" than AgF (Ag electronegativity is 1.44). The second compound may be less covalent (Tl electronegativity is 1.70), and we will check if that diminishes its reactivity compared to AgF.

Appendices

Supporting Information for:

Oxidative Functionalization of Pd[II]-C Bonds Using Hydrogen Peroxide: Exploring the Potential of the Pd[II] Hydrocarbyl – dpk System

Dave Jenkins

Department of Chemistry and Biochemistry, University of Maryland, College Park, MD 20742

Table of Contents

Materials and Methods

All reactions were carried out under ambient atmosphere unless otherwise noted. Dipyridyl ligands and oxazoline derivatives were prepared using literature procedures.[8-10] Commercial reagents used are available from Acros, Aldrich, Pressure Chemicals, Alfa Aesar, and were used without further purification. NMR spectra were obtained on a Bruker AVANCE 400 or Bruker DRX-500 (400 MHz for ^{1}H and ^{19}F), or a Bruker DRX-500 (500 MHz for ^{13}C NMR). [1]H and ^{13}C chemical shifts are reported in ppm and referenced to solvent resonance peaks. ESI-MS analysis was performed on a JEOL AccuTOF-CS instrument. Elemental analysis was obtained from Columbia Analytical Services, Tucson, AZ.

Experimental Data
Experimental Procedures and Compound Characterization

General Procedure

Conversion of palladium(II) complexes into various salts. Complex **8**, **10**, **17**, and **36** (30 mg, 0.07 mmol) were dissolved in 50 mL of water at 25°C. Addition of 5 eq. of NaX (X= BF_4, Ph_4 BAr^F_4, PF_6, OTf) led to immediate formation precipitate. The resulting precipitate was filtered and washed with hexanes.

Synthesis of 8-methylquinolyl Palladium(II) Acetato Complex (10a)

10a
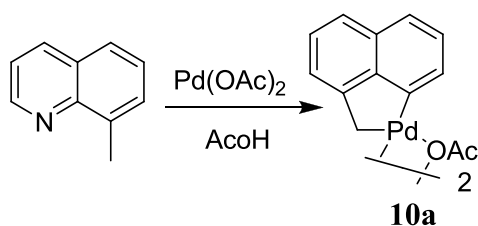
Complex **1** was prepared according to a published procedure. To 8-methylquinoline (1.00 g, 5.58 mmol) in AcOH (75 mL) at 25°C was added $Pd(OAc)_2$ (1.25 g, 5.58 mmol). After 2 h, the precipitate was isolated by filtration and washed sequentially with MeOH (50 mL) and Et2O (50 mL). The solid was dissolved in CH_2Cl_2 (250 mL) and filtered through a plug of Celite. Solvent was removed *in vacuo* to afford a yellow solid **10a** (88% yield). Compared to literature reference.[65]

Synthesis of 8-methylquinolyl Palladium(II) Di-2-pyridylketone Complex (10)
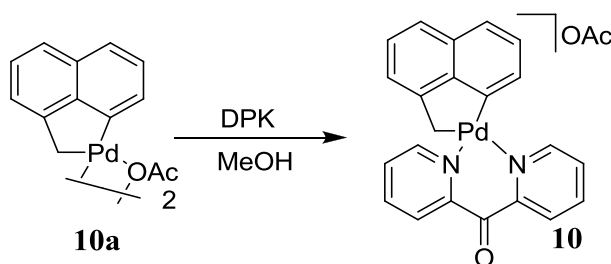
Di-(2-pyridyl) ketone (199 mg, 1.00 mmol) was dissolved in 10 mL of MeOH in a vial and the solution was added dropwise to a stir-bar equipped round bottom flask containing acetato palladium complex **10a** (315 mg, 1.05 mmol) in 10 mL of MeOH at 25°C. The reaction mixture was stirred at 25°C for 24h, and the solvent was removed *in vacuo*. To the solid residue was suspended in 10 mL of dichloromethane, followed by 50 mL of hexanes. The precipitate was filtered and washed with 10 mL of hexanes to afford light yellow solid **10**(80%). ^{1}H NMR (400 MHz, CD_2Cl_2, 22°C, δ ppm): 3.67(s, 2H), 7.54 (dd, *J*= 8.3, 5.2 Hz, 1H), 7.61 (t, *J*= 7.5 Hz, 1H), 7.69 (d, *J*= 7.1 Hz, 1H), 7.75 (d, *J*= 8.0 Hz, 1H), 7.88 − 7.79 (m, 1H), 8.12 − 8.04 (m, 1H),

8.18 – 8.11 (m, 2H), 8.20 (d, $J= 7.7$ Hz, 1H), 8.26 (t, $J= 7.8$ Hz, 1H), 8.33 (t, $J= 8.3$ Hz, 1H), 8.44 (d, $J= 8.3$ Hz, 1H), 8.82 (d, $J= 5.1$ Hz, 1H), 9.05 (d, $J = 5.1$ Hz, 1H). ^{13}CNMR 32.89 (s), 122.52 (s), 125.06 (s), 126.52 (s), 126.52 (s), 127.64 (s), 129.37 (d, $J = 21.0$ Hz), 130.39 (s), 139.97 (s), 141.42 (d, $J = 8.9$ Hz), 150.06 (s), 150.95 (s), 152.40 (s), 153.79 (s). Mass Spectrometry: ESI-MS (*m/z*): Anal. Calcd for $C_{21}H_{16}$ $BF_4N_3O^{106}Pd \cdot CH_3CN \cdot H_2O$: C, 47.69; H, 3.38; N, 7.79; found: C, 48.47; H, 3.90; N, 7.07.

Synthesis of 8-methylquinolylpalladium(IV) Hydroxo Di-2-pyridylketone Complex (10BAr$^F_4$)
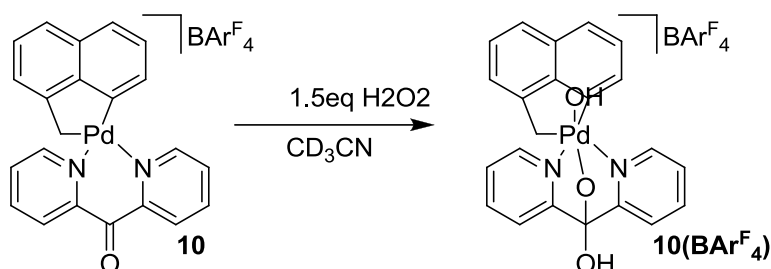
Complex **2** (30 mg, 0.06 mmol) was dissolved in 1 mL of CD$_3$CN at 25°C. Addition of H$_2$O$_2$ (14 μliters, 0.09 mmol) led to immediate formation of a deep yellow solution. The reaction mixture was stirred at 25 °C for 2 hr, to afford dark orange solution **10**(80%).^{1}H NMR is convoluted difficult to isolate major species in solution. Mass Spectrometry: ESI-MS (*m/z*): Calcd for $[C_{22}H_{18}N_3O_3^{106}Pd]$, 464.04. Found 463.95.

Synthesis of 4-amino-2-*tert*-butylpyridyl Palladium(II) Acetato Complex (16a)
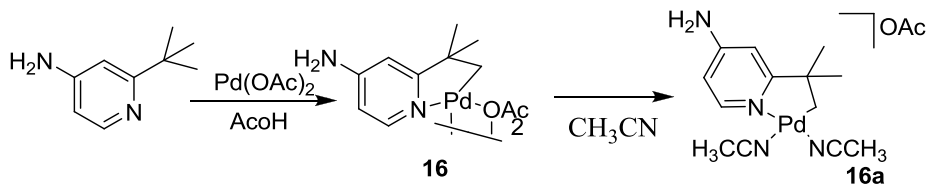


 To 2-(tert-butyl)pyridin-4-amine (200 mg, 1.32 mmol) in AcOH (75 mL) at 98ºC was added Pd(OAc)$_2$ (0.297 mg, 1.32 mmol). After 8 h, the resulting suspension was isolated by filtration and *in vacuo*.). The solid residue was washed with CH$_3$CN and filtered. Solvent was removed *in vacuo* to afford the title complex as an orange solid **16a**(82%).^{1}H NMR(400 MHz, CD$_3$OD, 22°C, δ ppm (**3**)): 1.31 (s, 9H), 2.07 (s, 3H), 6.36 (d, $J = 3.5$ Hz, 1H), 6.55 (s, 1H), 8.22 (d, $J= 5.5$ Hz, 1H).^{13}CNMR (400 MHz, CD$_3$OD, 22°C, δ ppm (**16a**)): 20.91 (s), 28.04 (s), 29.71 (s), 35.55 (s), 105.16 (s), 107.18 (s), 107.58 (s), 117.21 (s), 117.21 (s), 139.96 (s).

Synthesis of 4-amino-2-*tert*-butylpyridyl Palladium(II) Di-(2-pyridyl) Ketone Complex (17)
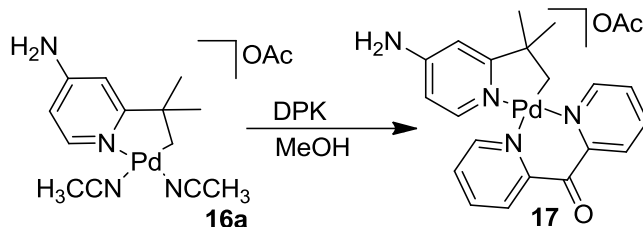
Di-(2-pyridyl) ketone (193 mg, 1.05 mmol) was dissolved in 10 mL of MeOH in a vial and the solution was added dropwise to a stir-bar equipped round bottom flask containing acetato palladium complex **16a** (319 mg, 1.00 mmol) in 10 mL of MeOH at 25°C. The reaction mixture was stirred at 25°C for 24h, and the solvent was removed *in vacuo*. To the solid residue was suspended in 10 mL of dichloromethane, followed by 50 mL of hexanes. The precipitate was filtered and washed with 10 mL of hexanes to afford light yellow solid **17**(75%).^{1}H NMR(400 MHz, CD$_3$OD, 22°C, δ ppm(**17(BF$_4$)**)): 1.28 (s, 1H), 1.60 (s, 2H), 1.93 (d, *J*= 8.4 Hz, 1H), 1.93 (d, *J*= 8.4 Hz, 1H), 2.49 (d, *J*= 8.2 Hz, 1H), 6.33 (dd, *J*= 6.5, 2.5 Hz, 1H), 6.43 (d, *J* = 2.5 Hz, 1H), 7.41 (dd, *J*= 13.1, 6.9 Hz, 1H), 7.48 (dt, *J*= 20.8, 10.3 Hz, 1H), 8.00 (ddd, *J*= 19.8, 14.8, 7.7 Hz, 4H), 8.66 − 8.58 (d, *J*= 5.3 Hz, 1H), 8.74 (d, *J*= 5.3 Hz, 1H).^{13}CNMR (400 MHz, CD$_3$OD, 22°C, δ ppm): 29.40 (s), 104.57 (s), 107.60 (s), 123.74 (s), 124.40 (s), 124.91 (s), 125.39 (s), 127.01 (s), 128.10 (s), 135.27 (s), 138.72 (s), 139.04 (s), 146.67 (s), 147.69 (s), 149.05 (s), 150.77 (d, *J* = 17.6 Hz), 152.16 (s), 154.35 (s). Mass Spectrometry: ESI-MS (*m/z*): Calcd for [C$_{20}$H$_{21}$N$_4$O^{106}Pd], 439.08. Found 439.03.

Synthesis of 4-amino-2-*tert*-butylpyridyl Palladium(IV) Hydroxo Di-(2-pyridyl) Ketone Complex (18)
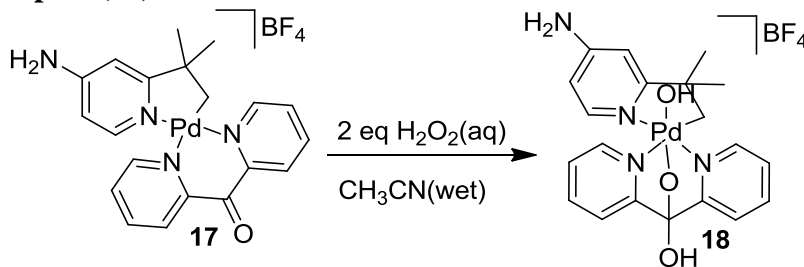
Complex **17** (30 mg, 0.07 mmol) was dissolved in 1 mL of CD$_3$CN at 25°C. Addition of H$_2$O$_2$ (15 μliters, 0.14 mmol) led to immediate formation of a deep yellow solution. The reaction mixture was stirred at 25°C for 2 hr, to afford dark orange solution **18**(80%). No ^{13}C NMR was acquired due to low stability of **18**. ^{1}H NMR (400 MHz, CD$_3$OD, 22°C, δ ppm): 1.46 (s, 3H), 1.52 (s, 3H), 4.56 (d, *J*= 5.7 Hz, 1H), 4.70 (d, *J*= 5.4 Hz, 1H), 5.73 (s, 2H-NH$_2$), 6.57 (s, 1H-Pd-OH), 6.57 (s, 1H-C-OH), 7.51 (m, 2H), 7.60 (m, 1 H), 7.68 (d, *J*= 8.0 Hz, 1H), 7.72 (d, *J*= 6.6 Hz, 1H), 7.83 (d, *J*= 7.8 Hz, 1H), 8.10 − 7.99 (m, 1H), 8.49 (d, *J*= 5.1 Hz, 1H), 9.00 (d, *J*= 2.2 Hz, 1H) ^{1}H NMR (400 MHz, DMSO, 22°C, δ ppm): 1.42 (s, 3H), 1.52 (s, 3H), 4.37 (d, *J*= 5.5 Hz, 1H), 4.66 (d, *J*= 5.1 Hz, 1H), 6.60 − 6.52 (m, 2H-C-OH,Pd-OH), 7.09

(s, 2H-NH$_2$), 7.66 – 7.61 (m, 1H), 7.76 – 7.66 (m, 3H), 7.89 (d, $J=$ 7.7 Hz, 1H), 8.16 (dd, $J=$ 15.5, 7.7 Hz, 2H), 8.35 (s, 1H), 8.60 (d, $J=$ 5.3 Hz, 1H), 9.16 (t, $J=$ 9.8 Hz, 1H), 9.15 (d, $J=$ 4.6 Hz, 1H). Mass Spectrometry: ESI-MS (*m/z*): Calcd for [C$_{20}$H$_{21}$N$_4$O^{106}Pd], 473.08. Found 473.04.

Synthesis of 4-amino-2-*tert*-butylpyridine Palladium(IV) Fluoro Di-(2-pyridyl) Ketone Complex (19)
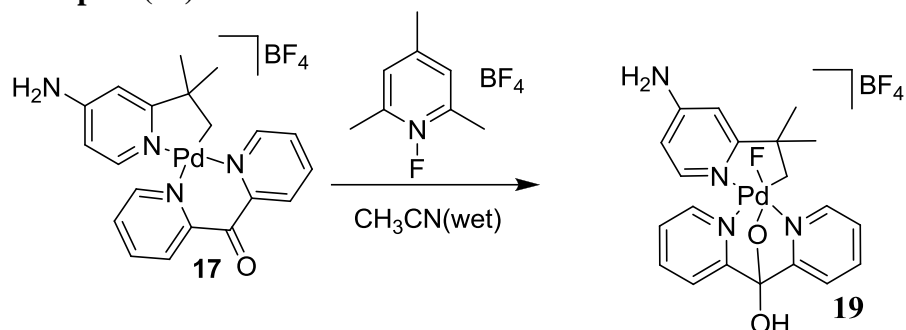
A solution of complex 17 (30 mg, 1.00 mmol) in 2 mL of CH$_3$CN at 25°C were treated with 1-Fluoro-2,4,6-trimethylpyridinium tetrafluoroborate (77 mg, 5 mmol). After stirring for 5 min, the resulting suspension afforded an orange solution 19(91%). No ^{13}C NMR was acquired due to low stability of 19. ^{1}H NMR (400 MHz, CD$_3$CN, 22°C, δ ppm): 1.43 (s, 3H), 1.56 (s, 3H), 4.96 4.81 (d, $J=$ 3.0 Hz, 1H), 4.94 (dd, $J=$ 13.4, 5.2 Hz, 1H), 5.80 (s, 2H-NH$_2$), 6.55 (dd, $J=$ 6.9, 2.7 Hz, 1H), 6.64 (d, $J=$ 2.7 Hz, 1H), 7.61 – 7.53 (m, 2H), 7.72 (d, $J=$ 7.9 Hz, 2H), 7.91 (d, $J=$ 7.8 Hz, 2H), 8.11 (td, $J=$ 7.7, 1.4 Hz, 3H), 8.43 (d, $J=$ 6.1 Hz, 2H), 9.06 – 9.01 (m, 1H) ^{1}H NMR (400 MHz, DMSO-*d6*, 22°C, δ ppm):   1.40 (s, 3H), 1.51 (s, 3H), 4.81 (d, $J=$ 3.0 Hz, 1H), 4.94 (dd, $J=$ 13.4, 5.2 Hz, 1H), 6.62 – 6.50 (m, 2H), 7.18 (s, 1H), 7.65 (t, $J=$ 6.4 Hz, 1H), 7.73 (dd, $J=$ 7.1, 4.1 Hz, 1H), 8.25 – 8.14 (m, 1H), 8.53 (d, $J=$ 5.4 Hz, 1H), 9.03 (s, 1H), 9.12 (d, $J=$ 4.9 Hz, 1H), ^{19}F NMR (400 MHz, CD$_3$CN, 22°C, δ ppm): -320.85 (d, $J=$ 13.4 Hz).

Synthesis of Benzo[*h*]quinolinyl Palladium(II) Acetato Complex (8a)
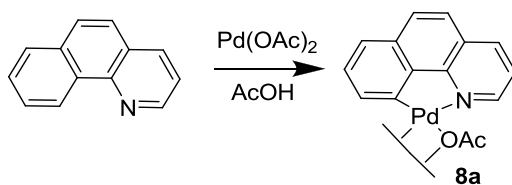
Complex **8a** was prepared according to a published procedure.[66] A solution of benzo[*h*]quinoline (179 mg, 1.00 mmol) in 100 mL of acetic acid at 25°C were treated with palladium acetate (224 mg, 1.00 mmol, 1.00 equiv). After stirring for 24 h, the resulting suspension was filtered through Celite and filtrate was allowed to crystallize overnight at 25°C to afford orange solid **8a**(80%).^{1}H NMR (400 MHz, CDCl$_3$, 22°C, δ ppm): 2.38 (s, 3H), 6.46 (dd, $J=$ 7.5, 5.0 Hz, 1H), 6.97 (d, $J=$ 9.0 Hz,

1H), 7.08 (dd, *J*= 7.0, 1.5 Hz, 1H), 7.24-7.18 (m, 3H), 7.43 (dd, *J*= 8.0, 1.5 Hz, 1H), 7.80 (dd, *J*= 5.5, 1.5 Hz, 1H).

Synthesis of Benzo[*h*]quinolinyl Palladium(II) Di-(2-pyridyl) Ketone Complex (8)
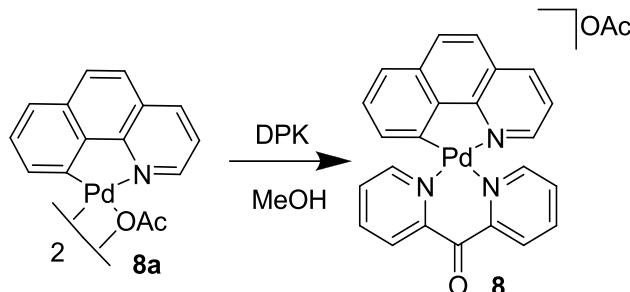
Di-(2-pyridyl) ketone (193 mg, 1.05 mmol) was dissolved in 10 mL of MeOH in a vial and the solution was added dropwise to a stir-bar equipped round bottom flask containing acetato palladium complex **8a** (343 mg, 1.00 mmol) in 10 mL of MeOH at 25°C. The reaction mixture was stirred at 25°C for 3h, and the solvent was removed *in vacuo*. To the solid residue was suspended in 10 mL of dichloromethane, followed by 50 mL of hexanes. The precipitate was filtered and washed with 10 mL of hexanes to afford light yellow solid **8**(85%). ^{1}H NMR (400 MHz, CD$_3$OD, 22°C, δ ppm): 1.72 (s, 3H), 6.86 (d, *J*= 7.9 Hz, 1H), 7.31 (t, *J*= 8.2 Hz, 1H), 7.59-7.48 (m, 5H), 7.70 (d, *J*= 8.9 Hz, 1H), 8.06 (m, 4H), 8.32 (d, *J*= 5.3 Hz, 1H), 8.40 (d, *J*= 8.4 Hz, 1H), 8.83 (d, *J*= 5.8 Hz, 1H), 8.92 (d, *J*= 5.3 Hz, 1H)^{13}C NMR (400 MHz, CD$_3$OD, 25 °C, δ): 23.6, 99.9, 122.7, 124.0, 124.2, 124.4, 124.5, 126.7, 129.9, 128.2, 129.4,129.9, 131.8, 134.5, 139.3, 141.1, 141.2, 141.9, 149.5, 152.1, 152.8, 155.5, 155.8, 158.5, 159.1, 179.5. Mass Spectrometry: ESI-MS (*m/z*): Anal. Calcd for C$_{26}$H$_{19}$N$_3$O$_3$^{106}Pd·2H$_2$O: C, 55.38; H, 4.11; N, 7.45; found: C, 55.68; H, 3.71; N, 7.41.

Synthesis of Benzo[*h*]quinolinyl Palladium(IV) Hydroxo Di-(2-pyridyl)
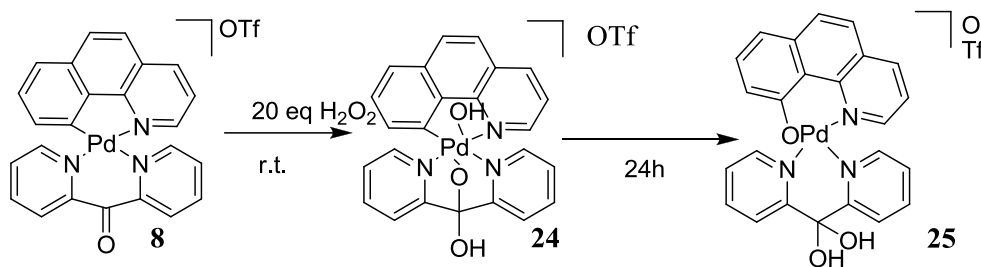
Complex(24)
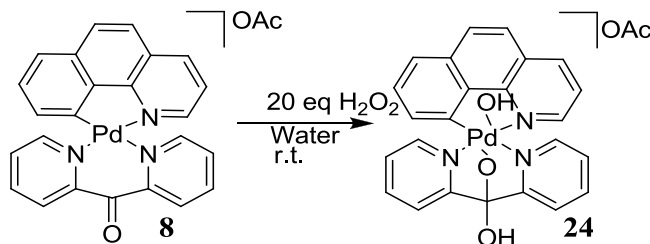
Complex **8** (10 mg, 0.02 mmol) was dissolved in 2 mL of D$_2$O at 25°C. Addition of H$_2$O$_2$ (20 μliters, 0.4 mmol) led to immediate formation of a deep yellow solution. The reaction mixture was stirred at 25°C for 15 min, followed by the addition of NaBF$_4$ (2 mg, 1.00 mmol, 1.00 equiv). The resulting precipitate was filtered and

washed with 0.15 mL of D$_2$O at 0 °C to afford dark yellow solid **24**(90%). No ^{13}C NMR was acquired due to low stability of **24**. ^{1}H NMR (400 MHz, D$_2$O, 22°C, δ ppm): 1.75f (s, 3H), 7.04 (d, *J*= 8.2 Hz, 1H), 7.57 (t, *J*= 7.8 Hz, 1H), 7.71 (dd, *J*= 5.8 , 2.5 Hz, 1H), 7.8 (ddd, *J*= 6.8, 6.8, 7.1 Hz, 2H), 8.01-7.85 (m, 5H), 8.21 (td, *J*= 8.0, 8.2 Hz, 1H), 8.27 (td, *J*= 8.0, 8.2 Hz, 1H), 8.53 (d, *J*= 6.7 Hz, 1H), 8.68 (d, *J*= 8.2 Hz, 1H), 8.82 (d, *J*= 6.7 Hz, 1H), 9.09 (d, *J*= 5.7 Hz, 1H); ^{1}H NMR (400 MHz, DMSO–*d6*, 22°C, δ ppm): 7.38 (d, *J*= 7.6 Hz, 1H), 7.43 (t, *J*= 7.8 Hz, 1H), 7.46 (d, *J*= 6.8 Hz, 1H), 7.66 (t, *J*= 7.8 Hz, 1H), 7.72 (t, *J*= 7.8 Hz, 1H), 7.87-7.73 (m, 2H), 8.07-7.94 (m, 2H), 8.19-8.06 (m, 3H), 8.29 (t, *J*= 7.8 Hz, 1H), 8.49 (d, *J*= 5.9 Hz, 1H), 8.71 (d, *J*= 6.2 Hz, 2H).

To confirm the formation of the Pd-OH and C-OH bond in **24** the oxidation of **8** using H$_2$O$_2$ was replicated with the exception of using H$_2$O as solvent instead of D$_2$O. The corresponding ^{1}H NMR is as follows:

^{1}H NMR (400 MHz, DMSO–*d6*, 22°C, δ ppm): 7.38 (d, *J*= 7.6 Hz, 1H), 7.43 (t, *J*= 7.8 Hz, 1H), 7.46 (d, *J*= 6.8 Hz, 1H), 7.66 (t, *J*= 7.8 Hz, 1H), 7.72 (t, *J*= 7.8 Hz, 1H), 7.87-7.73 (m, 2H), 8.07-7.94 (m, 2H), 8.19-8.06 (m, 3H), 8.29 (t, *J*= 7.8 Hz, 1H), 8.49 (d, *J*= 5.9 Hz, 1H), 8.67 (s, 1H) 8.71 (d, *J*= 6.2 Hz, 2H), 9.35 (s, 1H); ^{1}H NMR (400 MHz, CD$_3$OD, 22°C, δ ppm): 2.1 (s, 3H), 7.42 (d, *J*= 8.2 Hz, 1H), 7.48 (d, *J*= 8.2 Hz, 1H), 7.66 (t, *J*= 8.6 Hz, 2H), 7.79-7.71 (m, 2H), 8.01-7.91 (m, 3H), 8.15-8.09 (m, 2H), 8.23-8.19 (m, 2H), 8.35 (d, *J*= 6.4 Hz, 1H), 8.65 (d, *J*= 8.2 Hz, 1H), 8.86 (d, *J*= 6.4 Hz, 1H). Mass Spectrometry: ESI-MS (*m/z*): Calcd for [C$_{24}$H$_{18}$N$_3$O$_3$[106]Pd], 502.0383. Found 502.0382.

Oxapalladacycle of Benzo[*h*]quinolinyl Palladium(II) Di-(2-pyridyl) Complex (25)


Complex **7** (10 mg, 0.02 mmol) was dissolved in 2 mL of CD$_3$CN at 25°C. Addition of H$_2$O$_2$ (20 μliters, 0.4 mmol) led to immediate formation of a deep yellow solution. The reaction mixture was stirred at 25°C for 24 h, to afford dark orange solid **25**(40%). ^{1}H NMR (400 MHz, CD$_3$CN, 22°C, δ ppm): 6.98 (t, *J*= 7.5 Hz, 1H), 7.20 − 7.14 (m, 4H), 7.59 − 7.52 (m, 2H), 7.67 − 7.59 (m, 2H), 8.07 − 7.94 (m, 4H), 8.73 − 8.67 (m, 2H). Mass Spectrometry: ESI-MS (*m/z*): Calcd for [C$_{24}$H$_{18}$N$_3$O$_3$[106]Pd], 502.04. Found 502.03.

Synthesis of 2-(difluoro(phenyl)methyl)pyr..idyl Palladium(II) Acetonitrile complex (36a)
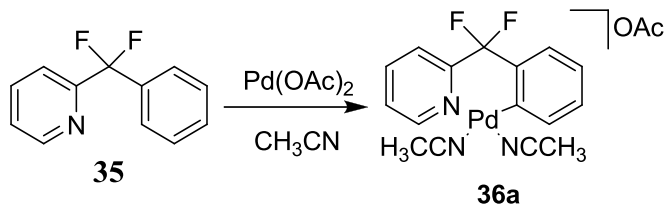
To 2-(difluoro(phenyl)methyl)pyridine (500 mg, 2.43 mmol) in CH_3CN (100 mL) at 65ºC was added $Pd(OAc)_2$ (546 mg, 2.43 mmol) and stirred for 24 hrs. After 24 hrs, the resulting suspension was evaporated *in vacuo* to afford title compound as a brown solid **36a**(82%). ^{1}H NMR (400 MHz, CD_3CN, 22°C, δ ppm): 7.43 − 7.36 (m, 1H), 7.57 (ddd, *J*= 5.1, 2.3, 1.1 Hz, 2H), 7.74 − 7.66 (m, 2H), 7.86 − 7.75 (m, 2H), 8.64 (d, *J*= 4.0 Hz, 1H). ^{13}C NMR (400 MHz, CD_3CN, 22°C, δ ppm): 25.00 (s), 124.22 (s), 125.48 (s), 125.58 − 125.38 (m), 127.73 (dd, *J*= 374.9, 119.2 Hz), 131.03 − 130.50 (m), 134.61 (s), 137.46 (s), 139.16 (s), 150.10 (s), 153.89 − 153.69 (m). ^{19}F NMR (400 MHz, CD_3CN, 22°C, δ ppm): -95.13(s).

## Synthesis of 2-(difluoro(phenyl)methyl)pyridyl Palladium(II) Di-2-pyridylketone Complex (36)
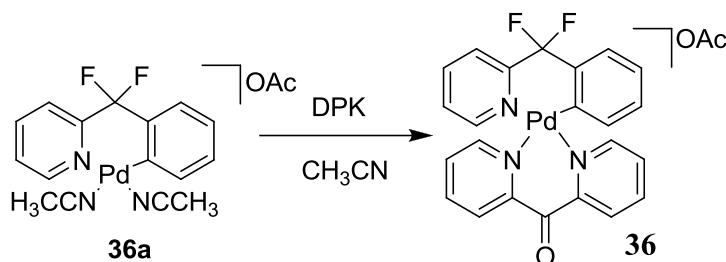
Di-(2-pyridyl) ketone (105 mg, 0.57 mmol) was added to the acetato palladium complex **10** (200 mg, 0.54 mmol) in 25 mL of CH_3CN at 25°C. The reaction mixture was stirred at 65 °C for 5 h, and the solvent was removed *in vacuo*. To the solid residue was suspended in 50 mL of dichloromethane, followed by 50 mL of hexanes. The precipitate was filtered and washed with 10 mL of hexanes to afford light brown solid **36**(49%). ^{1}H NMR (400 MHz, CD_3CN, 22°C, δ ppm): 6.68 (dd, *J*= 7.7, 0.9 Hz, 1H), 7.11 − 7.02 (m, 1H), 7.24 (td, *J*= 7.4, 0.8 Hz, 1H), 7.53 − 7.45 (m, 1H), 7.53 − 7.45 (m, 1H), 7.68 − 7.57 (m, 1H), 7.78 − 7.70 (m, 1H), 8.08 (dd, *J*= 10.7, 5.1 Hz, 1H), 8.21 − 8.14 (m, 1H), 8.27 − 8.21 (m, 1H), 8.37 − 8.27 (m, 1H). ^{13}CNMR (400 MHz, CD_3CN, 22°C, δ ppm): 120.33 (s), 122.13 (t, *J*= 12.8 Hz), 123.10 (d, *J* = 13.3 Hz), 125.92 (s), 127.67 (s), 127.86 (s), 126.98 (s), 128.92 (s), 129.42 (d, *J* = 15.2 Hz), 130.18 (d, *J* = 8.3 Hz), 131.70 (s), 133.98 (s), 136.95 (s), 141.90 (s), 142.14 (s), 142.33 (s), 151.12 (s), 151.79 (s), 152.64 (s), 153.94 (s), 155.72 (s). ^{19}F NMR (400 MHz, CD_3CN, 22°C, δ ppm): -121.90(d), -121.88(d). Mass Spectrometry: ESI-MS (*m/z*): Calcd for $[C_{23}H_{16}F_2N_3O^{106}Pd]$, 494.04. Found 493.03.

Oxidative Halogenation of 8-methylquinoline using H_2O_2

General Procedure

Complex **10(BF₄)** or **17(BF₄)** (30 mg) was dissolved in 1 mL of Solvent (CH_3CN, CH_2Cl_2, MeOH, or THF) at 25°C. Addition of LiX (X= Cl, Br, I, and OH) (10 equiv), AgF and TBAF(3eq), AgF and CuF_2, or TBABF followed by H_2O_2 (2 eq.) led to immediate formation of a deep yellow solution. The reaction mixture was stirred at 25°C for 1 hr or 24hrs for fluorination, to afford a dark orange solution. The solvent was evaporated by air. The resulting precipitate was extracted with 25 mL of chloroform. The precipitate was filtered and he filtrate was evaporated *in vacuo* to yield dark orange residue **11a-f**.

Synthesis of 8-(iodomethyl)-quinoline (11d)
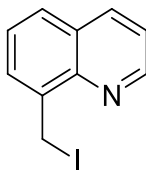
Product **11d** was also obtained from above transformation (82% isolated yield). ^{1}H NMR (400 MHz, CDCl₃, 22°C, δ ppm): 5.14 (s, 2H), 7.39 − 7.44 (m, 2H), 7.774 (d, J= 8.5 Hz, 1H), 7.82 (d, J= 8.5 Hz, 1H), 8.13 (d, J= 8.5, 1H), 8.98 (d, J= 4.4, 1H). Mass Spectrometry: ESI-MS (*m/z*): Calcd for [H+] [$C_{10}H_8IN$], 269.98. Found 269.94. Compared to literature reference.[67]

**Synthesis of 8-(bromomethyl)-quinoline (11c)**
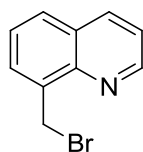
 Product **11c** was also obtained from this transformation (82% isolated yield).   ^{1}H NMR (400 MHz, CDCl₃, 22°C, δ ppm): 5.26 (s, 2H), 7.48 (dd, J= 8.3, 4.2 Hz, 1H), 7.54 (dd, J= 8.2, 7.2 Hz, 1H), 7.90 − 7.77 (m, 2H), 8.19 (dd, J= 8.3, 1.7 Hz, 1H), 9.04 (dd, J= 4.2, 1.8 Hz, 1H). Mass Spectrometry: ESI-MS (*m/z*): Calcd for [H+] [$C_{10}H_8BrN$], 221.99. Found 221.09. Compared to literature reference.[68]

Synthesis of 8-(chloromethyl)quinoline (11b)
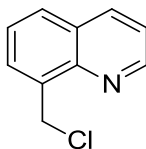
Product **11b** was also obtained from this transformation (80% isolated yield)   ^{1}H NMR (400 MHz, CDCl$_3$, 22°C, δ ppm):   5.36 (s, 2H), 7.48 (dd, *J*= 8.3, 4.2 Hz, 1H), 7.56 (dd, *J*= 14.4, 7.2 Hz, 1H), 7.86 − 7.81 (d, *J*= 7.1 Hz, 1H), 7.88 (d, *J*= 7.1 Hz, 1H), 8.20 (dd, *J*= 8.3, 1.8 Hz, 1H), 9.01 (dd, *J* = 4.2, 1.7 Hz, 1H). Mass Spectrometry: ESI-MS (*m/z*): Calcd for [H+] [C$_{10}$H$_8$ClN], 178.04. Found 178.03. Compared to literature reference.[69]

Synthesis of 8-(fluoromethyl)-quinoline (11a)
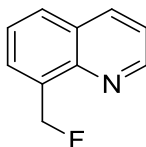
Product **11a** was also obtained from this transformation (45% isolated yield).   ^{1}H NMR (400 MHz, CDCl3, 22°C, δ ppm): 8.93 (dd, *J*= 4.2, 1.7 Hz, 1H), 8.18 (dd, *J*= 8.2, 1.8 Hz, 1H), 7.83-7.81 (multiple peaks, 2H), 7.58 (t, *J*= 7.7 Hz, 1H), 7.44 (dd, *J*= 8.3, 4.2 Hz, 1H), 6.15 (d, *J*$_{FH}$= 48 Hz, 2H). ^{19}F NMR (400 MHz, CD$_3$CN, 22°C, δ ppm): −219.2 (d, *J*$_{FH}$= 48 Hz). Mass Spectrometry: ESI-MS (*m/z*): Calcd for [H+] [C$_{10}$H$_8$FN], 162.18. Found 162.12. Compared to literature reference.[70]

Synthesis of quinoline-8-carbaldehyde (11f)
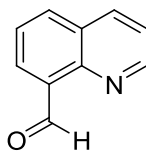
Product **11f** was also obtained from this transformation (45% isolated yield). ^{1}H NMR (400 MHz, CDCl$_3$, 22°C, δ ppm): 7.51 (dd, *J*= 8.3, 4.2 Hz, 1H), 7.66 (dd, *J*= 16.5, 8.6 Hz, 1H), 8.09 (dd, *J*= 8.2, 1.4 Hz, 1H), 8.24 (dd, *J*= 8.4, 1.8 Hz, 1H), 8.33 (dd, *J*= 7.2, 1.5 Hz, 1H), 9.05 (dd, *J*= 4.2, 1.8 Hz, 1H), 11.45 (s, 1H). Mass Spectrometry: ESI-MS (*m/z*): Calcd for [H+] [C$_{10}$H$_8$ClN], 158.18. Found 158.11.[71]

Synthesis of quinolin-8-ylmethanol (11e)
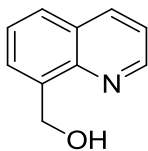
Product **11e** was also obtained from this transformation (35% isolated yield). ^{1}H NMR (400 MHz, CDCl$_3$, 22°C, δ ppm): ^{1}H NMR δ 8.77 (dd, J = 3.9, 1.2 Hz, 1 H), 8.07 (dd, J = 8.2, 1.2 Hz, 1 H), 7.65 (d, J = 8.2 Hz, 1 H), 7.55 (d, J = 7.0 Hz, 1 H), 7.40 (t, J = 7.6 Hz, 1 H), 7.32 (dd, J = 8.2, 4.3 Hz, 1 H), 5.20 (s, 2 H). Mass Spectrometry: ESI-MS (*m/z*): Calcd for [H+] [C$_{10}$H$_8$ClN], 160.08. Found 160.04. Compared to literature reference.[71]

**Synthesis of 2-(4-aminopyridin-2-yl)-2-methylpropan-1-ol (18d)**
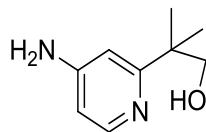
Product **18d** was also obtained from this transformation (15% isolated yield). ^{1}H NMR (400 MHz, CDCl$_3$, 22°C, δ ppm): 1.37 (s, 3H), 1.47 (s, 3H), 4.24 (s, 2H), 7.38 − 7.32 (m, 1H), 7.76 (dt, J= 12.8, 5.6 Hz, 1H), 8.62 − 8.56 (m, 1H) (NH$_2$excluded). Mass Spectrometry: ESI-MS (*m/z*): Calcd for [H+] [C$_9$H$_{15}$N$_2$O], 167.12. Found 167.04.

Synthesis of 2-(1-fluoro-2-methylpropan-2-yl)pyridin-4-amine (19d)
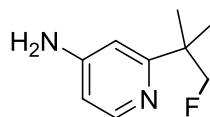
Product **19d** was also obtained from this transformation (54% isolated yield). ^{1}H NMR (400 MHz, CDCl$_3$, 22°C, δ ppm): 2.32 (s, 3H), 2.37 (s, 3H), 5.39 (d, J = 47.1 Hz, 2H), 7.61 − 7.53 (m, 1H), 8.47 − 8.40 (m, 2H), 9.03 − 8.97 (m, 1H), (NH$_2$excluded). ^{19}F NMR (400 MHz, CD$_3$CN, 22°C, δ ppm): -216.13(t, J_{FH}= 48 Hz).

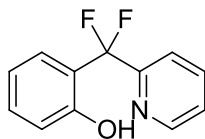**Synthesis of 10-hydroxy-benzo[*h*]quinoline (24a)**
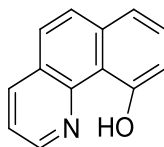
Complex **8** (10 mg, 0.02 mmol) was dissolved in 2 mL of D_2O at 25°C. Addition of H_2O_2 (20 μliters, 0.4 mmol) led to immediate formation of a deep yellow solution. The reaction mixture was stirred at 25°C for 24 h, to afford dark orange solid, followed by the addition of trifluoroacetic acid (9 mg, 0.08 mmol) and pyridine (1.6 mg, 0.02 mmol). The resulting precipitate was filtered and washed with 5 mL of water. Extractions using dichloromethane (3 X 1 mL) were combined and evaporated *in vacuo*, to afford dark orange solid **24a**(75%).^{1}H NMR (400 MHz, CDCl$_3$, 22°C, δ ppm): 7.41 (d, *J*=7.1 Hz, 1H), 7.60 − 7.53 (m, 1H), 7.63 (dd, *J*=8.4, 2.8 Hz, 2H), 7.81 (d, *J*=8.9 Hz, 1H), 8.25 (dd, *J*=8.1, 1.7 Hz, 1H), 8.83 (dd, *J*=4.6, 1.7 Hz, 1H). Mass Spectrometry: ESI-MS (*m/z*): Calcd for [H+] [$C_{13}H_{10}NO$], 196.08. Found 196.04.

**The Homocoupling of Benzo[*h*]quinoline (28)**
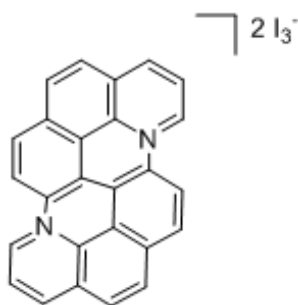
Complex **8(BF$_4$)** (25 mg, 0.05 mmol) was dissolved in 10 mL of CH_3CN at 25°C. Addition of iodine (68 mg, 0.25 mmol) led to immediate formation of a deep brown solution. The reaction mixture was stirred at 25°C for 3 weeks, to afford dark redish brown solution **28**(65%). ^{1}H NMR (400 MHz, CDCl$_3$, 22°C, δ ppm): 6.96 (dd, *J*= 7.9, 4.3 Hz, 1H), 7.46 (dd, *J*= 7.2, 1.3 Hz, 1H), 7.59 (t, *J*= 9.0 Hz, 1H), 7.72 − 7.67 (m, 1H), 7.79 (dd, *J*= 4.3, 1.8 Hz, 1H), 7.91 −7.84 (m, 1H), 7.93 (dt, *J* = 12.5, 3.0 Hz, 1H). ^{13}C NMR (400 MHz, CDCl$_3$, 22°C, δ ppm): 120.57 (s), 125.51 (s), 126.92 (s), 127.48 (s), 128.76 (s), 128.97 (d, *J*= 9.9 Hz), 128.97 (d, *J* = 9.9 Hz), 130.67 (s), 134.61 (s), 134.97 (s), 146.27 (s). Mass Spectrometry: ESI-MS (*m/z*): Calcd for [H+] [$C_{26}H_{14}N_2$], 177.06. Found 177.04.

**Synthesis of 2-(difluoro(pyridin-2-yl)methyl)phenol (39a)**

Complex **36(BF₄)** (10 mg, 0.02 mmol) was dissolved in 2 mL of CH_3CN at 25°C. Addition of H_2O_2 (10 μliters, 0.4 mmol) led to immediate formation of a deep brown solution. The reaction mixture was stirred at 25°C for 5 min, to afford dark brown solid **22**(70%).^{1}H NMR (400 MHz, $CDCl_3$, 22°C, δ ppm): 6.46 (dd, J= 8.1, 5.3 Hz, 1H), 6.97 (t, J= 6.5 Hz, 1H), 7.07 (dd, J= 6.8, 1.4 Hz, 1H), 7.20 (dd, J= 8.2, 1.5 Hz, 1H), 7.27 – 7.17 (m, 1H), 7.43 (dd, J= 8.1, 1.4 Hz, 1H), 7.80 (dd, J = 5.2, 1.4 Hz, 2H) ^{19}F NMR (400 MHz, CD_3CN, 22°C, δ ppm): -109(s).

Synthesis of 2-(1-bromo-2-methylpropan-2-yl)pyridin-4-amine(21)
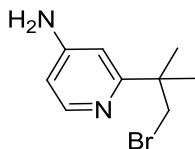
A solution of complex 4 (30 mg, 1.00 mmol) in 2 mL of CH_3CN at 25°C were treated with 1-N-Bromosuccinimide (77 mg, 5 mmol). After stirring for 1 hr, the resulting suspension afforded an orange solution 21(42%). ^{1}H NMR (400 MHz, $CDCl_3$, 22°C, δ ppm): 1.37 (s, 6H), 3.76 (s, 2H), 7.23 (s, 1H), 7.44 (d, J= 5.6 Hz, 1H), 8.90 (d, J= 5.6 Hz, 1H) (NH_2excluded).

Synthesis of (E)-1,2-bis(5-bromo-2-(1-bromo-2-methylpropan-2-yl)pyridin-4-yl)diazene (23)
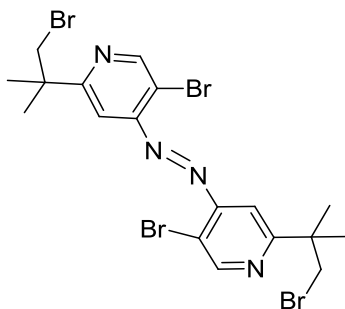
A solution of complex 17 (30 mg, 1.00 mmol) in 2 mL of CH_3CN at 25°C were treated with 1-N-Bromosuccinimide (77 mg, 5 mmol). After stirring for 3 weeks, the resulting suspension afforded an orange solution 23(31%). Characterization by X-ray Crystallography.

# Oxidative Chlorination of 8-methylquinoline using O_2

General Procedure

A solution of 8-methylquinoline (179 mg, 1.00 mmol) in 20mL of CH_3CN at 78 °C were treated with palladium acetate (224 mg, 1.00 mmol), 2,6-pyridine dicarboxylic acid(h2pda), lithium chloride, and TSOH.H2O. After stirring for 5 d, the resulting suspension was filtered and filtrate evaporated *in vacuo* dissolved in CHCl3 and treated with Na2CO3, followed by filtration. The resulting residue afforded **11b** in 65% yield.. ^{1}HNMR (400 MHz, CDCl3, 22°C, δ ppm): 5.36 (s, 2H), 7.48 (dd, *J*= 8.3, 4.2 Hz, 1H), 7.56 (dd, *J*= 14.4, 7.2 Hz, 1H), 7.86 − 7.81 (d, *J*= 7.1 Hz, 1H), 7.88 (d, *J*= 7.1 Hz, 1H), 8.20 (dd, *J*= 8.3, 1.8 Hz, 1H), 9.01 (dd, *J*= 4.2, 1.7 Hz, 1H).

Fluorination of Unactivated 8-methylquinoline using Deoxofluor

General Procedure

A solution of 8-methylquinoline (179 mg, 1.00 mmol) in 2 mL of CH_3CN at 90 °C were treated with tetrakis(acetonitrile)palladium(II) tetrafluoroborate (556 mg, 1.00 mmol) and Deoxofluor(1.66 g, 7.51 mmol). After stirring for 24 hr, the resulting suspension was diluted with 20 mL of dichloromethane and quenched with brine (5mL). The resulting precipitate was filtered and the filtrate extracted with water (3 X 3). The organic layer collected and dried with MgSO4 followed by filtration. The liquid were evaporated *in vacuo* and the resulting residue afforded **11a** in 11% yield. ^{1}H NMR (400 MHz, CDCl3, 22°C, δ ppm): 8.93 (dd, *J*= 4.2, 1.7 Hz, 1H), 8.18 (dd, *J*= 8.2, 1.8 Hz, 1H), 7.83-7.81 (multiple peaks, 2H), 7.58 (t, *J*= 7.7 Hz, 1H), 7.44 (dd, *J*= 8.3, 4.2 Hz, 1H), 6.15 (d, J_{FH}= 48 Hz, 2H). ^{19}F NMR (400 MHz, CD3CN, 22°C, δ ppm): −219.2 (d, J_{FH}= 48 Hz). Mass Spectrometry: ESI-MS (*m/z*): Calcd for [H+] [$C_{10}H_8FN$], 162.18. Found 162.12.

**Synthesis of 4-*tert*-Butyl-2-methyl-2-oxazoline (41a)**
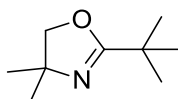
Reference.[8] Product **41a** (89% isolated yield). ^{1}H NMR (400 MHz, CDCl3, 22°C, δ ppm): 0.78 (s, 9H), 1.85 (s, 3H), 3.72 (dd, *J*=10.3, 9.0 Hz, 1H), 4.08 − 3.97 (m, 1H), 4.22 − 4.08 (m, 1H). Mass Spectrometry: ESI-MS (*m/z*): Calcd for [H+] [$C_9H_{18}NO$], 156.14. Found 156.10. Compared to literature reference.[72]

Synthesis of (4S)-4-*tert*-Butyl-2-methyl-2-oxazoline (41b)
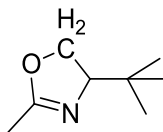
Reference.[9] Product **41b** (85% isolated yield) ^{1}H NMR (400 MHz, CDCl$_3$, 22°C, δ ppm): 0.78 (s, 9H), 1.85 (s, 3H), 3.72 (dd, *J*=10.3, 9.0 Hz, 1H), 4.08 – 3.97 (m, 1H), 4.22 – 4.08 (m, 1H ESI-MS (*m/z*): Calcd for [H+] [C$_8$H$_{15}$NO], 142.12. Found 142.10. Compared to literature reference.[73]

Synthesis of 2-(difluoro(phenyl)methyl)pyridine (35)
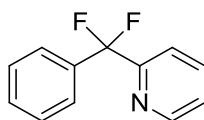
Reference.[10] Product **35** (82% isolated yield). ^{1}H NMR (400 MHz, CDCl$_3$, 22°C, δ ppm): 7.32 (dd, *J*=7.1, 5.2 Hz, 1H), 7.44 – 7.35 (m, 3H), 7.57 (s, 2H), 7.71 (d, *J*=7.9 Hz, 1H), 7.79 (t, *J*=7.7 Hz, 1H), 8.64 (d, *J*=4.7 Hz, 1H).^{13}CNMR(400 MHz, CDCl$_3$, 22°C, δ ppm): 120.30 (s), 121.77 (s), 127.53 – 127.09 (m), 127.93 (s), 129.50 (d, *J* = 3.4 Hz), 130.06 (s), 131.49 (s), 135.40 (s), 137.13 (s), 150.01 (s), 161.99 (s).^{19}F NMR (400 MHz, CD$_3$OD, 22°C, δ ppm): -100.12(s). Calcd for [H+] [C$_{12}$H$_9$F$_2$], 206.08. Found 206.02. Compared to literature reference.[74]

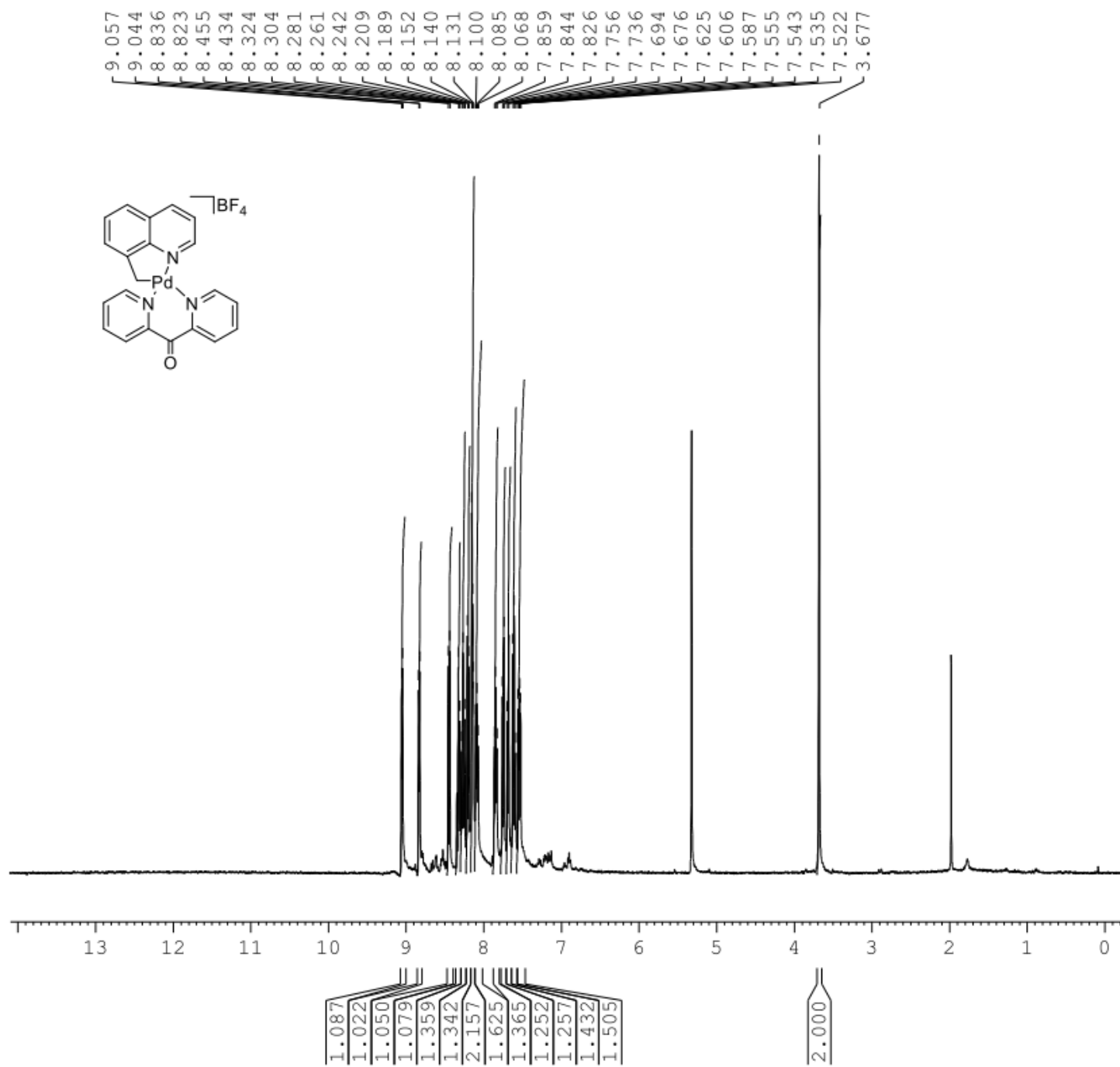Figure 1. ^{1}H NMR of 8-methylquinolylpalladium(II)Di-2-pyridylketone **(10)** in CD$_2$Cl$_2$, 22°C..

Figure 2. ^{13}C NMR of 8-methylquinolylpalladium(II)Di-2-pyridylketone **(10)** in CD$_2$Cl$_2$, 22°C.
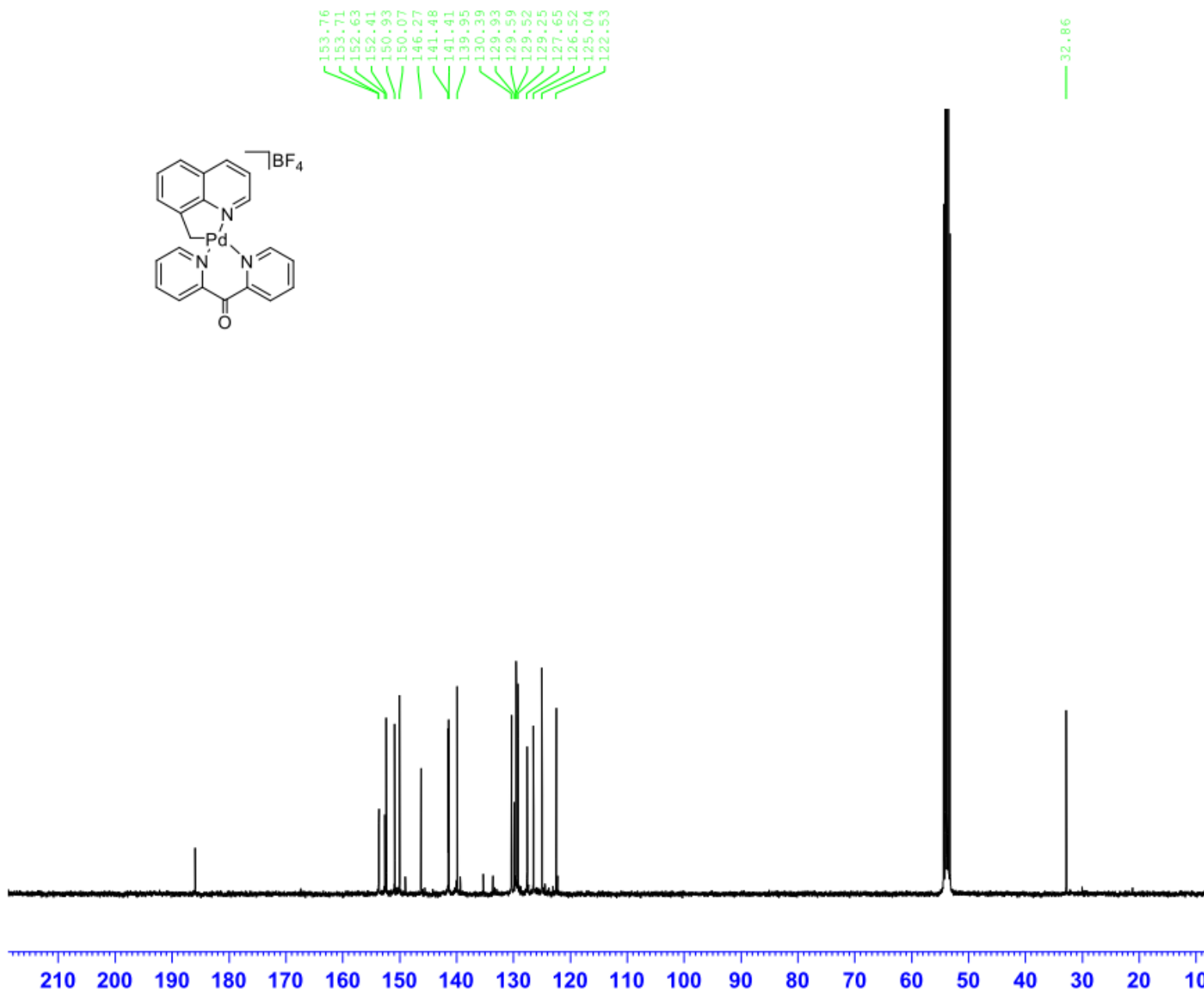
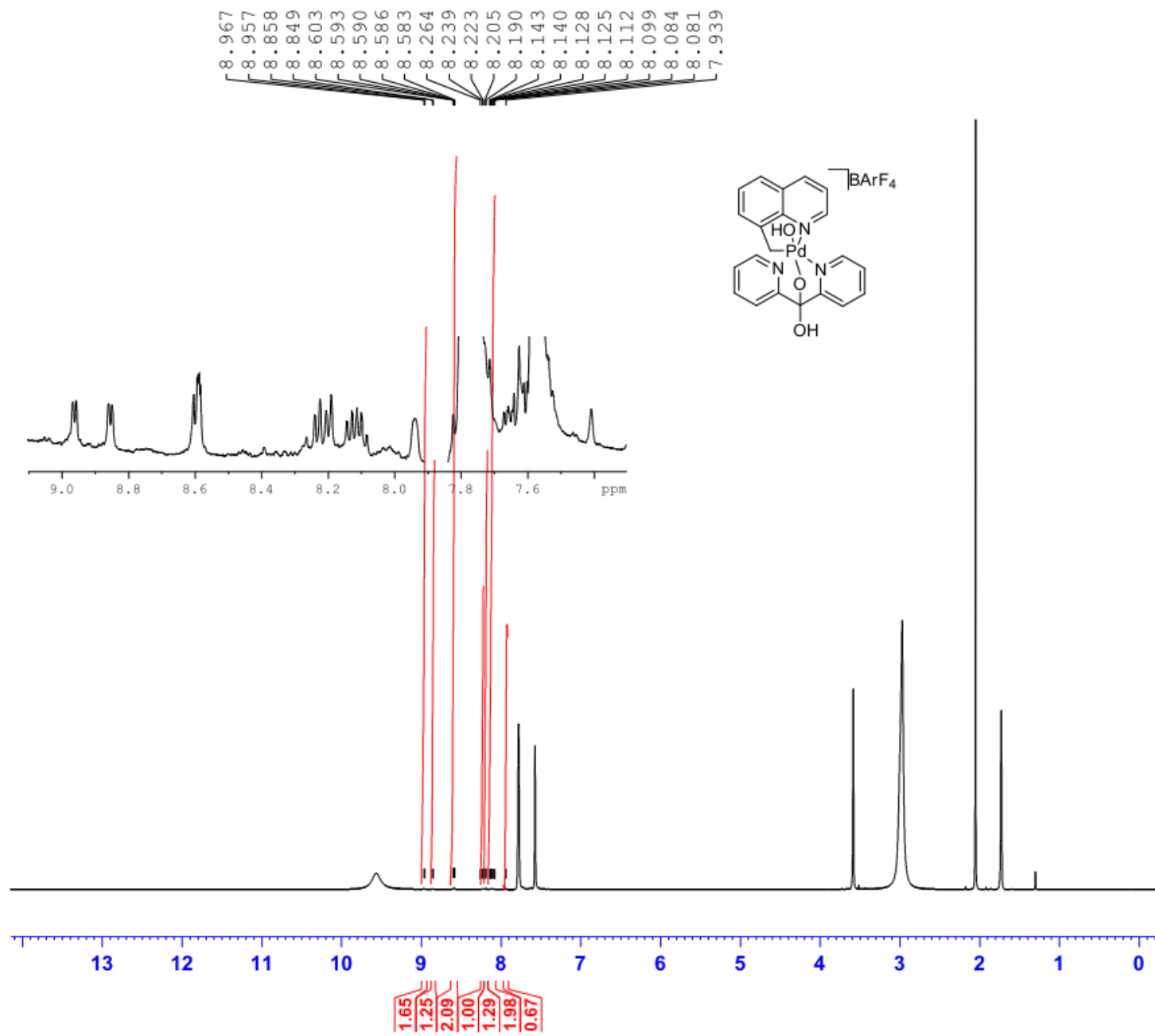Figure 3. ^{13}C NMR of 8-methylquinolylpalladium(II) Hydroxo Di-2-pyridylketone **(10)** in THF-*d8*, 22°C.

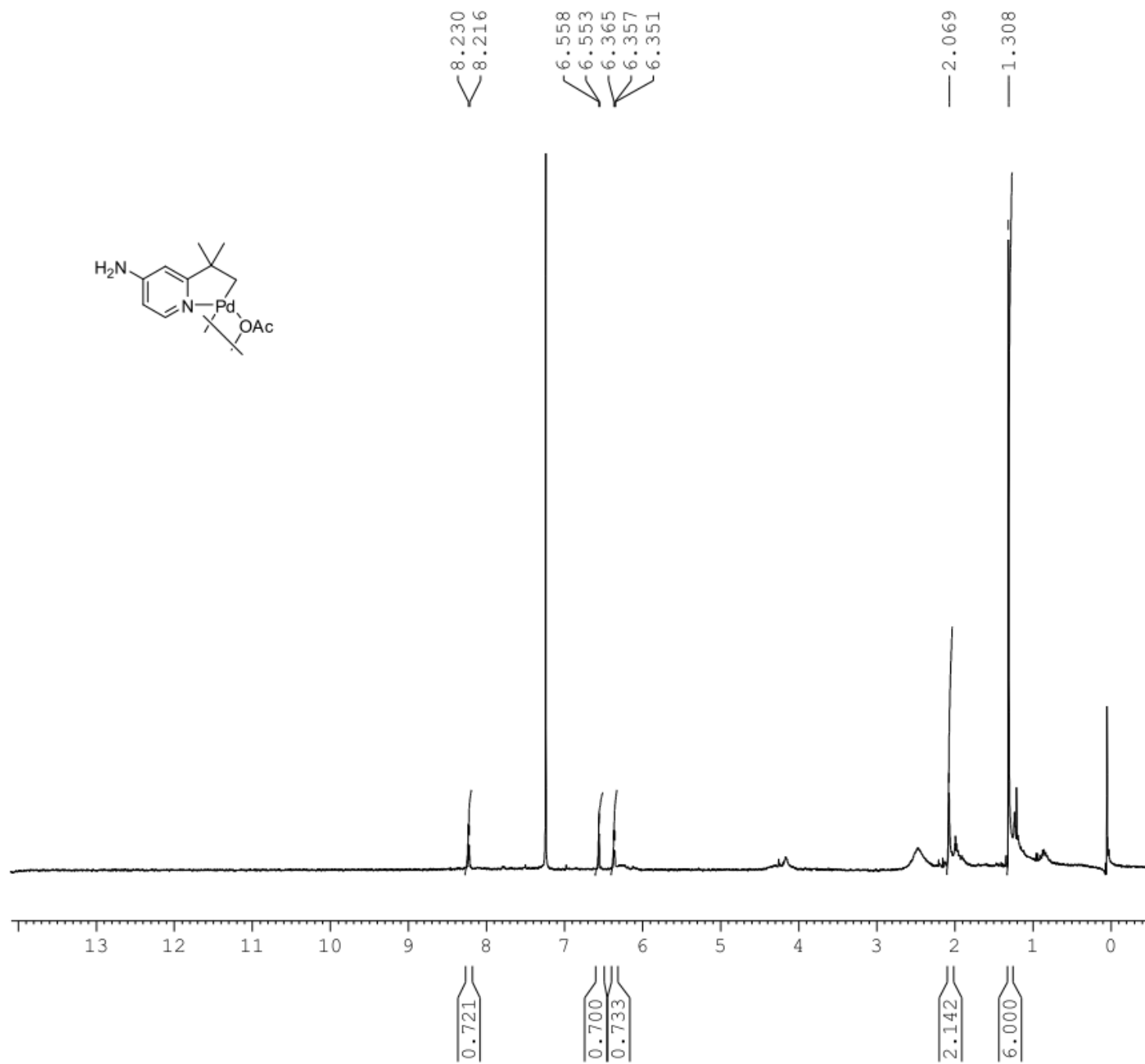Figure 4. ¹H NMR of 4-amino-2-*tert*-butylpyridyl Palladium(II) Acetato Complex (**16**)in CDCl₃, 22°C.

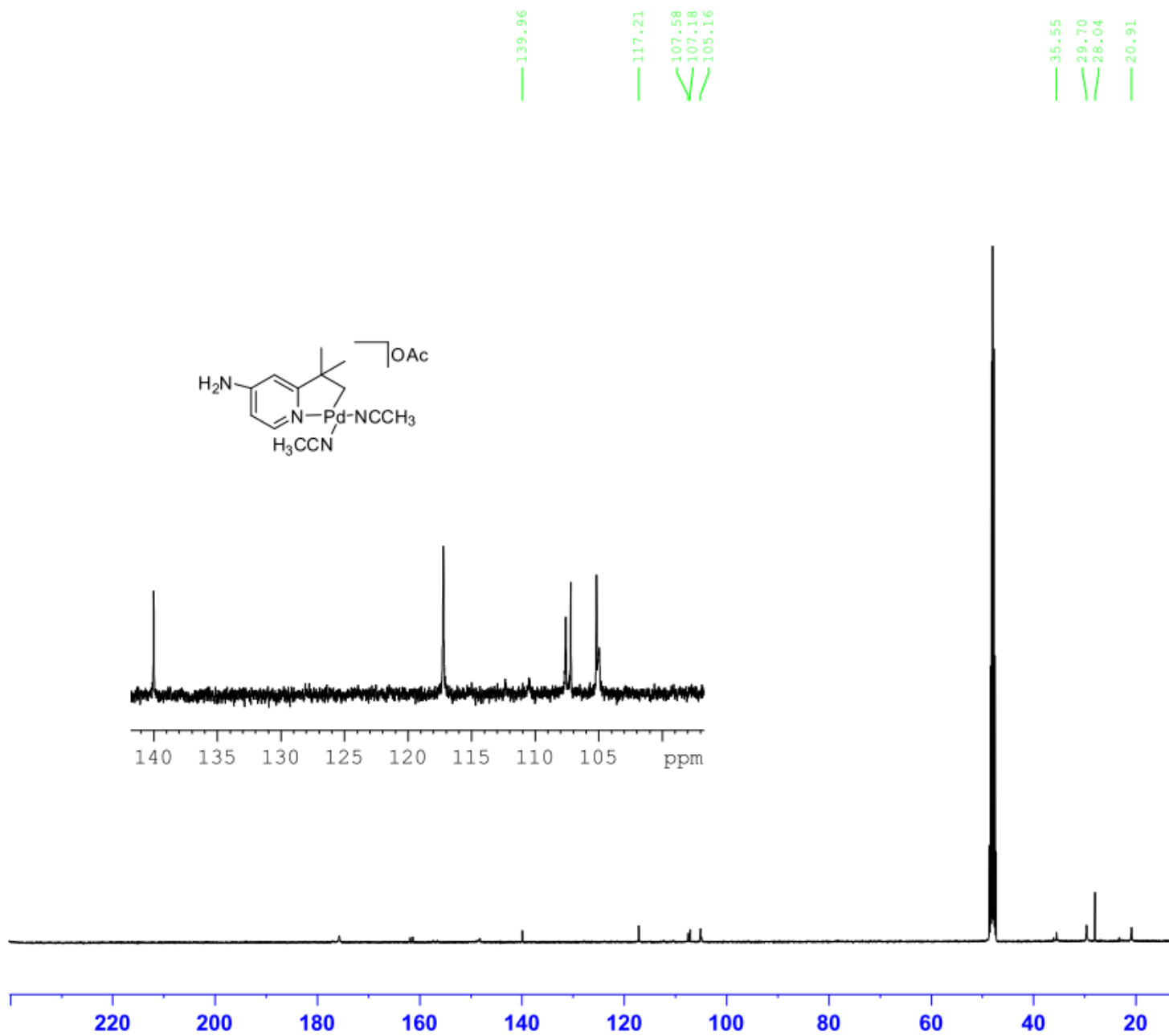Figure 5. ¹H NMR of 4-amino-2-*tert*-butylpyridyl Palladium(II) Acetonitrile Complex **(16a)** in CDCl₃, 22°C.

Figure 6. ^{1}H NMR of 4-amino-2-*tert*-butylpyridyl Palladium(II) Di-(2-pyridyl) Ketone Complex **(17)** in CD$_3$OD, 22°C.
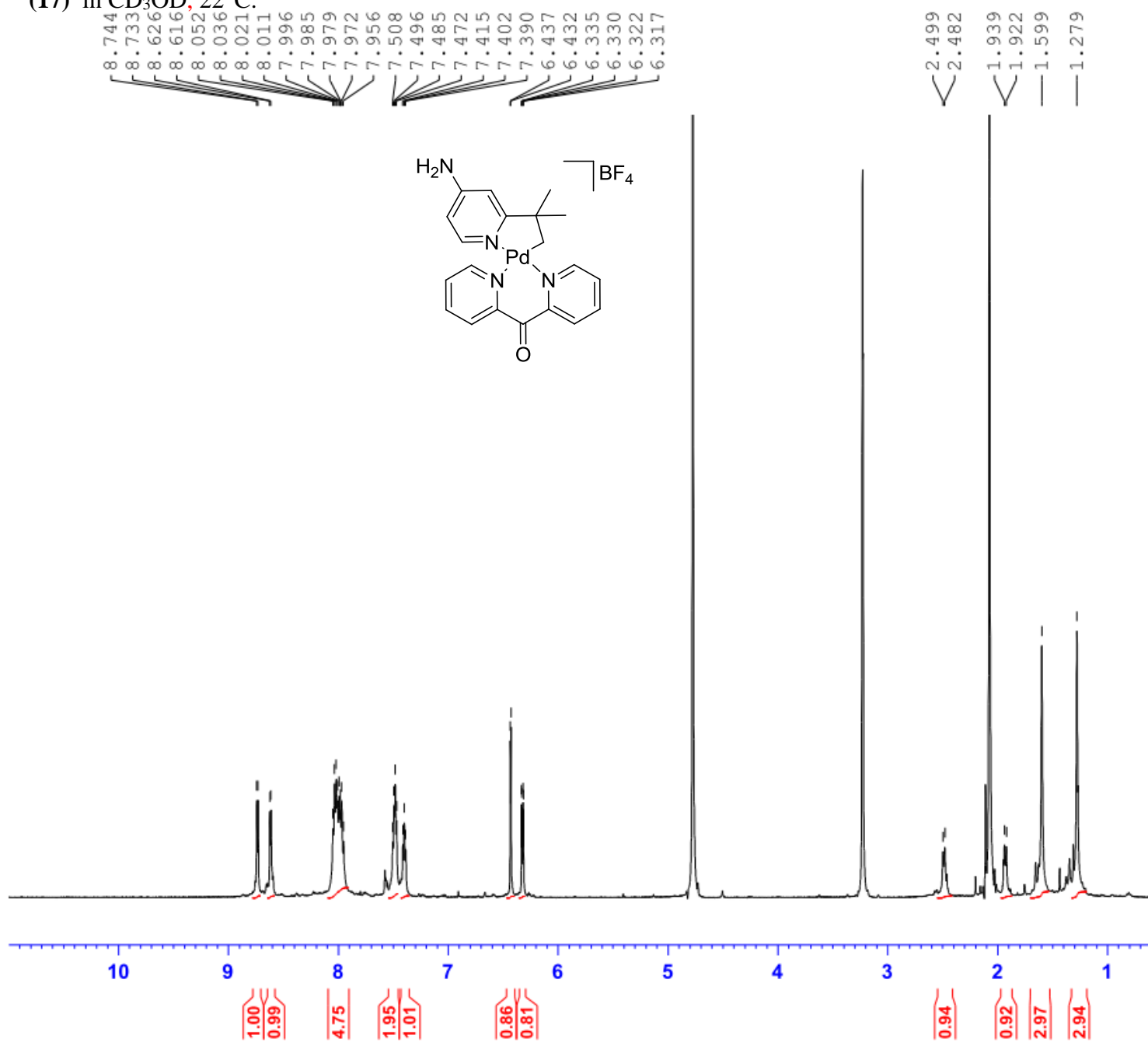
Figure 7. ^{13}C NMR of 4-amino-2-*tert*-butylpyridyl Palladium(II) Di-(2-pyridyl) Ketone Complex (**17**) in CD$_3$OD, 22°C.

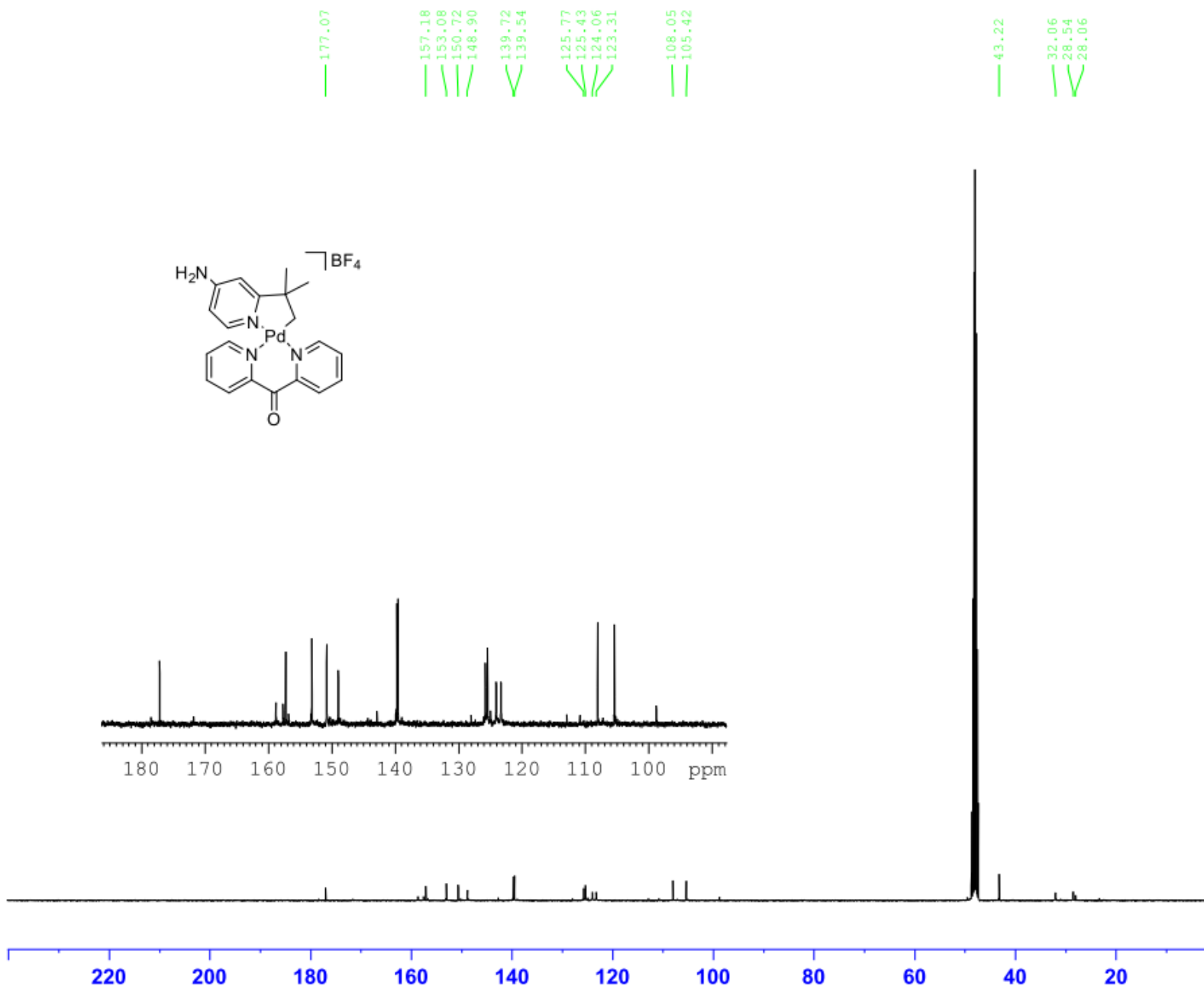Figure 8. ^{1}H NMR of 4-amino-2-*tert*-butylpyridyl Palladium(II) Hydroxo Di-(2-pyridyl) Ketone Complex **(18)** in DMSO-*d6*, 22°C.

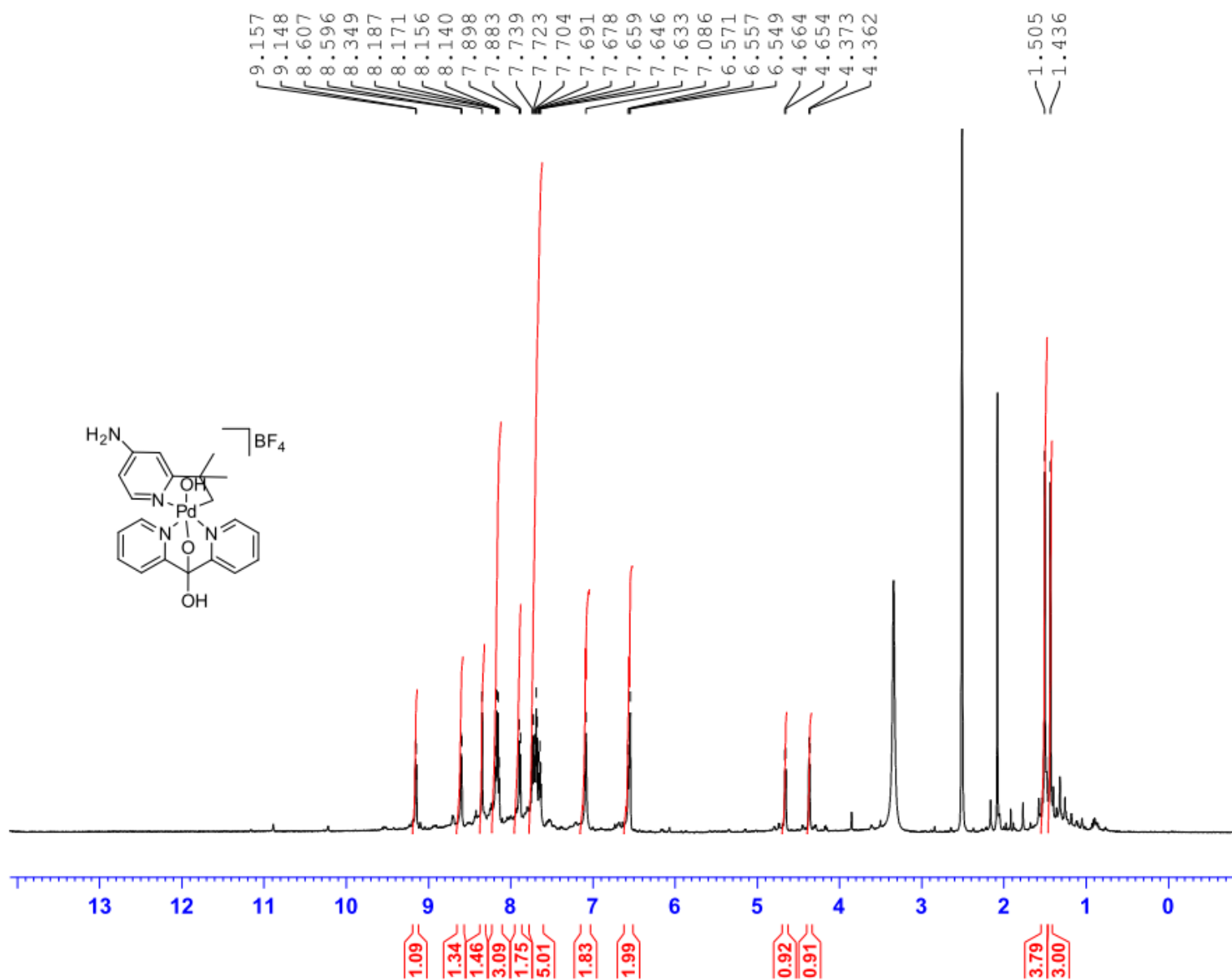Figure 9. ^{1}H NMR of 4-amino-2-*tert*-butylpyridyl Palladium(II) Hydroxo Di-(2-pyridyl) Ketone Complex **(18)** in CD$_3$CN, 22°C.

Figure 10. ^{1}H NMR of 4-amino-2-*tert*-butylpyridyl Palladium(II) Fluoro Di-(2-pyridyl) Ketone Complex **(19)** Complex in DMSO-*d6*, 22°C.
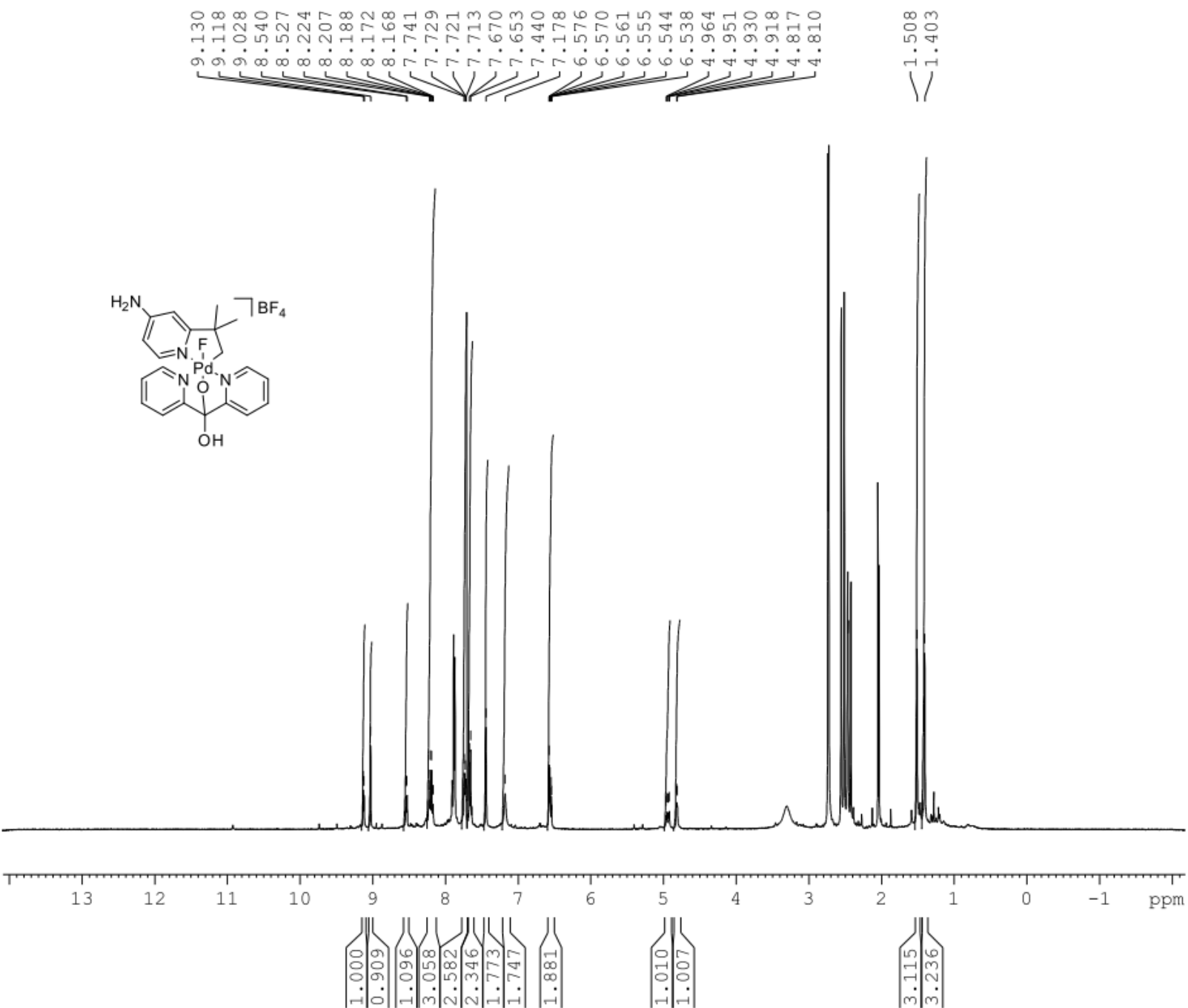
Figure 11. ^{1}H NMR of 4-amino-2-*tert*-butylpyridyl Palladium(II) Fluoro Di-(2-pyridyl) Ketone Complex **(19)** Complex in CD$_3$CN, 22°C.
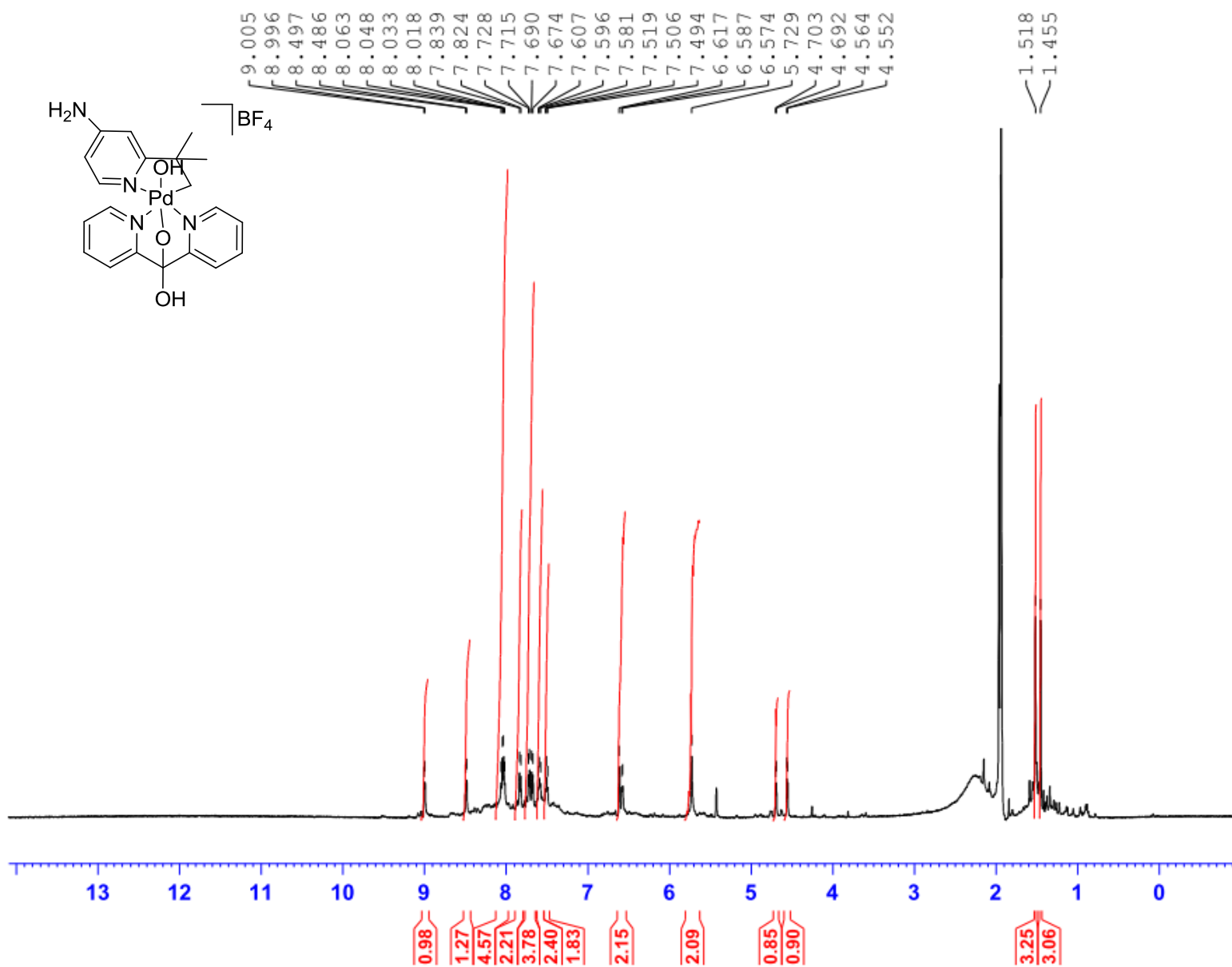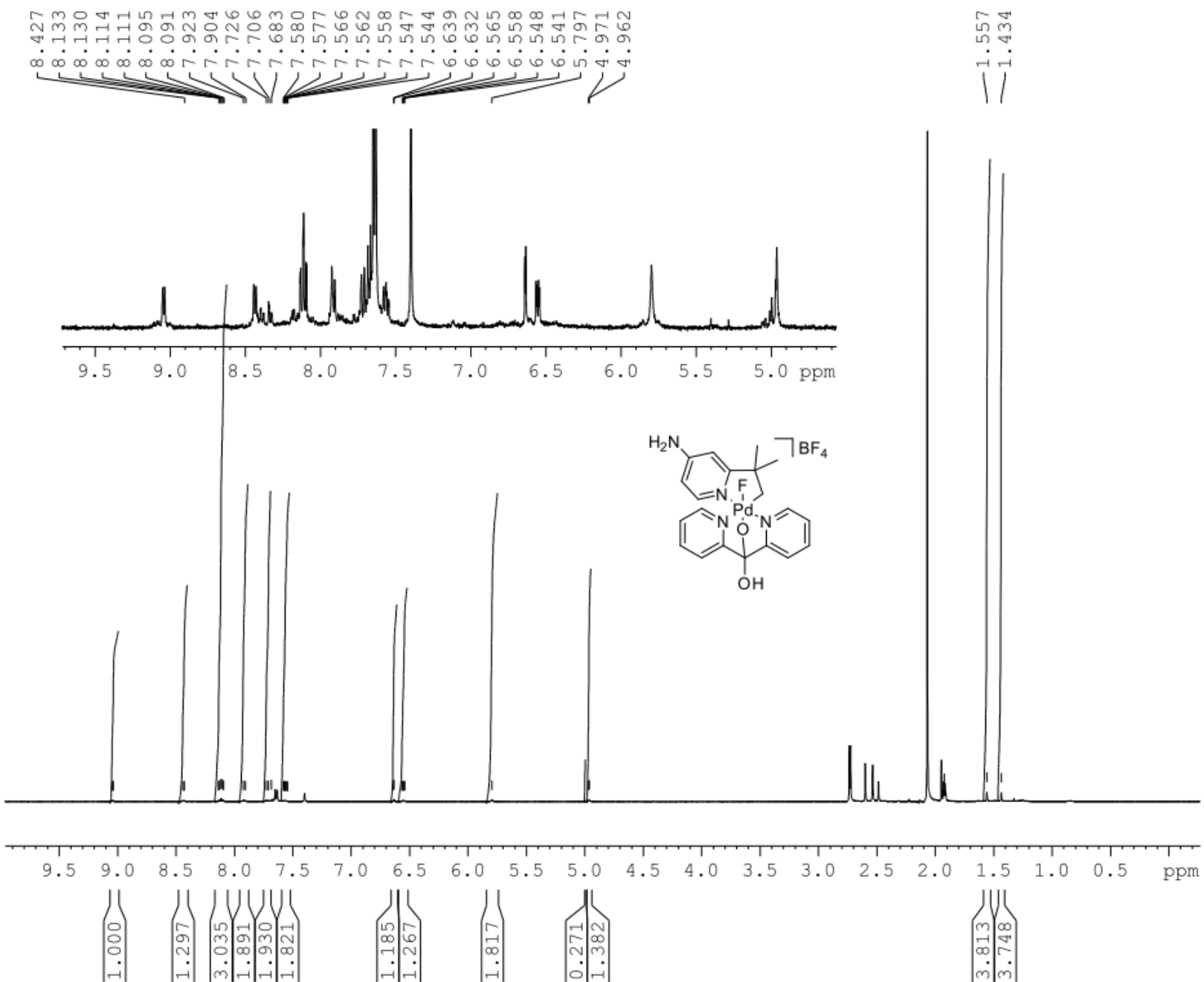
Figure 12. ^{19}F NMR of 4-amino-2-*tert*-butylpyridyl Palladium(II) Fluoro Di-(2-pyridyl) Ketone Complex **(19)** Complex in CD$_3$CN, 22°C.
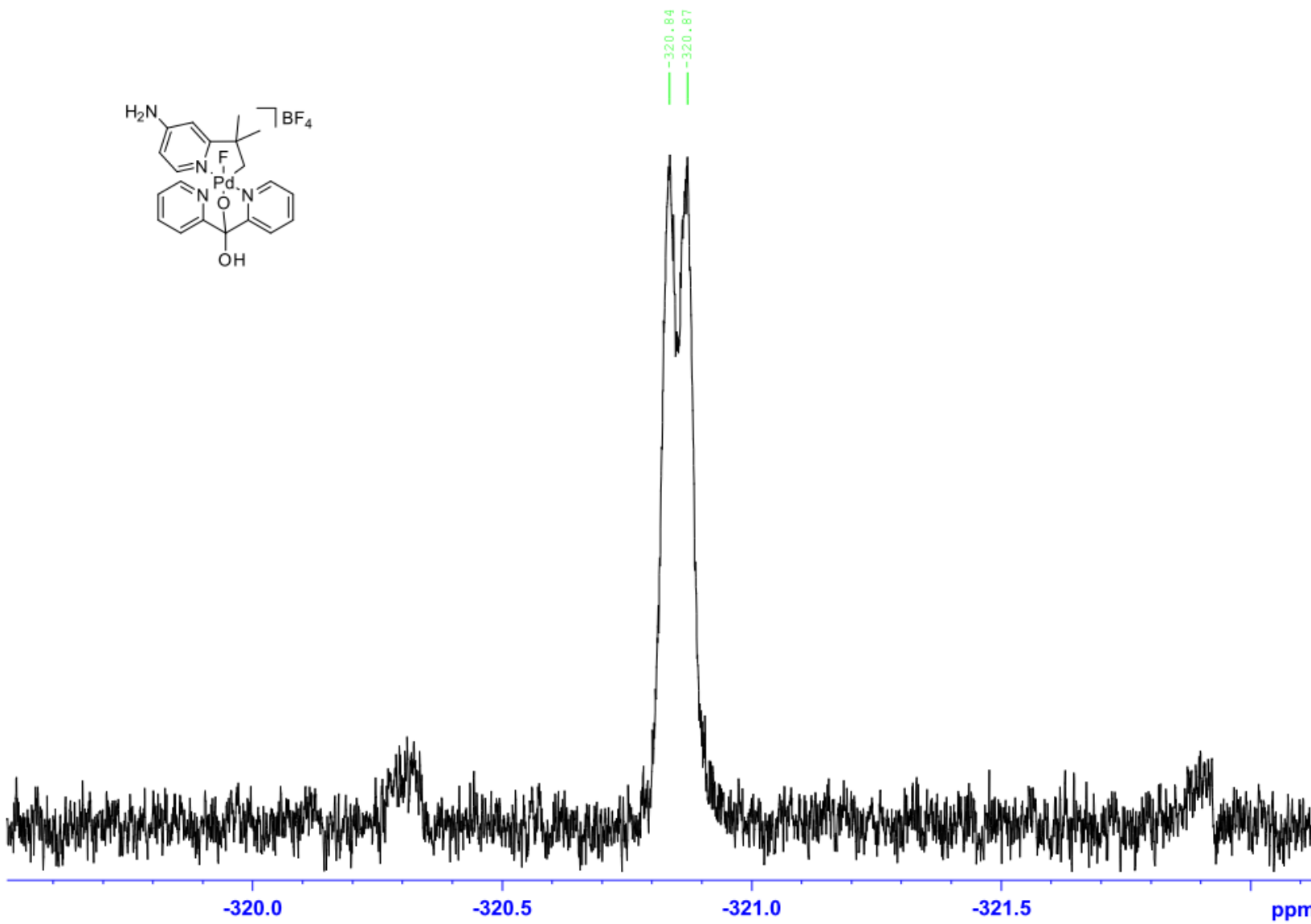
Figure 13. ^{1}H NMR of Benzo[*h*]quinolinyl Palladium(II) Acetato Complex **(8a)** in CDCl$_3$, 22°C.
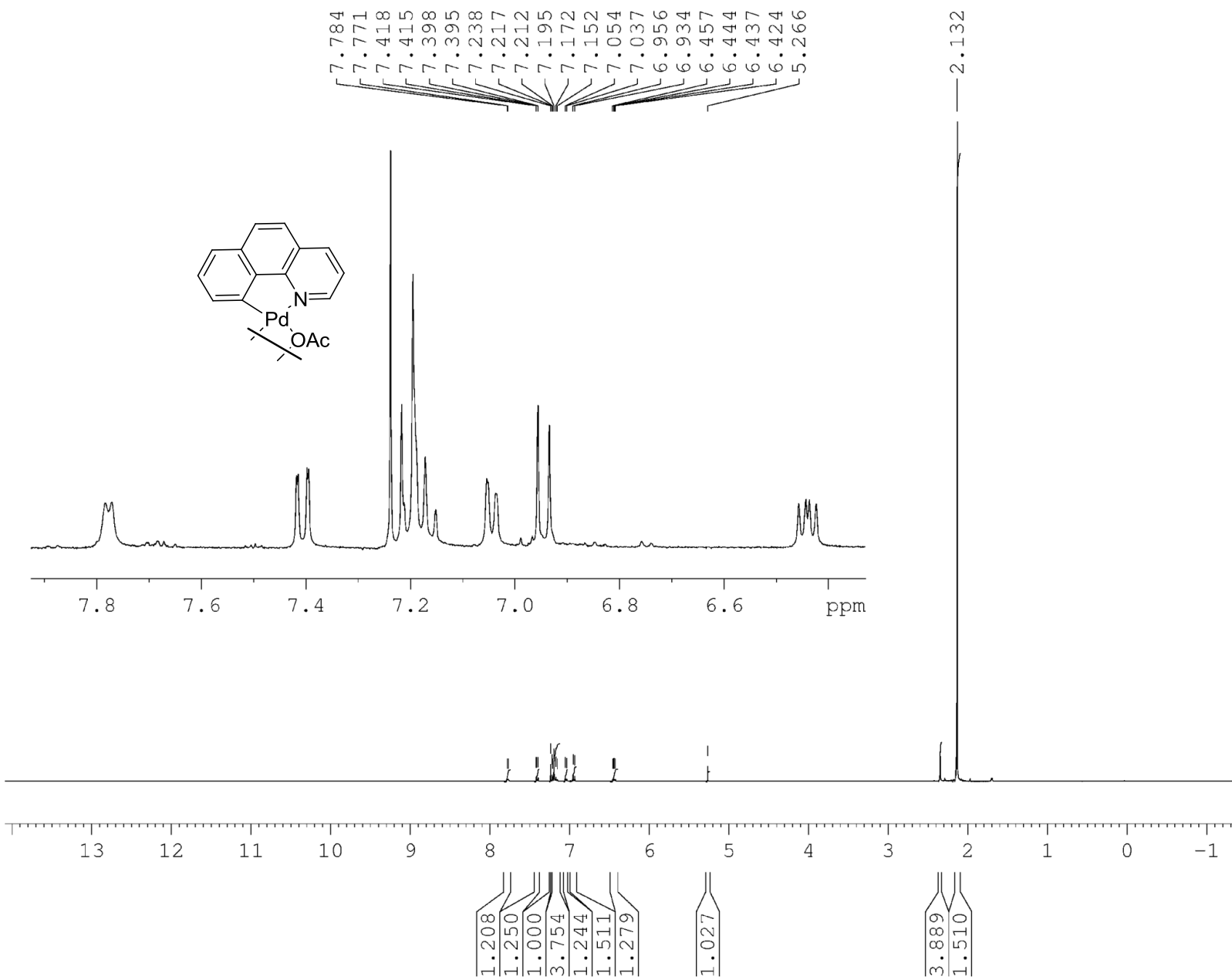
Figure 14. ^{1}H NMR of Benzo[*h*]quinolinyl Palladium(II) Di-(2-pyridyl) Ketone Complex **(8)** in CD$_3$OD, 22°C.
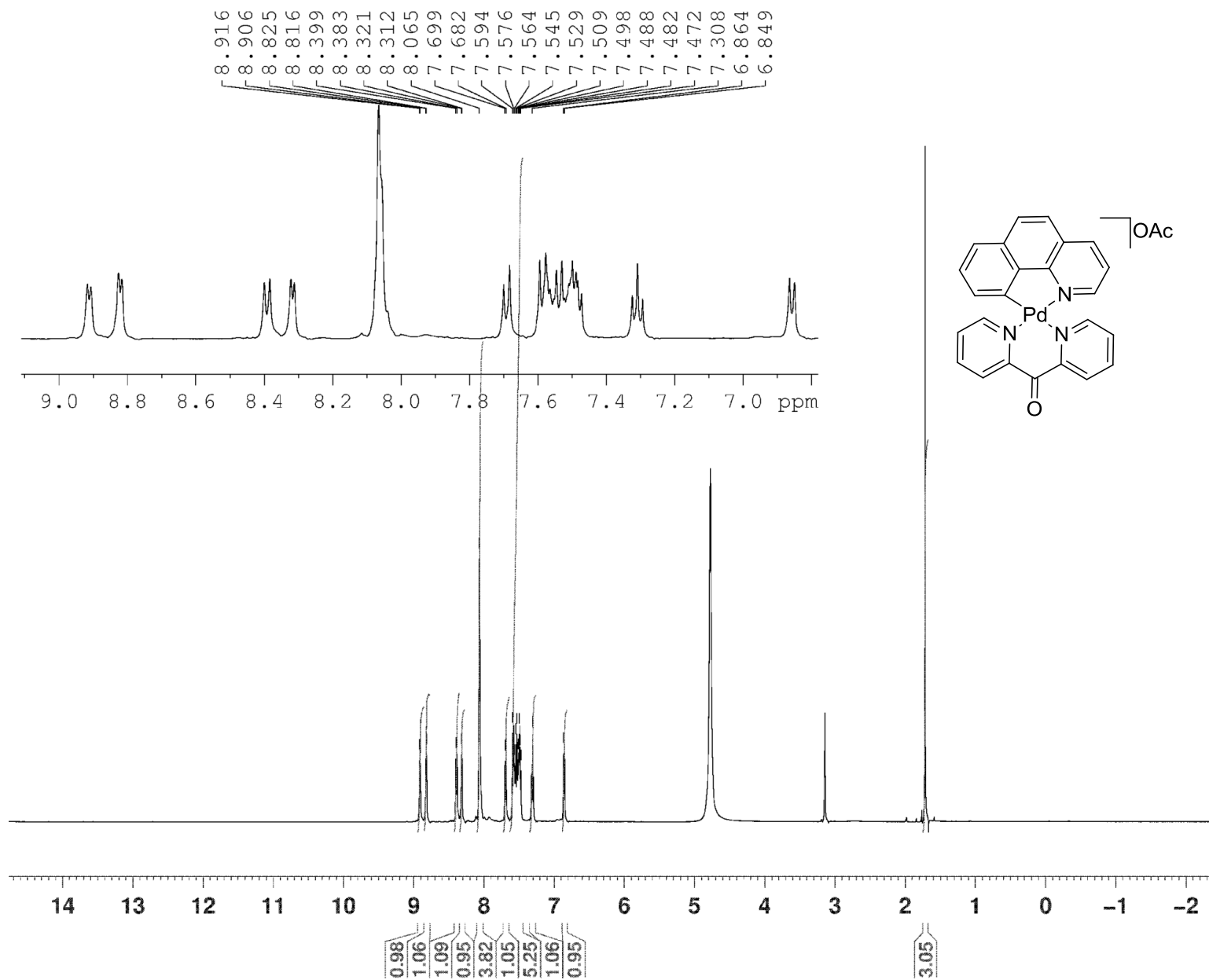
Figure 15. ^{13}C NMR of Benzo[*h*]quinolinyl Palladium(II) Di-(2-pyridyl) Ketone Complex **(8)** in CD$_3$OD, 22°C.
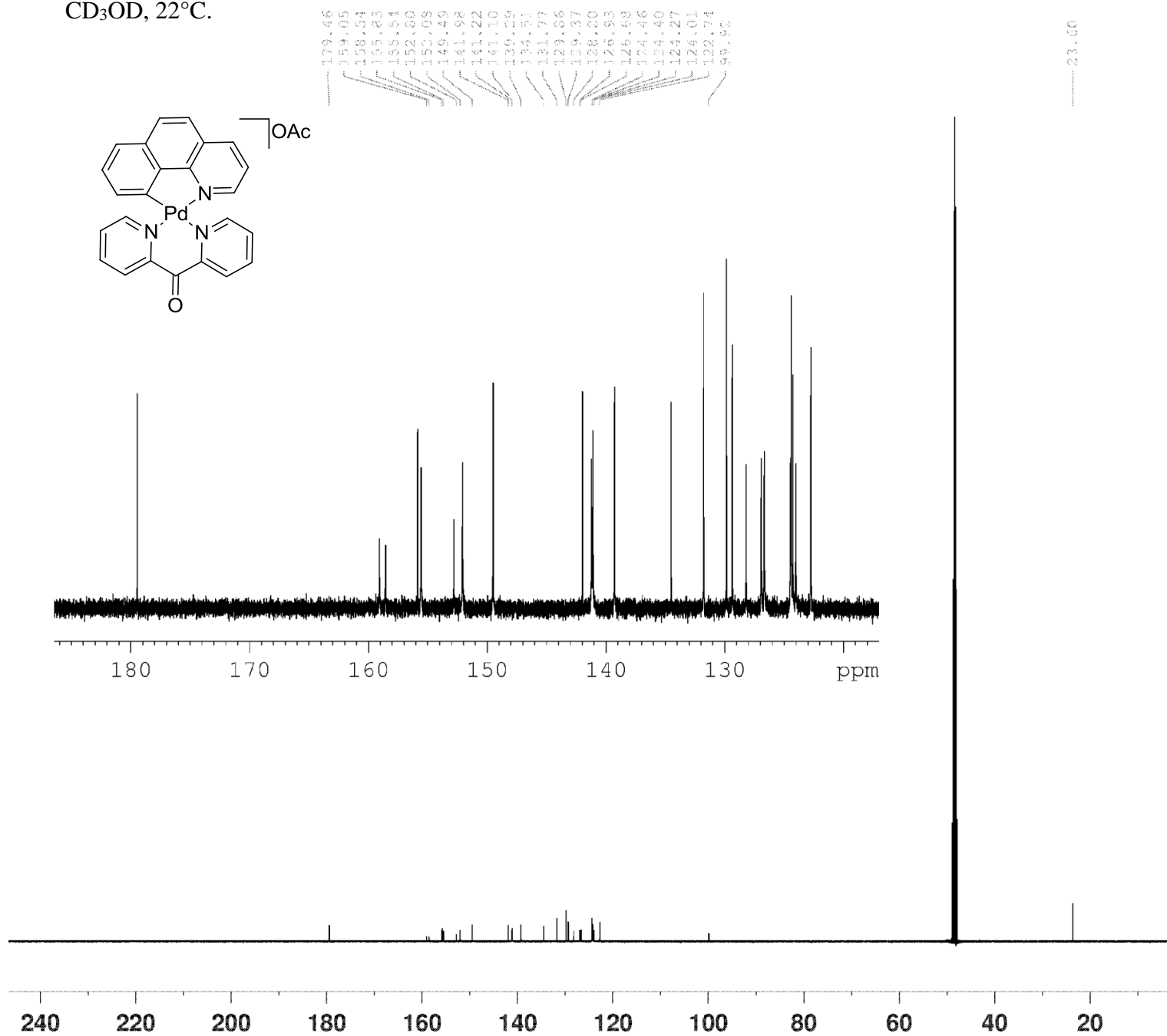
Figure 16. ^{1}H NMR of Benzo[*h*]quinolinyl Palladium(II) Hydroxo Di-(2-pyridyl) Ketone Complex **(24)** in D$_2$O, 22°C.
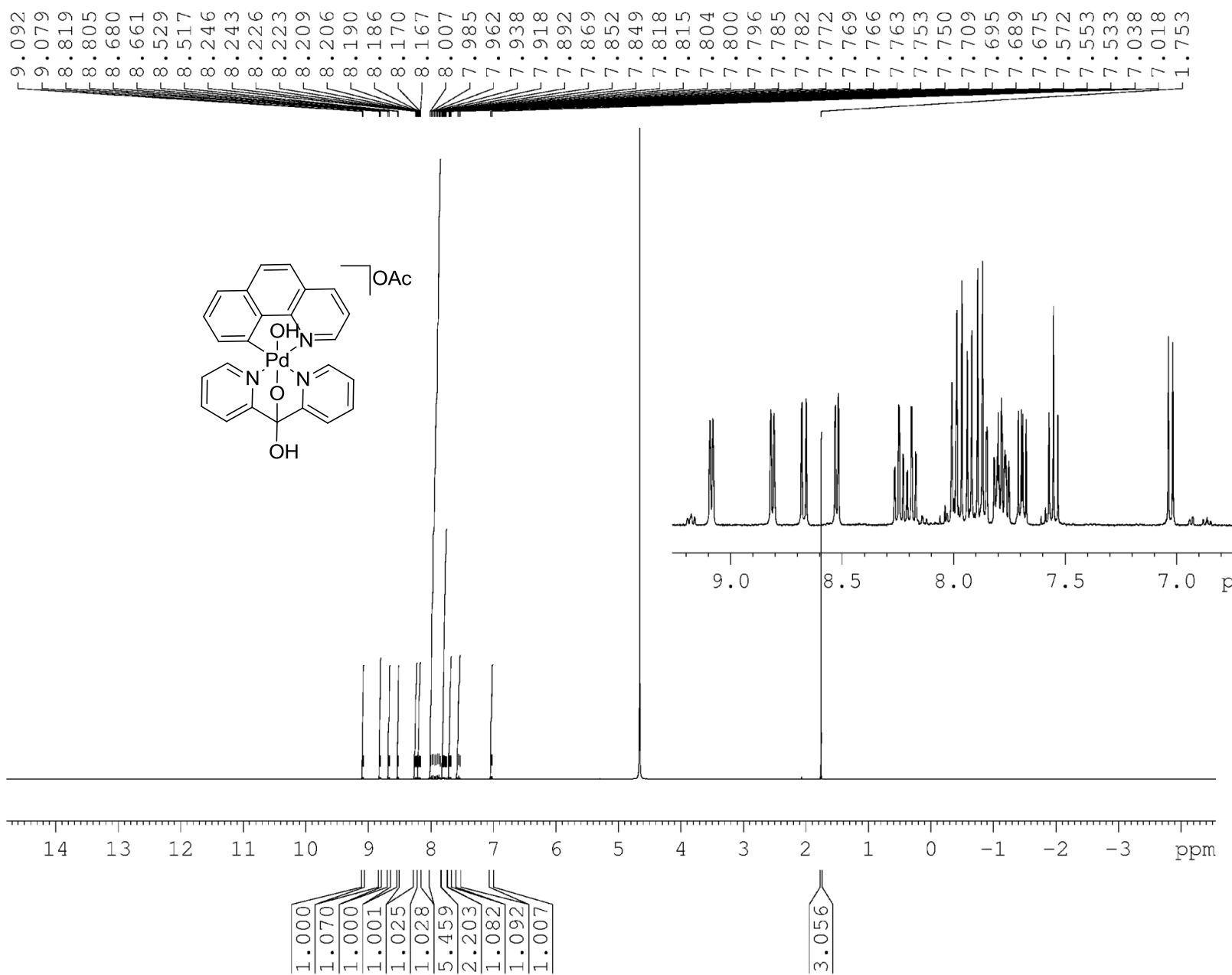
Figure 17. ^{1}H NMR of Benzo[*h*]quinolinyl Palladium(II) Hydroxo Di-(2-pyridyl) Ketone Complex (**24**) in DMSO–*d6*/D$_2$O, 22°C.
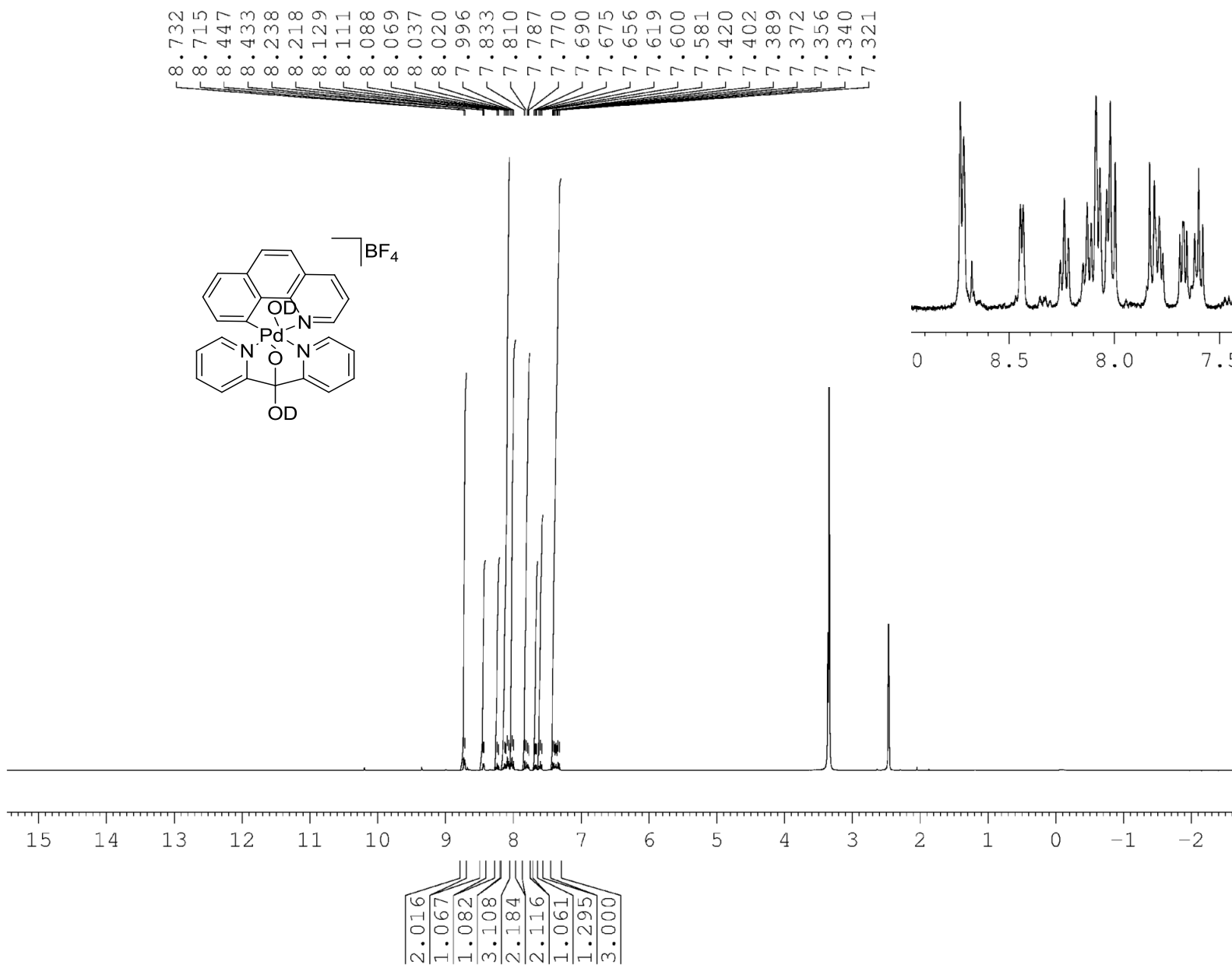
Figure 18. ^{1}H NMR of Benzo[*h*]quinolinyl Palladium(II) Hydroxo Di-(2-pyridyl) Ketone Complex H **(24)** in DMSO–*d6*/H$_2$O, 22°C.
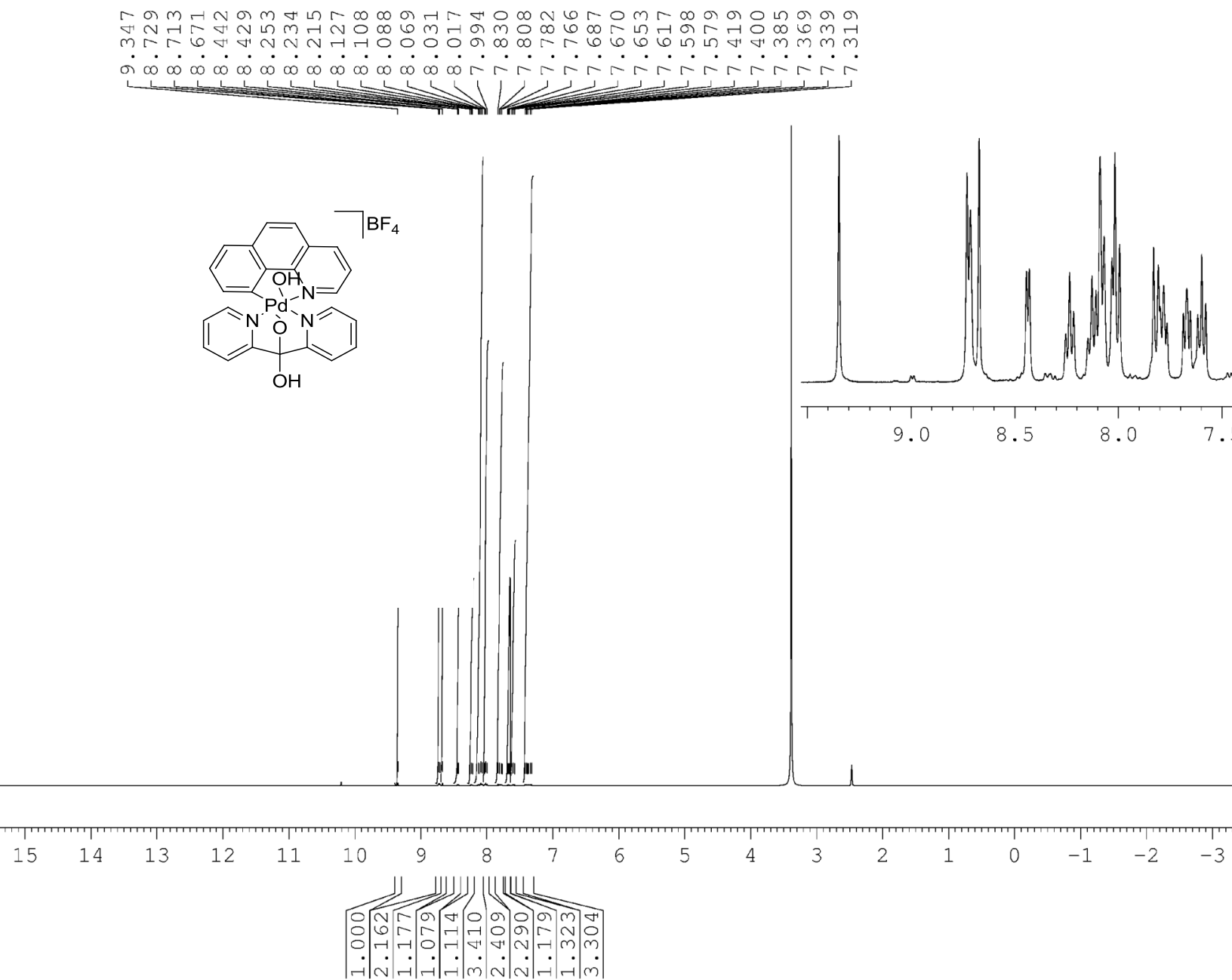
Figure 19. ^{13}C NMR Oxapalladacycle of Benzo[*h*]quinolinyl Palladium(II) Di-(2-pyridyl) Complex **(25)** in DMSO–*d6*.
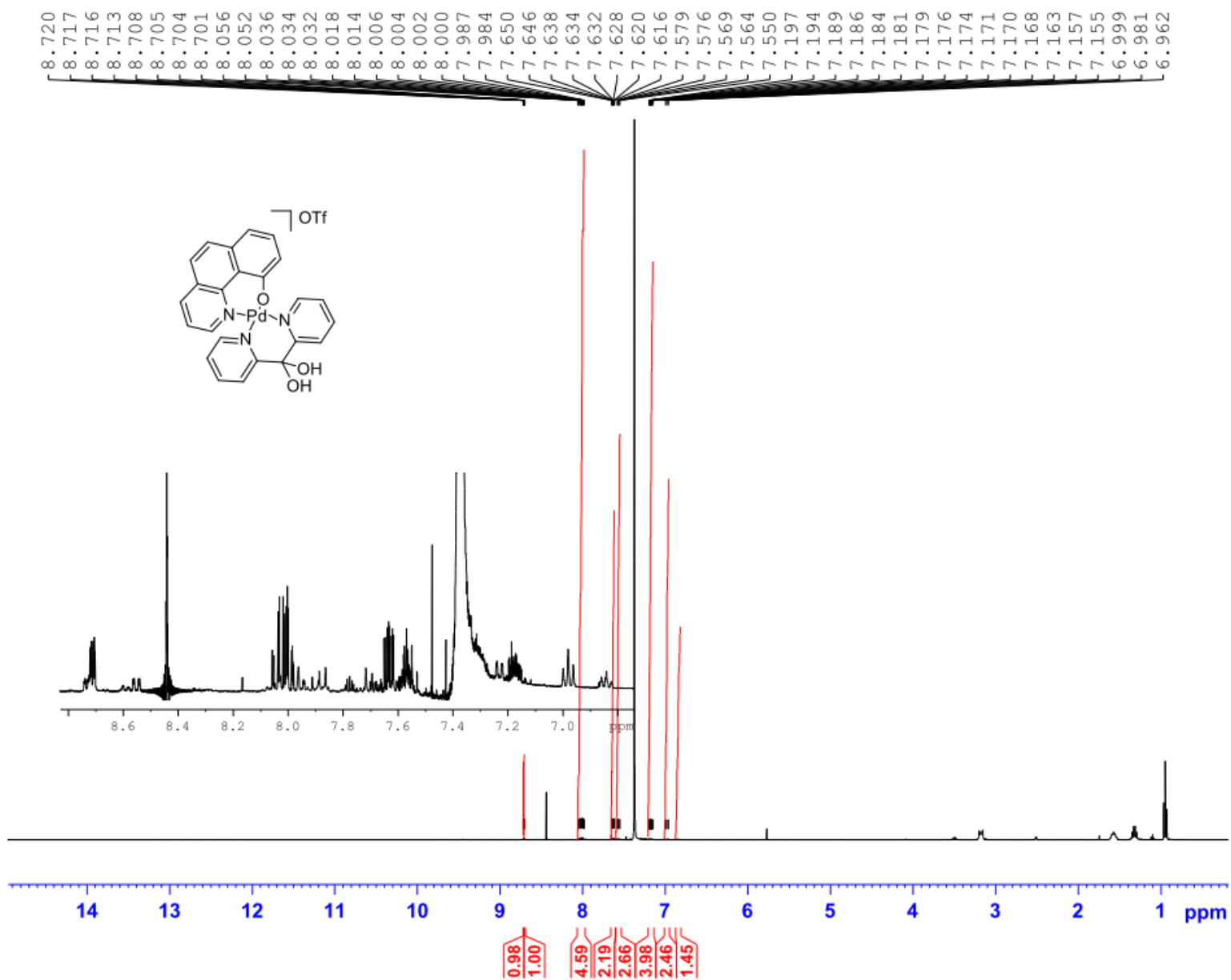
Figure 20. ^{1}H NMR of 2-(difluoro(phenyl)methyl)pyridyl-Palladium(II) Acetonitrile Complex **(36a)** in CDCl$_3$, 22°C.
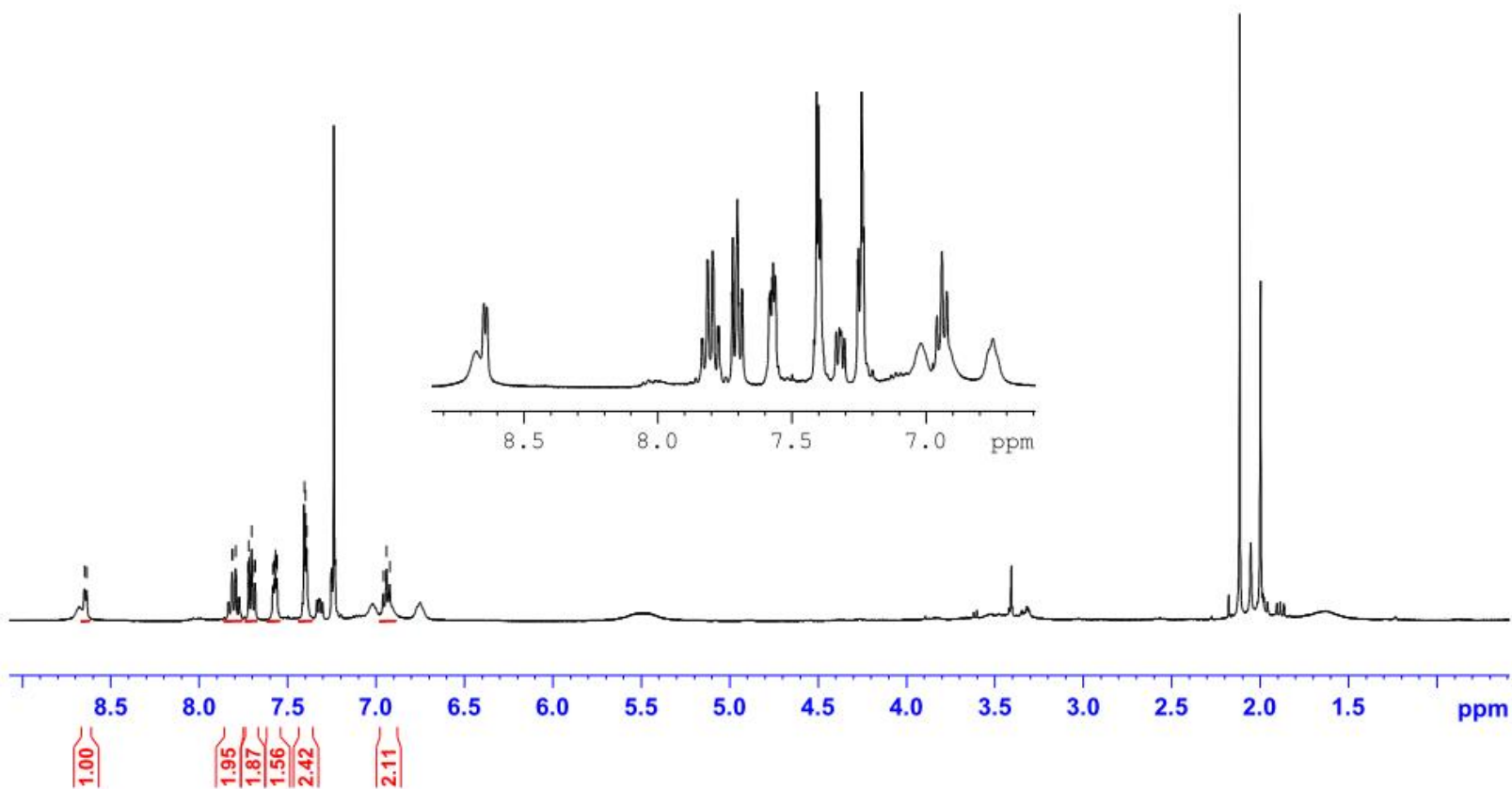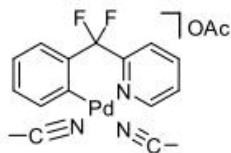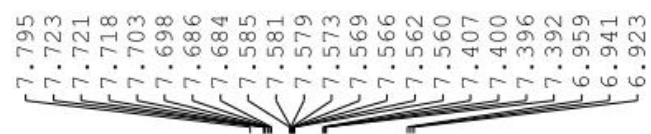
Figure 21. ^{13}C NMR of 2-(difluoro(phenyl)methyl)pyridyl-Palladium(II) Acetonitrile Complex **(36a)** in CDCl$_3$, 22°C.
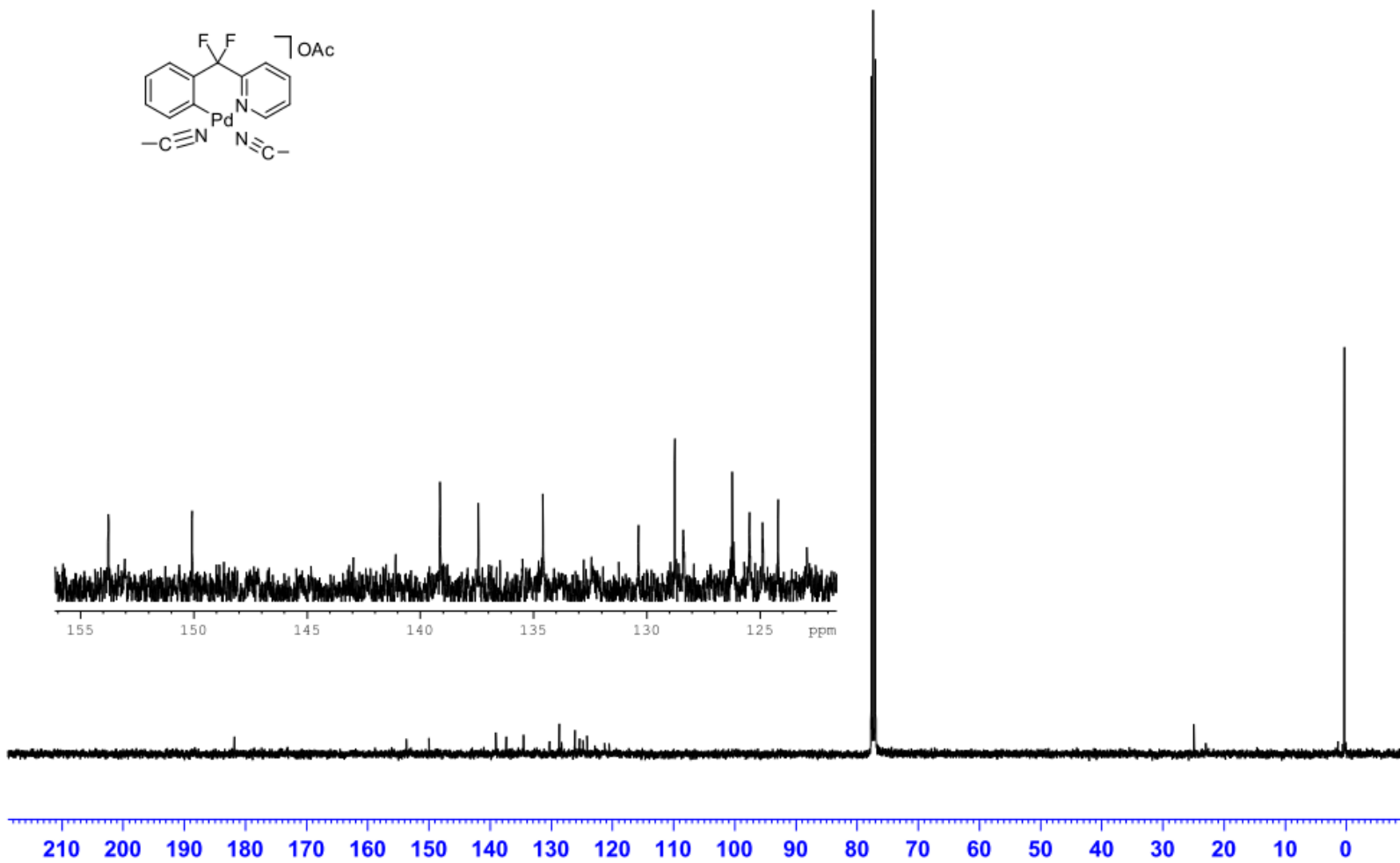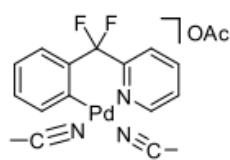
Figure 22. ^{19}F NMR of 2-(difluoro(phenyl)methyl)pyridine-Palladium(II) Acetonitrile Complex**(36a)** in CD$_3$CN, 22°C.
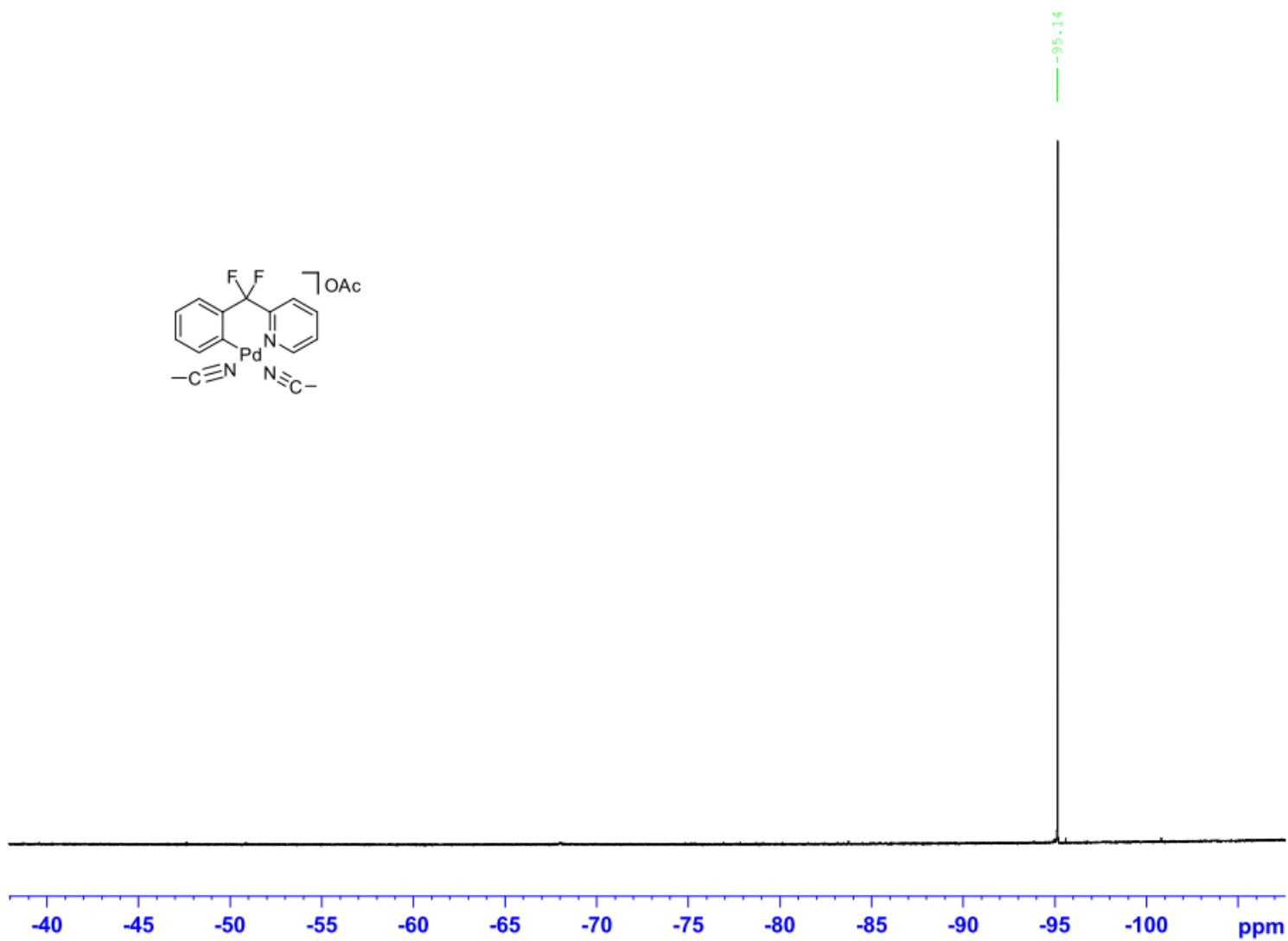
Figure 23. ^{1}H NMR of 2-(difluoro(phenyl)methyl)pyridyl Palladium(II) Di-2-pyridylketone Complex **(36)** in CD₃CN, 22°C.
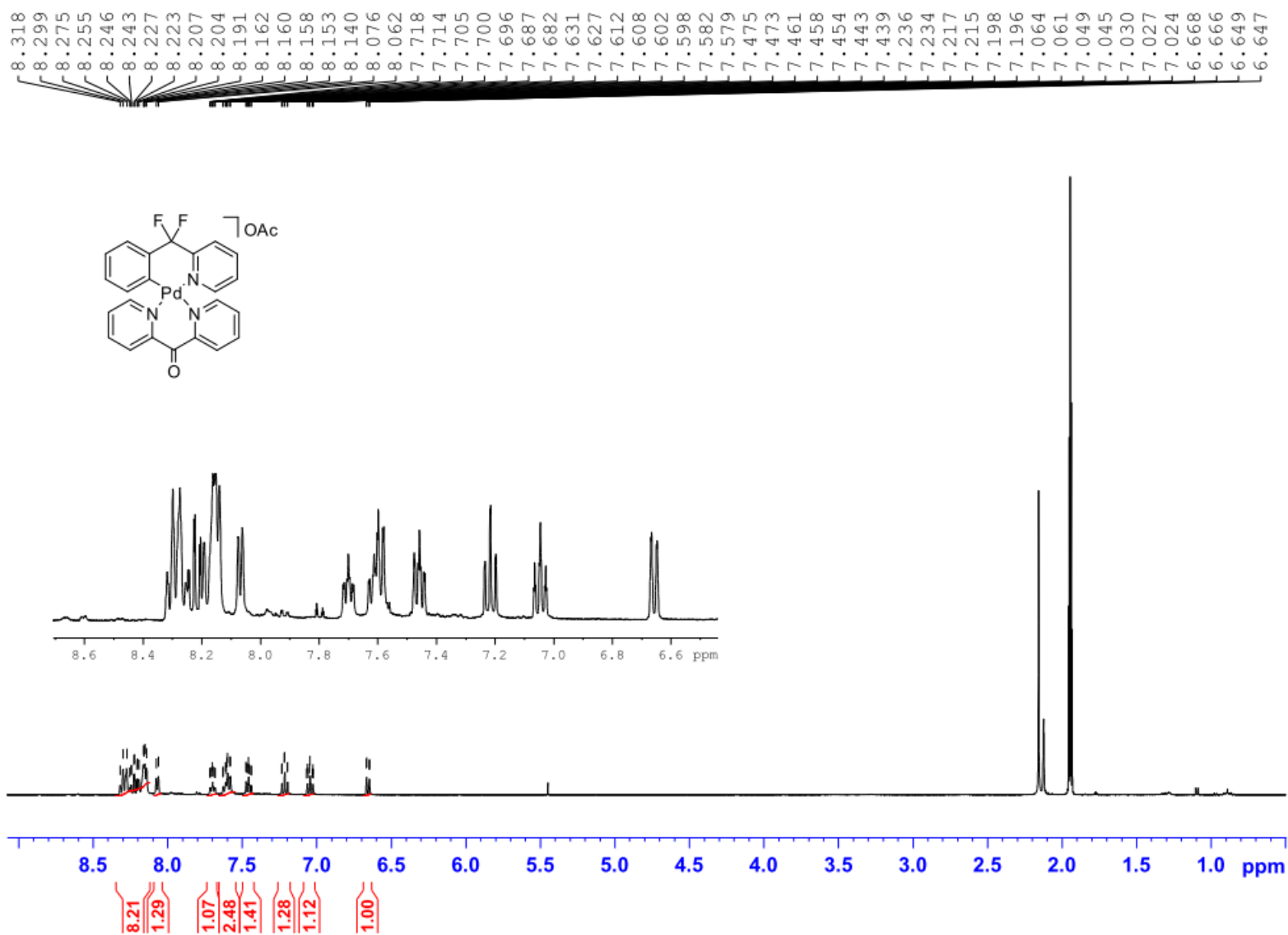
Figure 24. ^{13}C NMR of 2-(difluoro(phenyl)methyl)pyridyl Palladium(II) Di-2-pyridylketone Complex **(36)** in CD$_3$CN, 22°C.
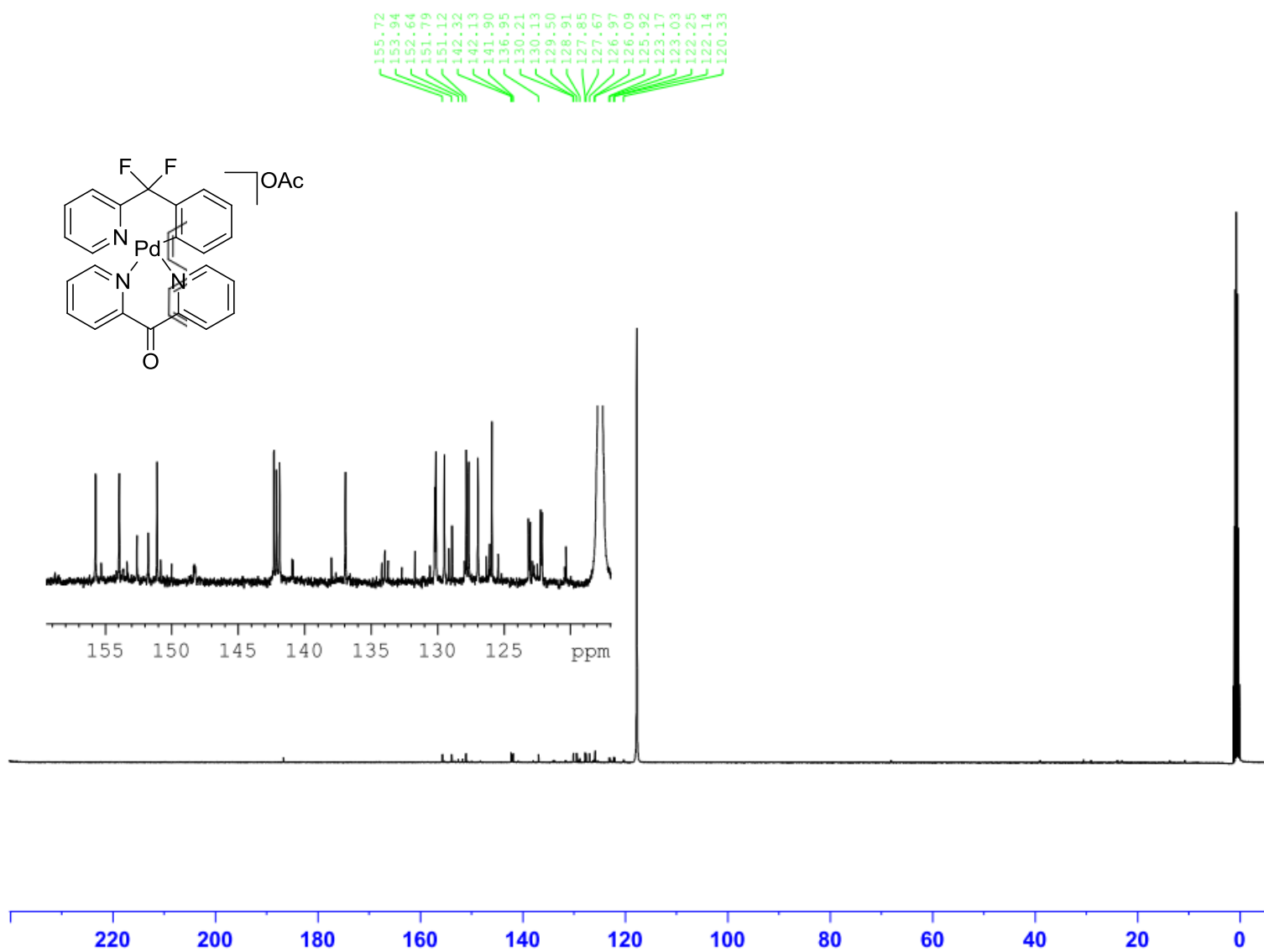
Figure 25. ^{19}F NMR of of 2-(difluoro(phenyl)methyl)pyridyl Palladium(II) Di-2-pyridylketone Complex **(36)** in CD$_3$CN , 22°C.
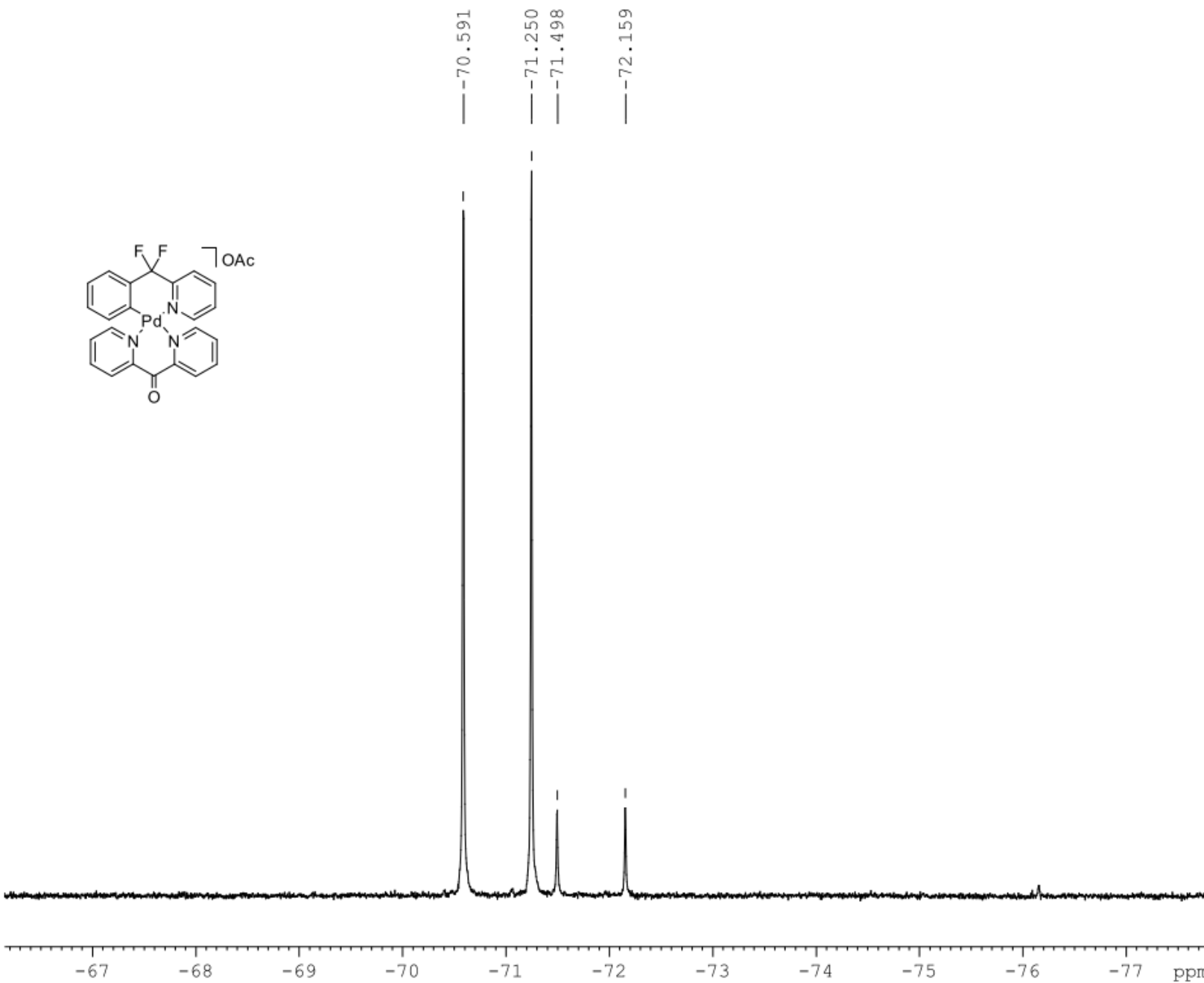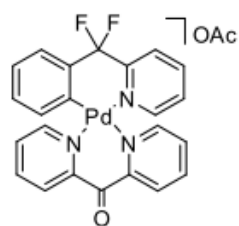
Figure 26. ^{1}H NMR of 8-(iodomethyl)quinoline(**11d**) in CDCl$_3$, 22°C.
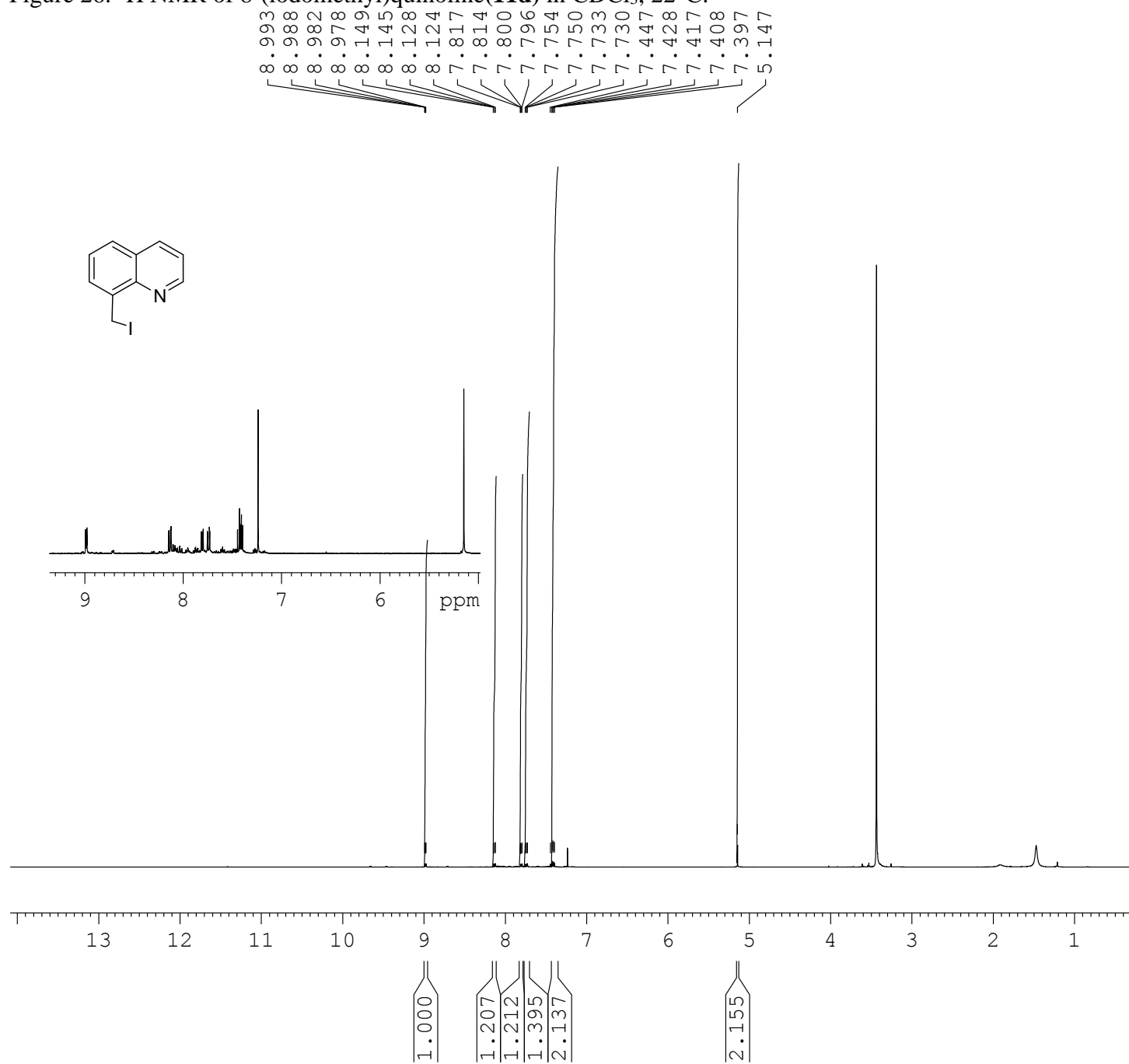
Figure 27. ¹H NMR of 8-(bromomethyl)quinoline(**11c**) in CDCl₃, 22°C.
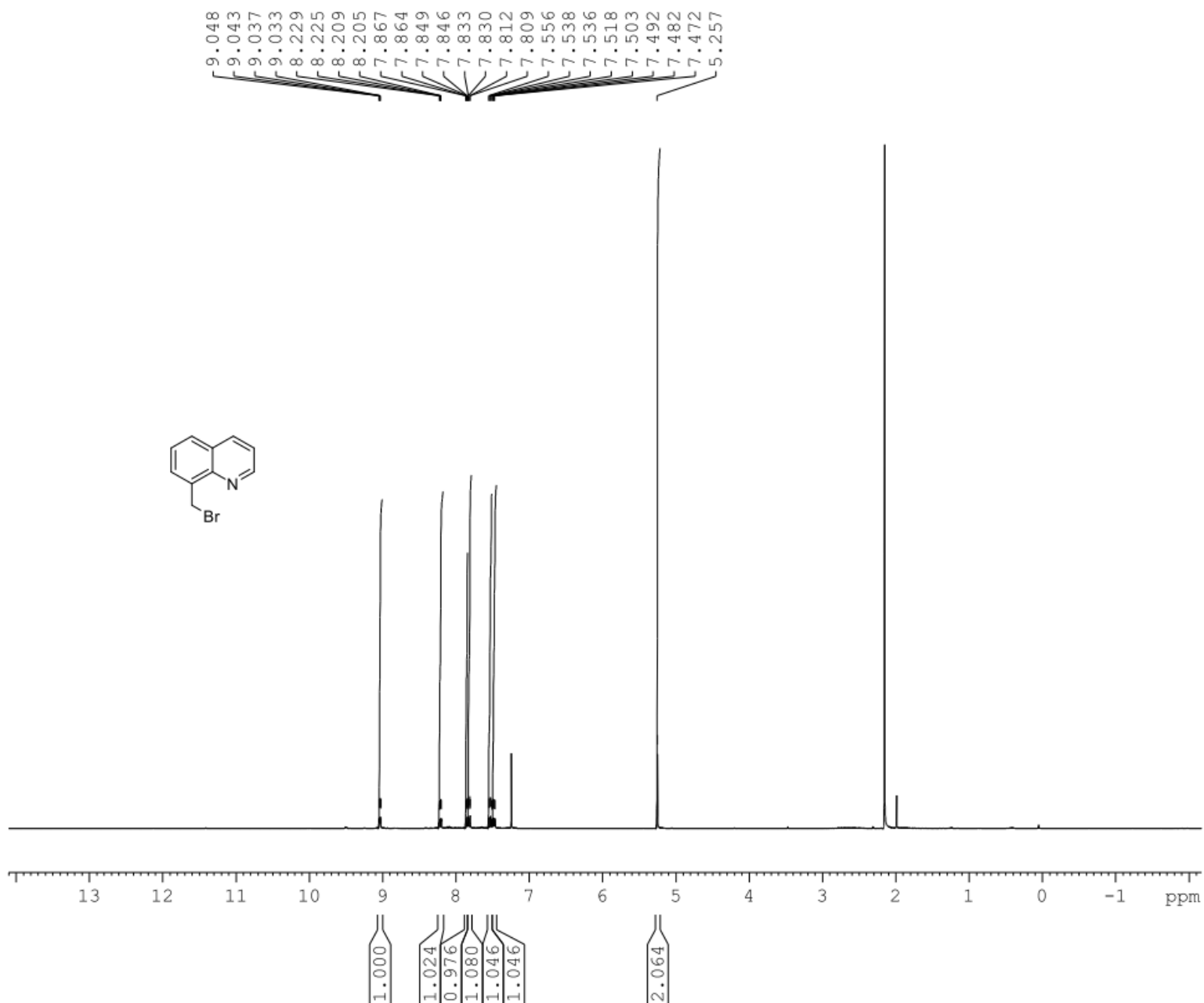
Figure 28. ^{1}H NMR of 8-(chloromethyl)quinoline(**11b**) in CDCl$_3$, 22°C.
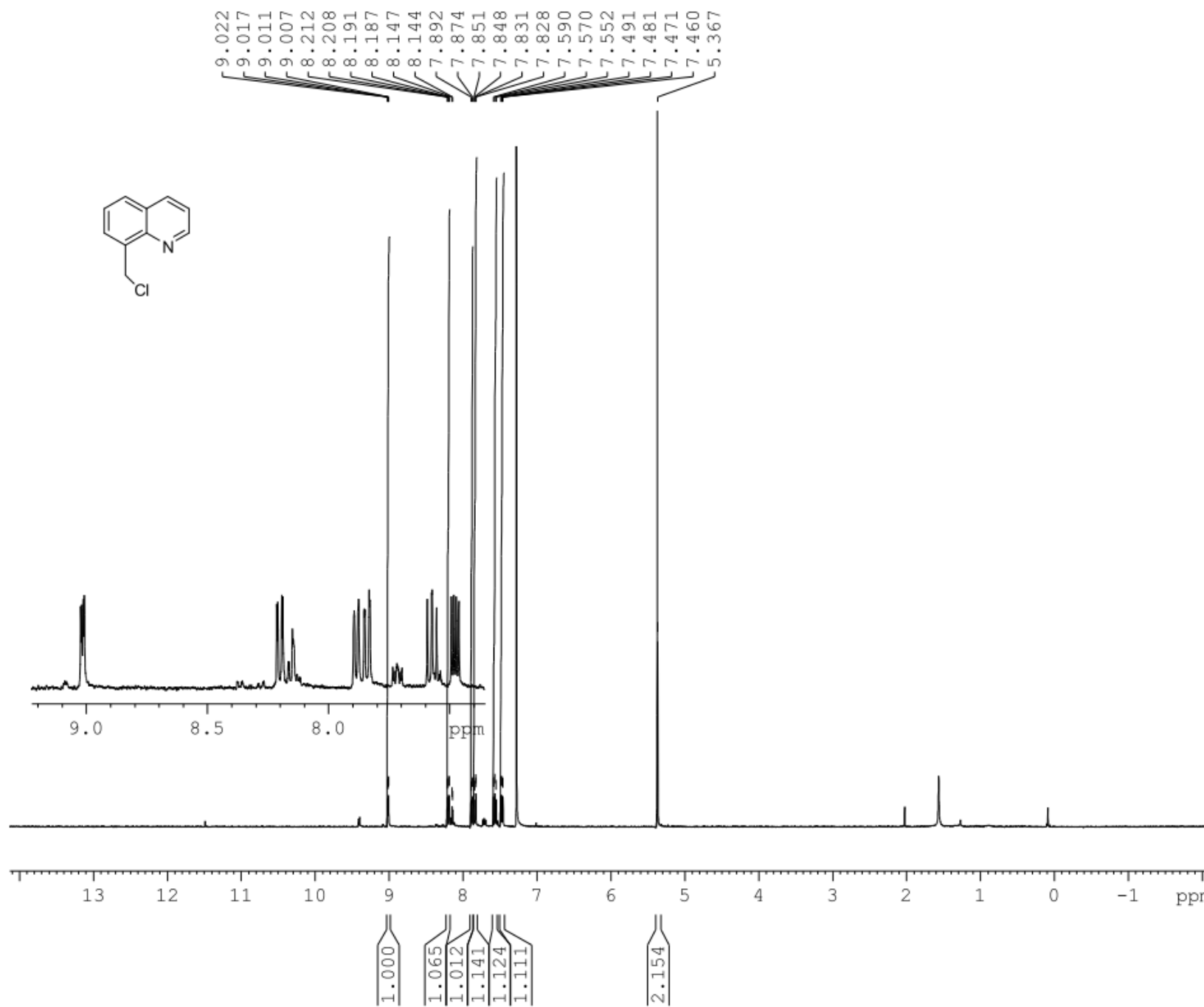
Figure 29. ^{1}H NMR of 8-(fluoromethyl)quinoline (**11a**) in CDCl$_3$, 22°C

8.912
8.905
8.902
8.169
8.151
8.148
7.817
7.809
7.802
7.789
7.580
7.560
7.542
7.439
7.429
7.419
7.408
6.190
6.071

1.068
1.196
2.000
1.197
1.132
2.022
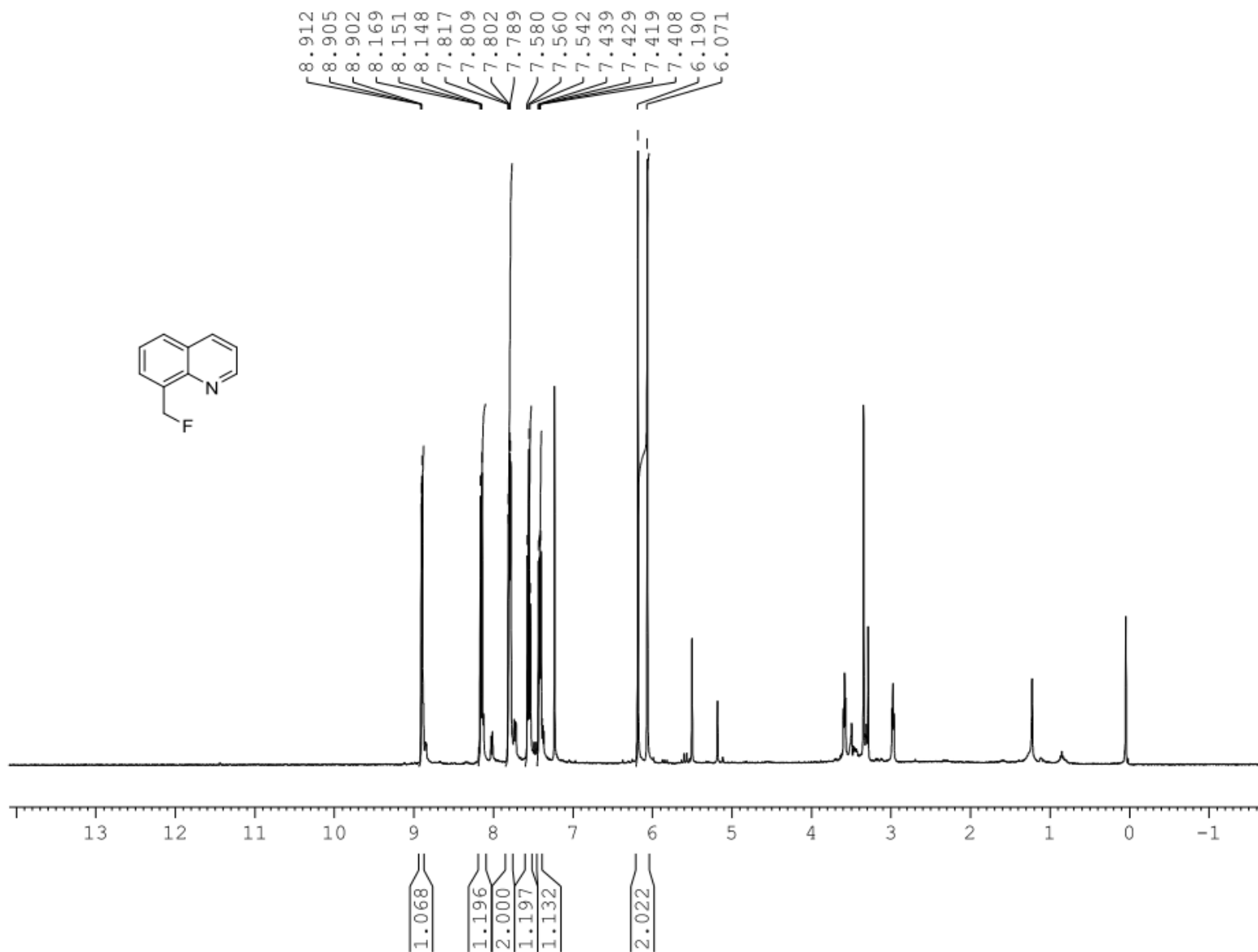
Figure 30. ^{19}F NMR of 8-(fluoromethyl)quinoline(**11a**) in CDCl$_3$, 22°C.
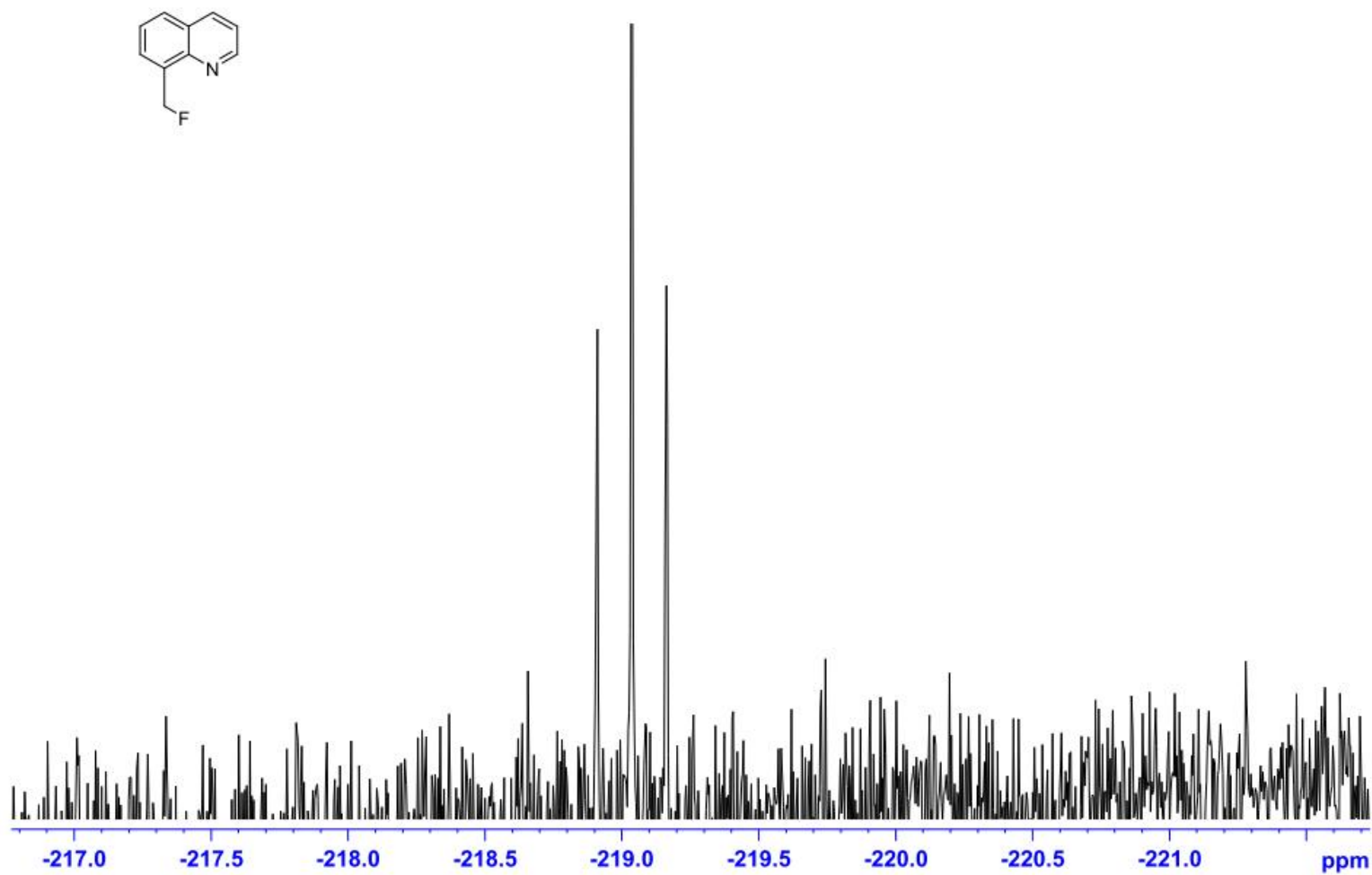
Figure 31. ^{1}H NMR of quinoline-8-carbaldehyde(**11f**) in CDCl$_3$, 22°C.
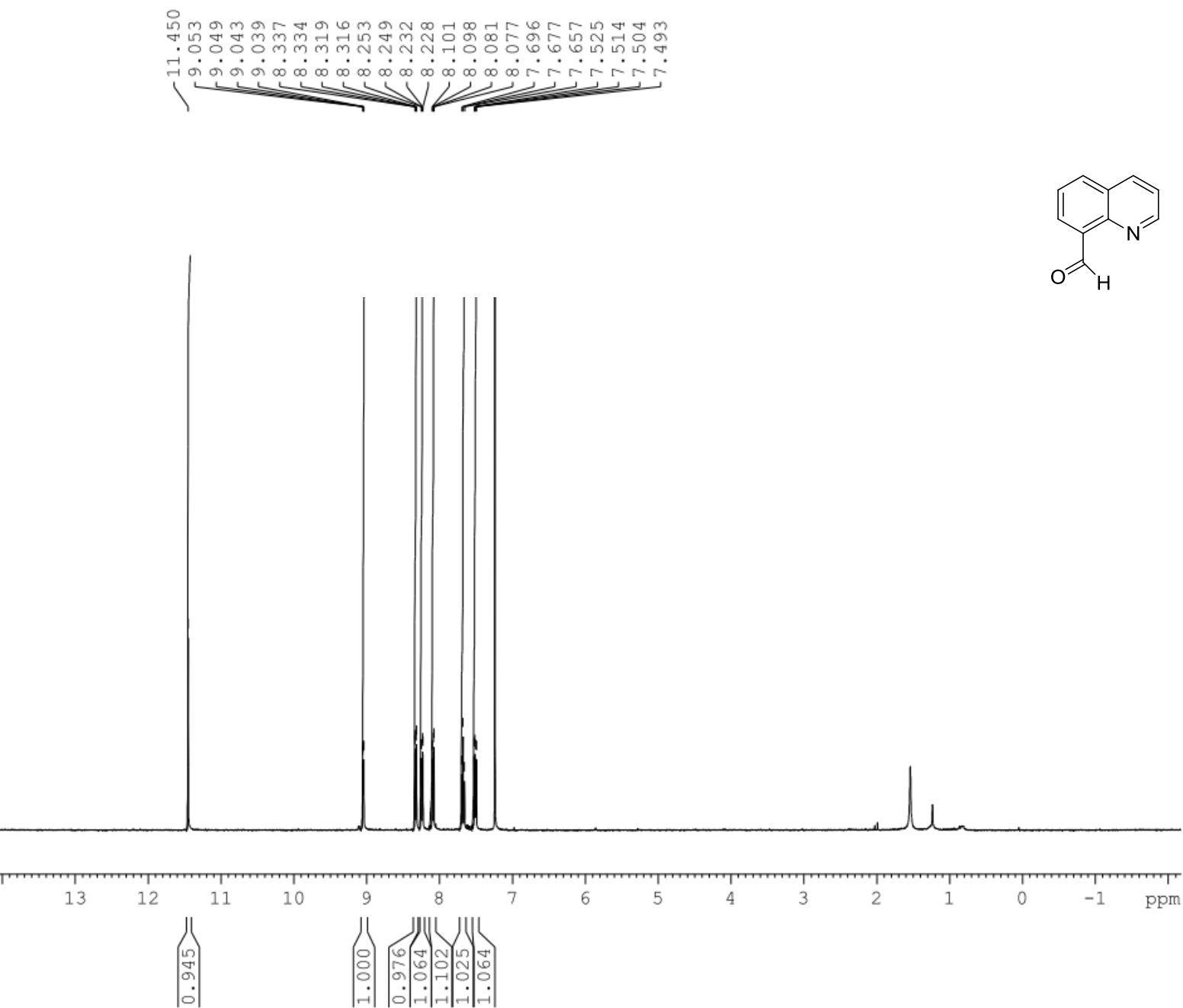
Figure 32. ^{1}H NMR of quinoline-8-quinomethanol(**11e**) in CDCl$_3$, 22°C.

8.866
8.861
8.855
8.851
8.197
8.192
8.176
8.172
7.757
7.753
7.736
7.733
7.579
7.577
7.561
7.496
7.479
7.476
7.458
7.446
7.435
7.425
7.414
5.189
5.056

1.000
1.005
1.015
1.007
0.804
1.293
1.983
0.864
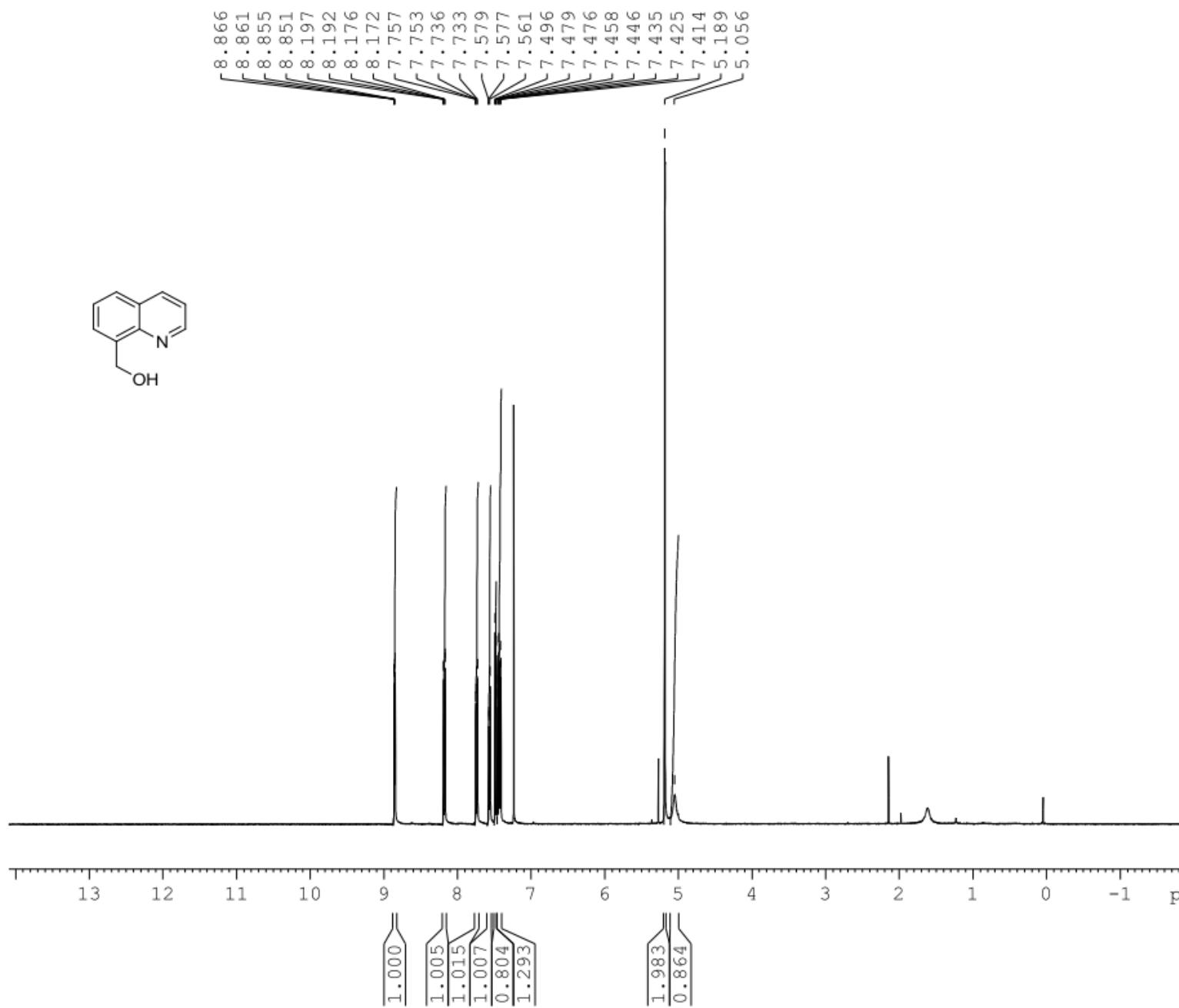
Figure 33. ^{1}H NMR of Synthesis of 2-(4-aminopyridin-2-yl)-2-methylpropan-1-ol **(18d)** in CDCl$_3$, 22°C.
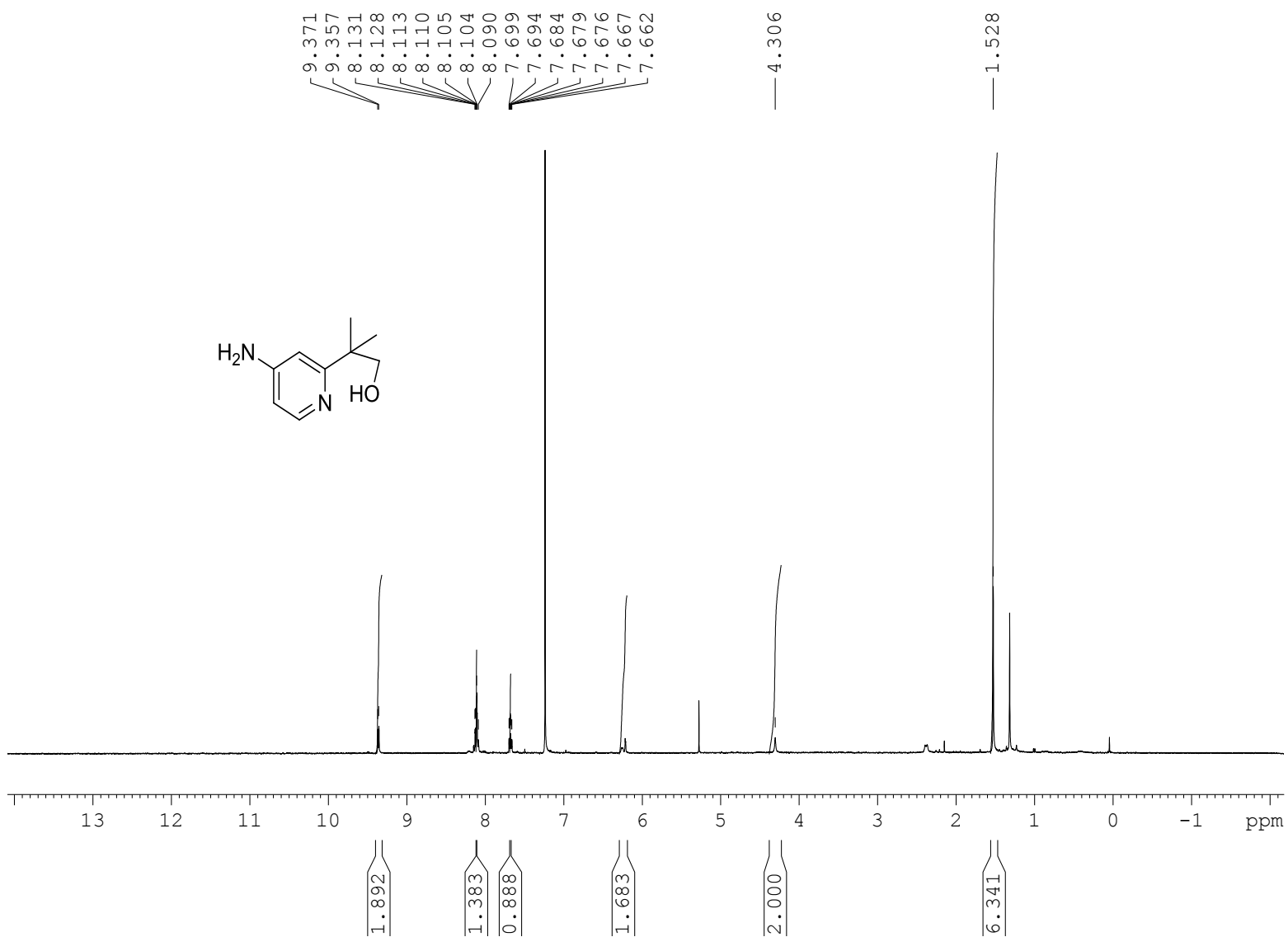
Figure 34. ^{1}H NMR of 2-tert-butylpyridin-4-amine-Fluoro(**19d**) in CD$_3$CN, 22°C.
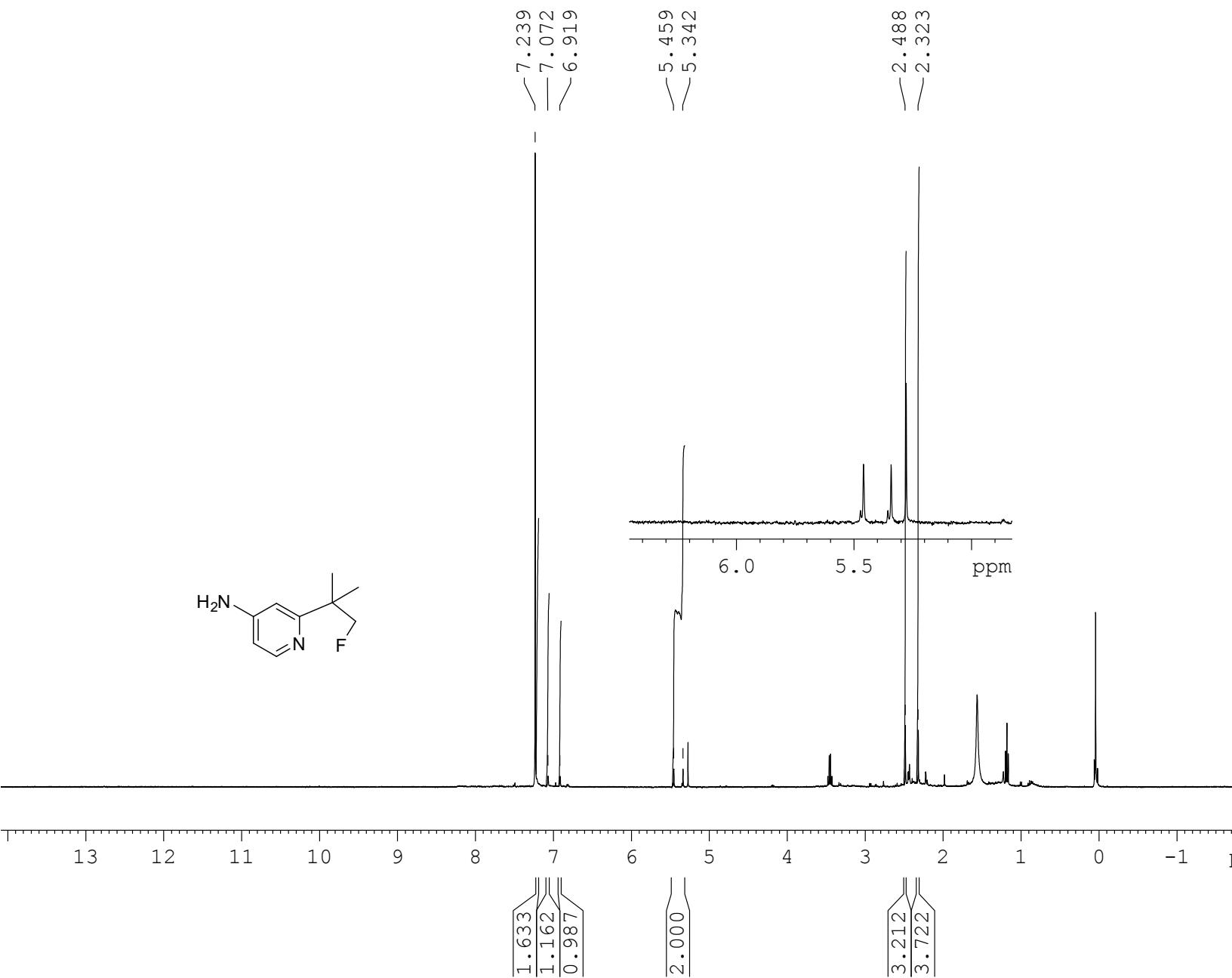
Figure 35. ^{19}F NMR of 2-tert-butylpyridin-4-amine-Fluoro(**19d**) in CD$_3$CN, 22°C.
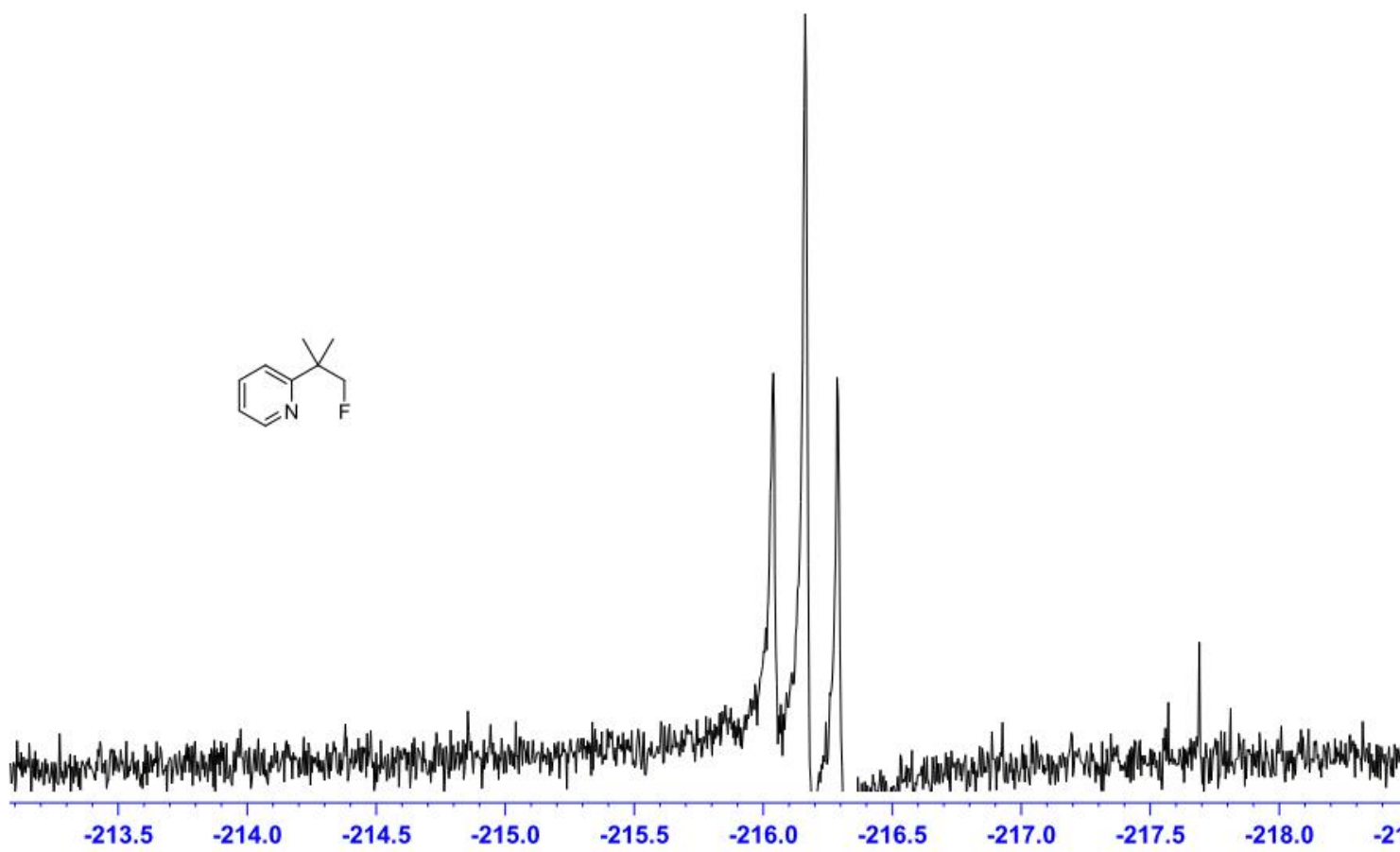
Figure 36. ^{1}H NMR of Benzo[*h*]quinolin-10-ol **(24a)** in CDCl$_3$, 22°C.
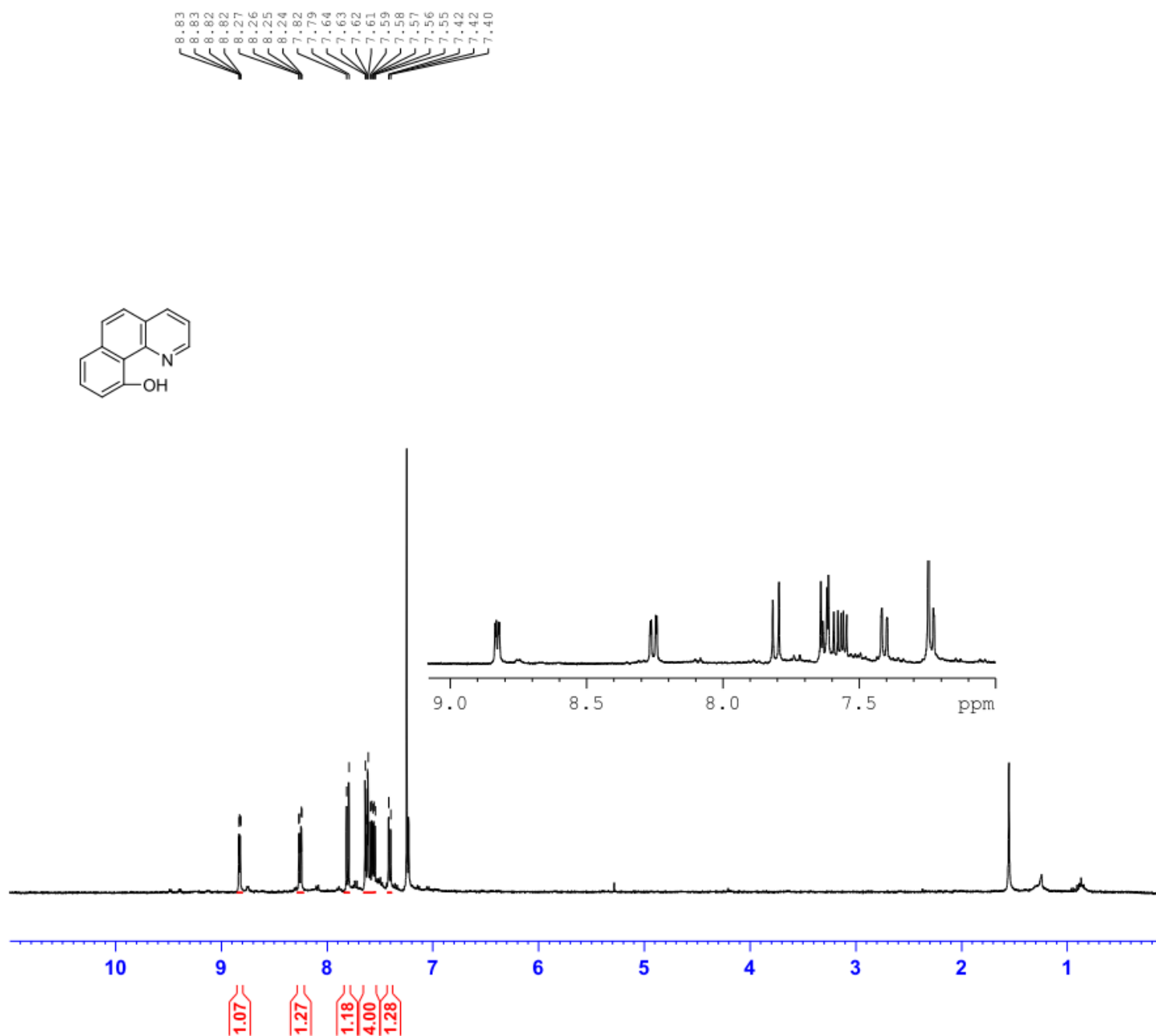
Figure 37. ^{1}H NMR of Homocoupling of Benzo[*h*]quinolone (**28**) in CDCl$_3$, 22°C.
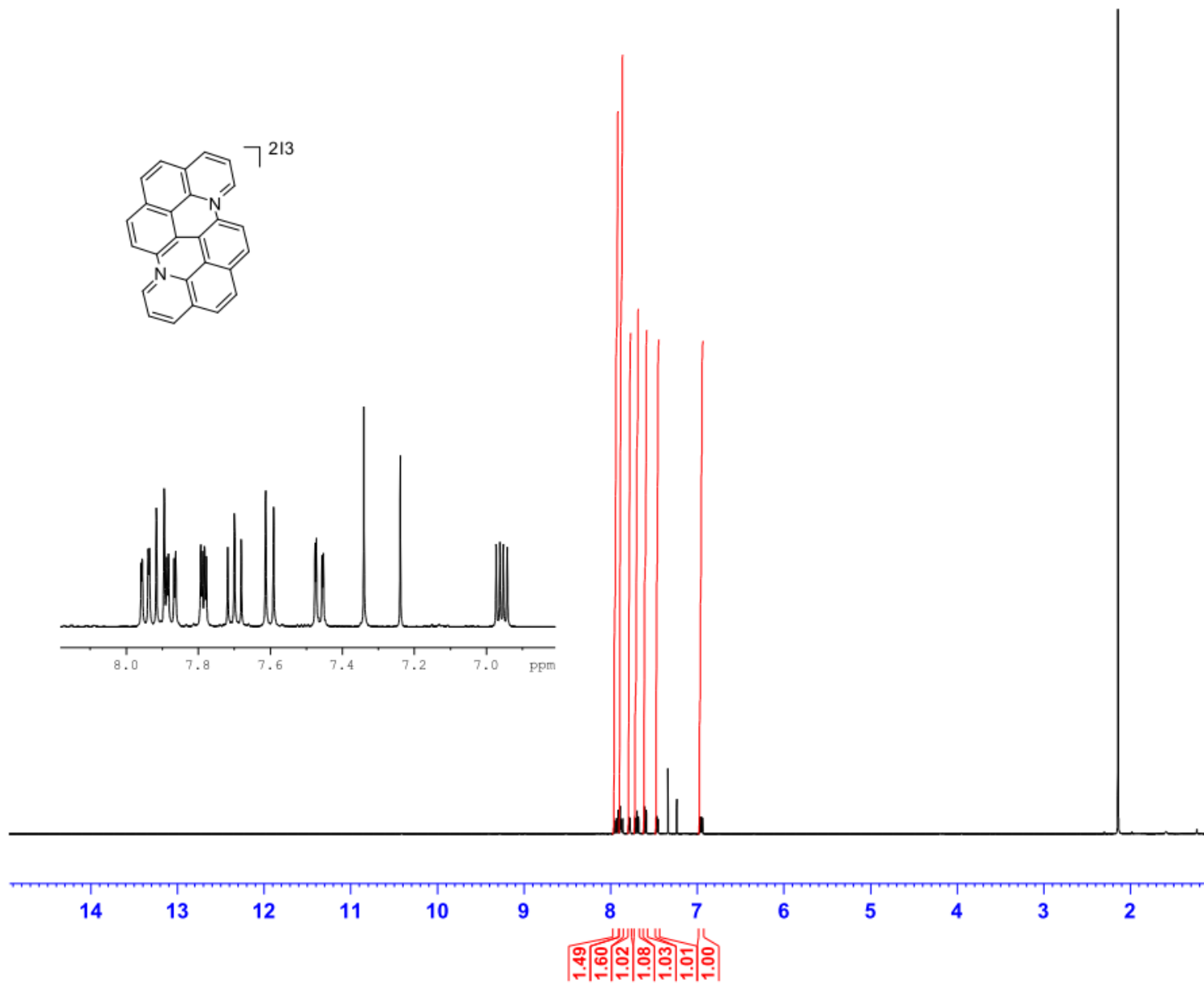
Figure 38. ^{13}C NMR of Homocoupling of Benzo[*h*]quinoline **(28)** in CDCl$_3$, 22°C.

147.69
146.95
146.26
134.97
134.60
130.67
129.02
128.92
128.75
127.48
126.92
125.50
120.56

213
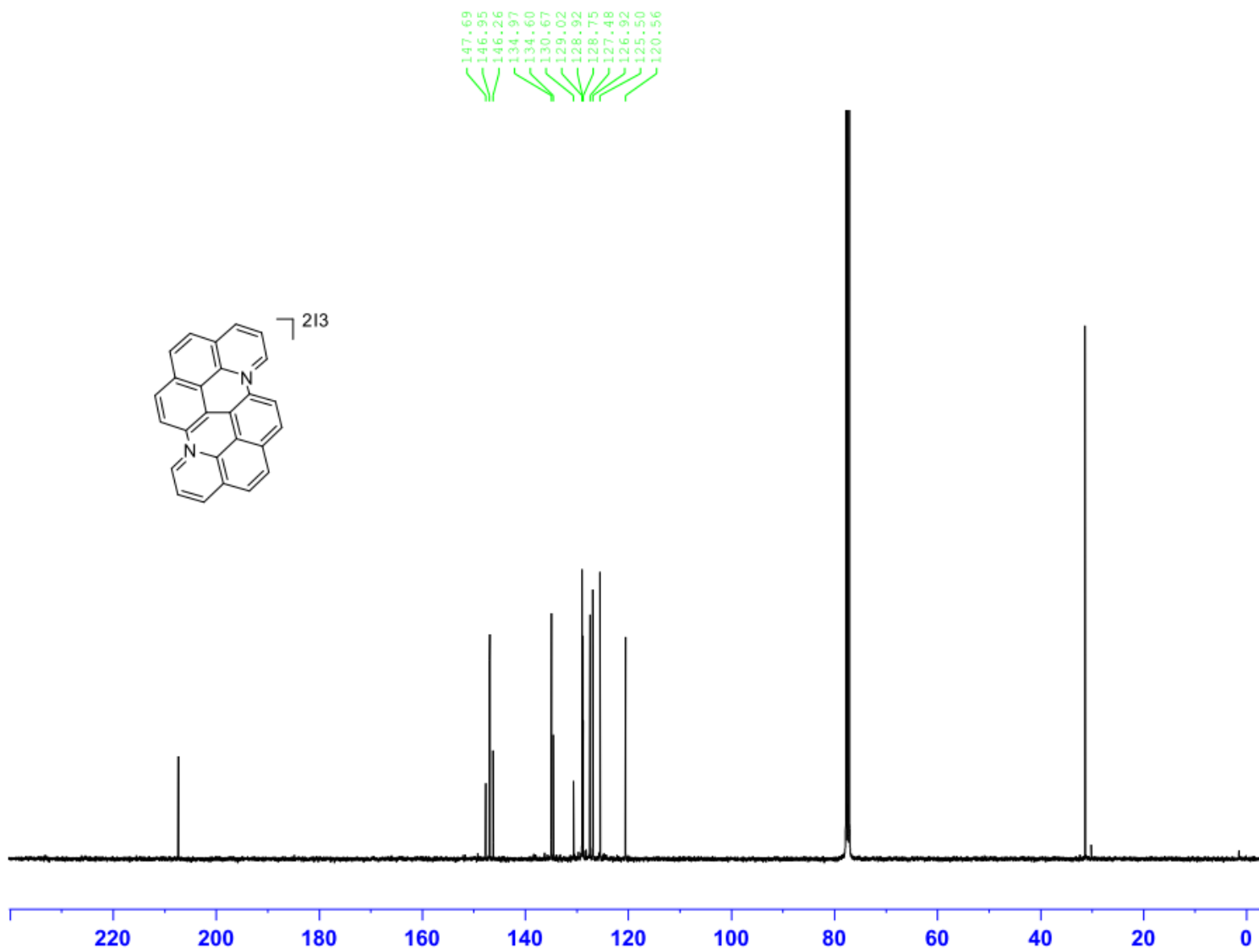
Figure 39. ^{1}H NMR of 2-(difluoro(pyridin-2-yl)methyl)phenol **(39a)** in CDCl$_3$ and DPK, 22°C.
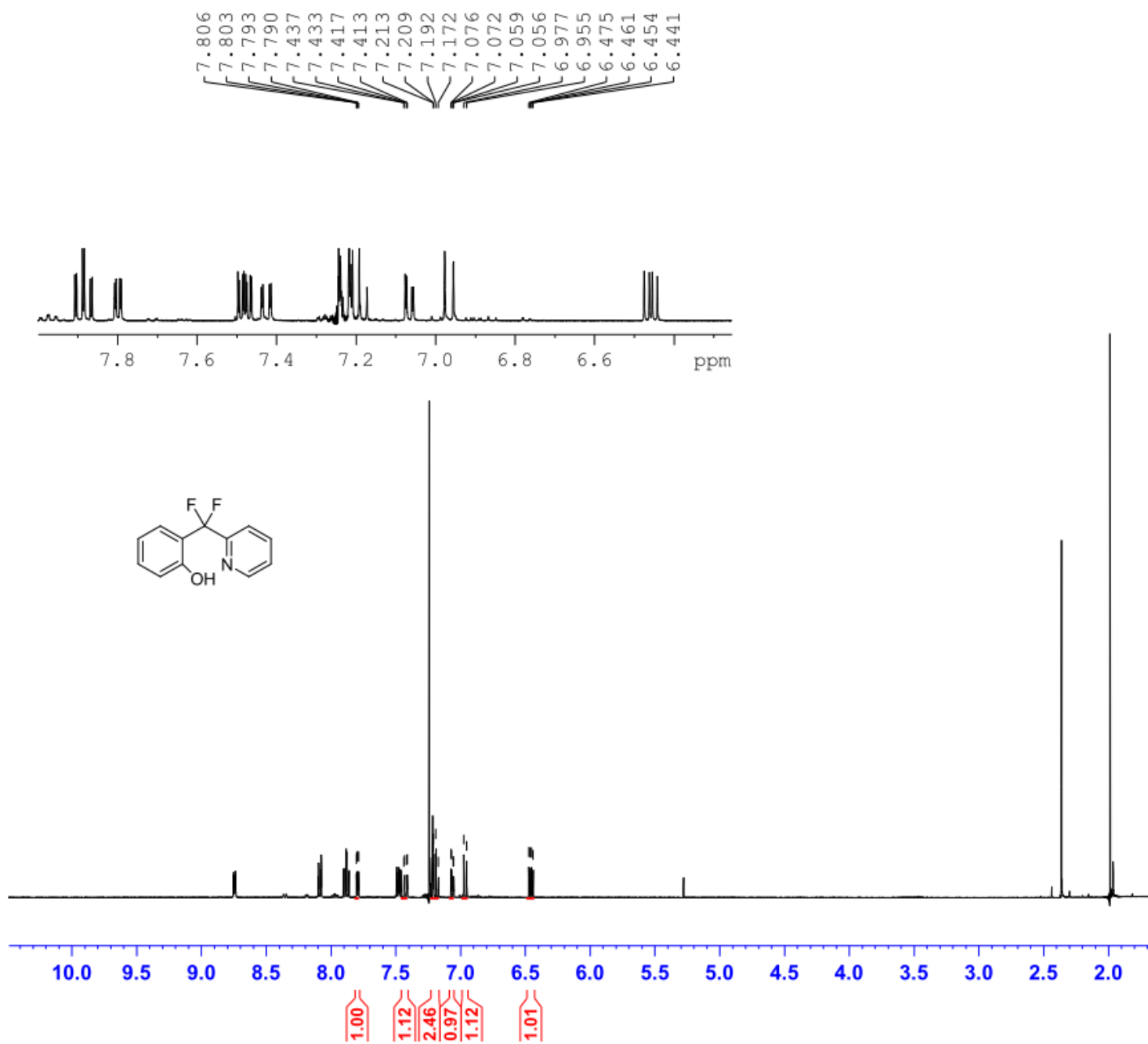
Figure 40. ^{1}H NMR of 2-(1-bromo-2-methylpropan-2-yl)pyridin-4-amine **(21)** and DPK in CDCl₃, 22°C.
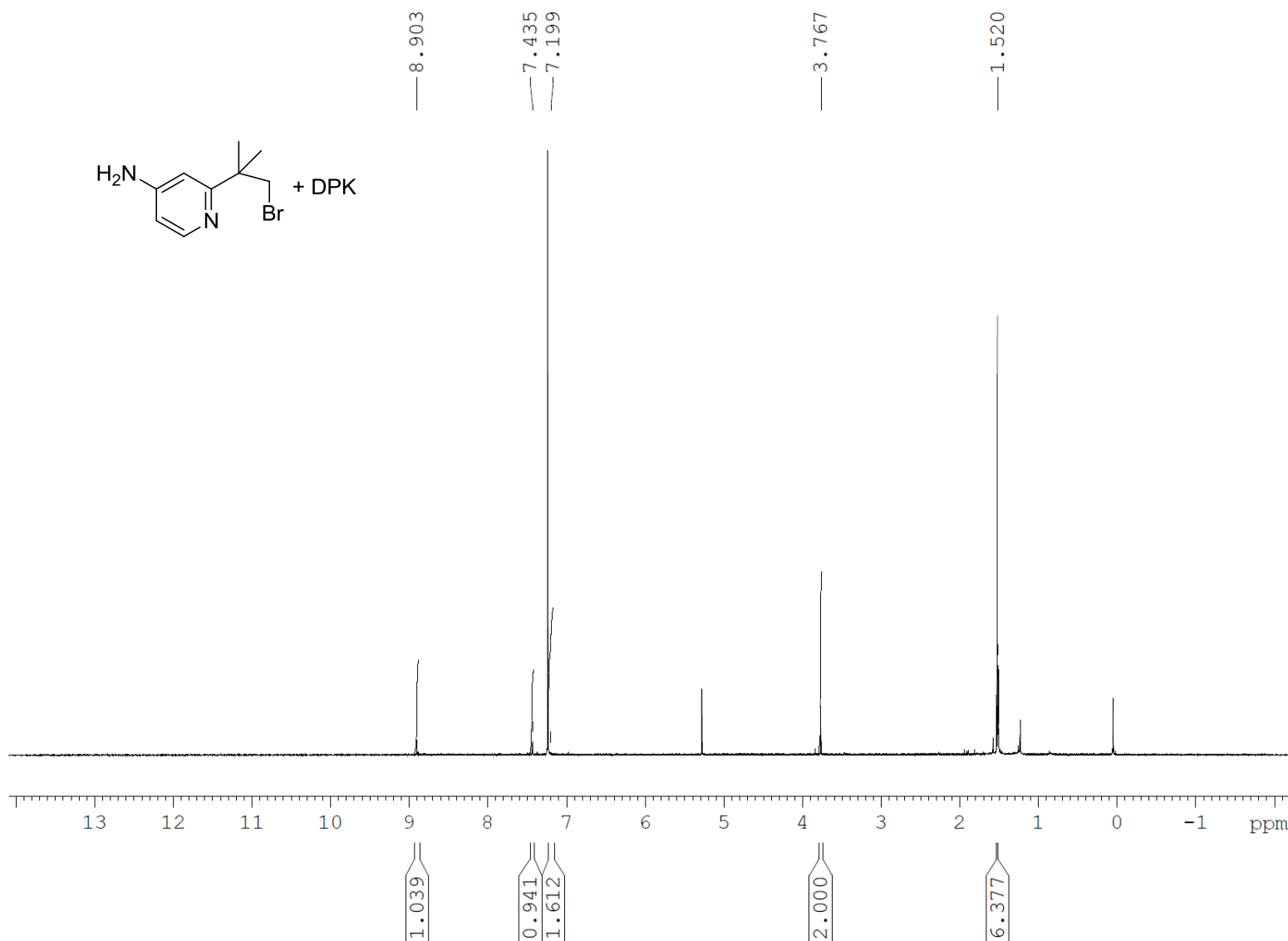
Figure 41. ^{1}H NMR of 2-tert-butyl-5,5-dimethyl-4,5-dihydrooxazole**(40a)** in CDCl$_3$, 22°C.
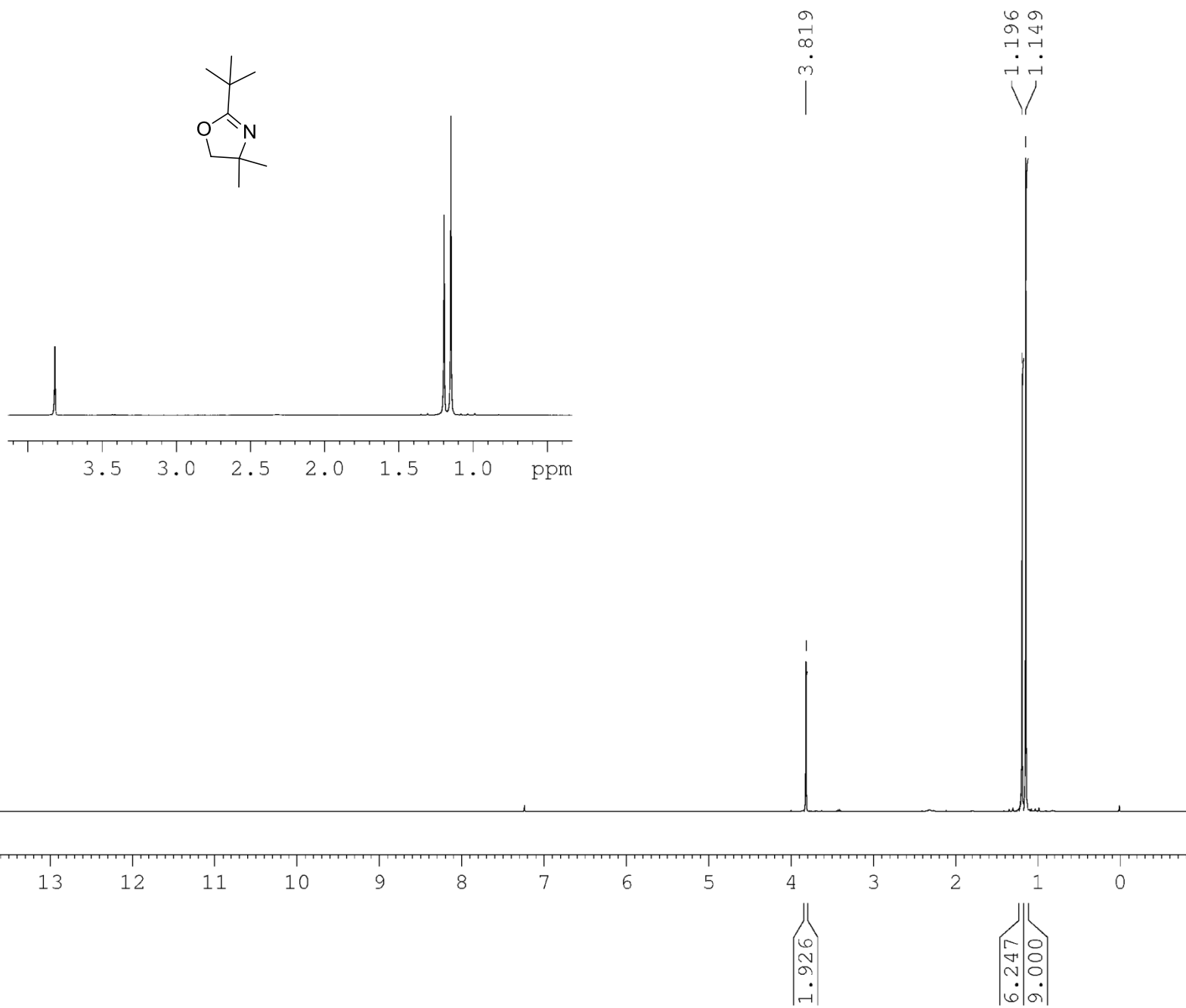
Figure 42. ^{1}H NMR of 4-tert-butyl-2-methyl-4,5-dihydrooxazole(**40b**) in CD$_2$Cl$_2$, 22°C.
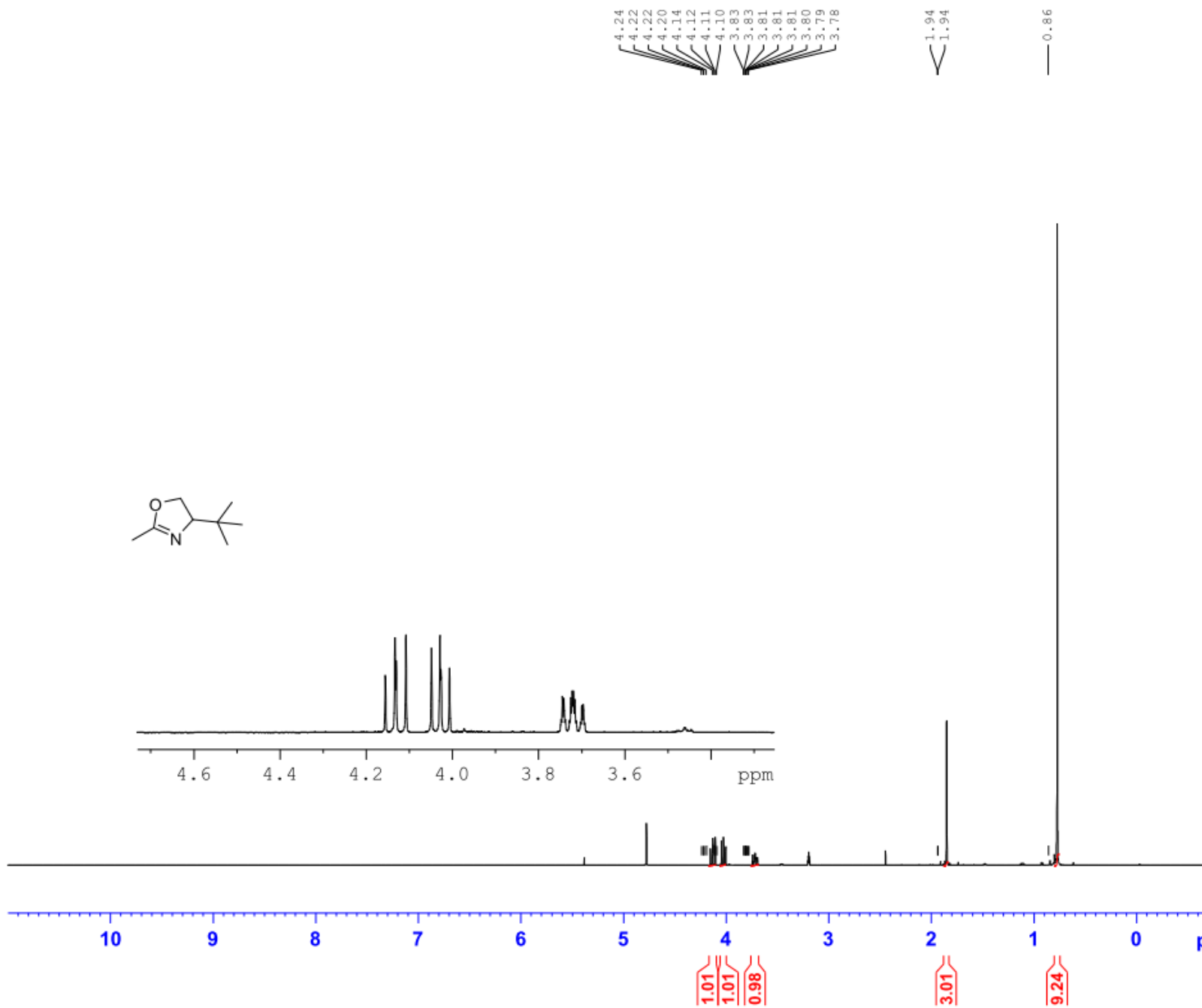
Figure 43. ^{1}H NMR of 2-(difluoro(phenyl)methyl)pyridine(**35**) in CDCl$_3$, 22°C.
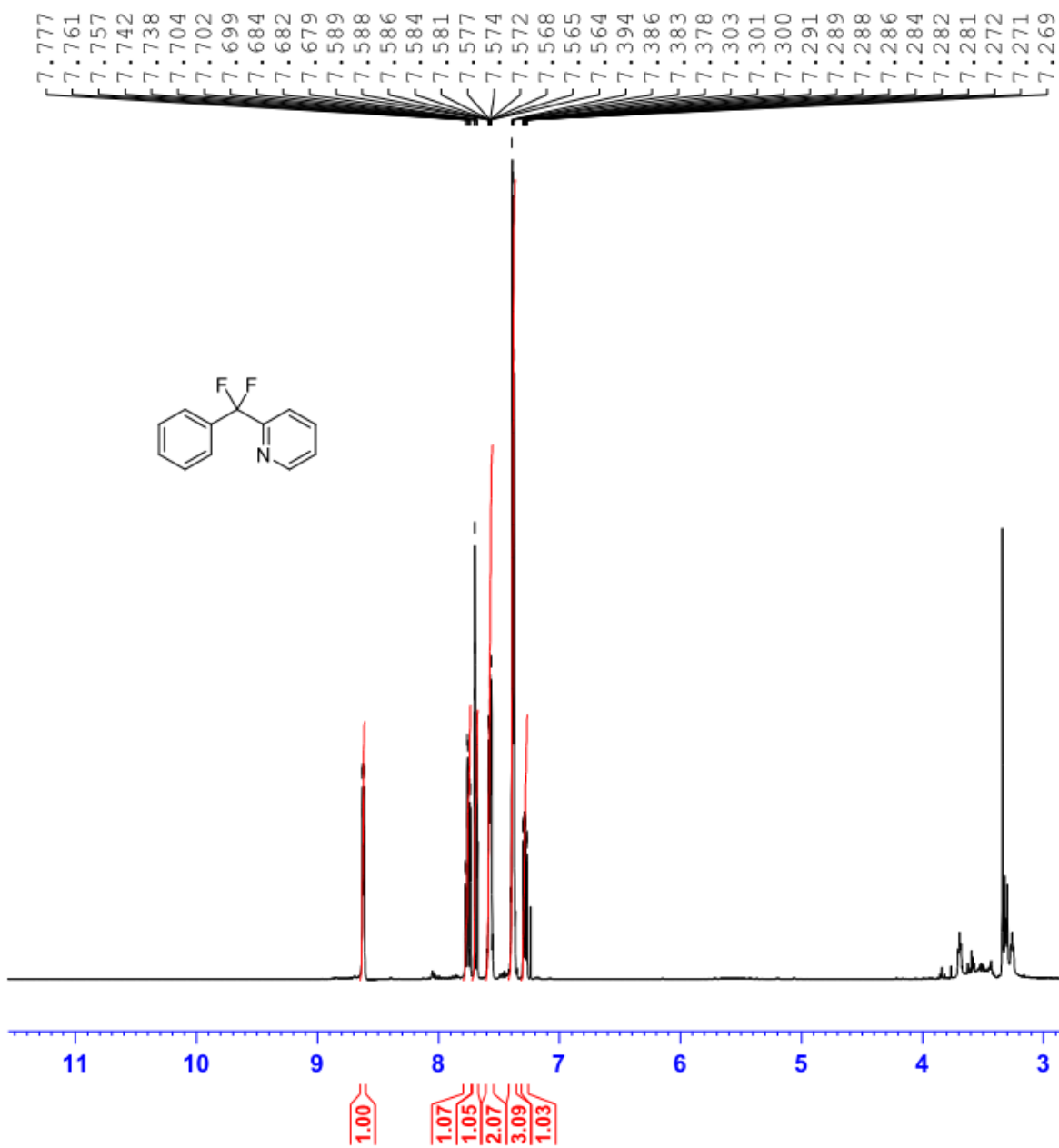
Figure 44. ^{13}C NMR of 2-(difluoro(phenyl)methyl)pyridine **(35)** in CDCl$_3$, 22°C.
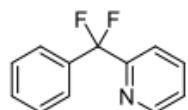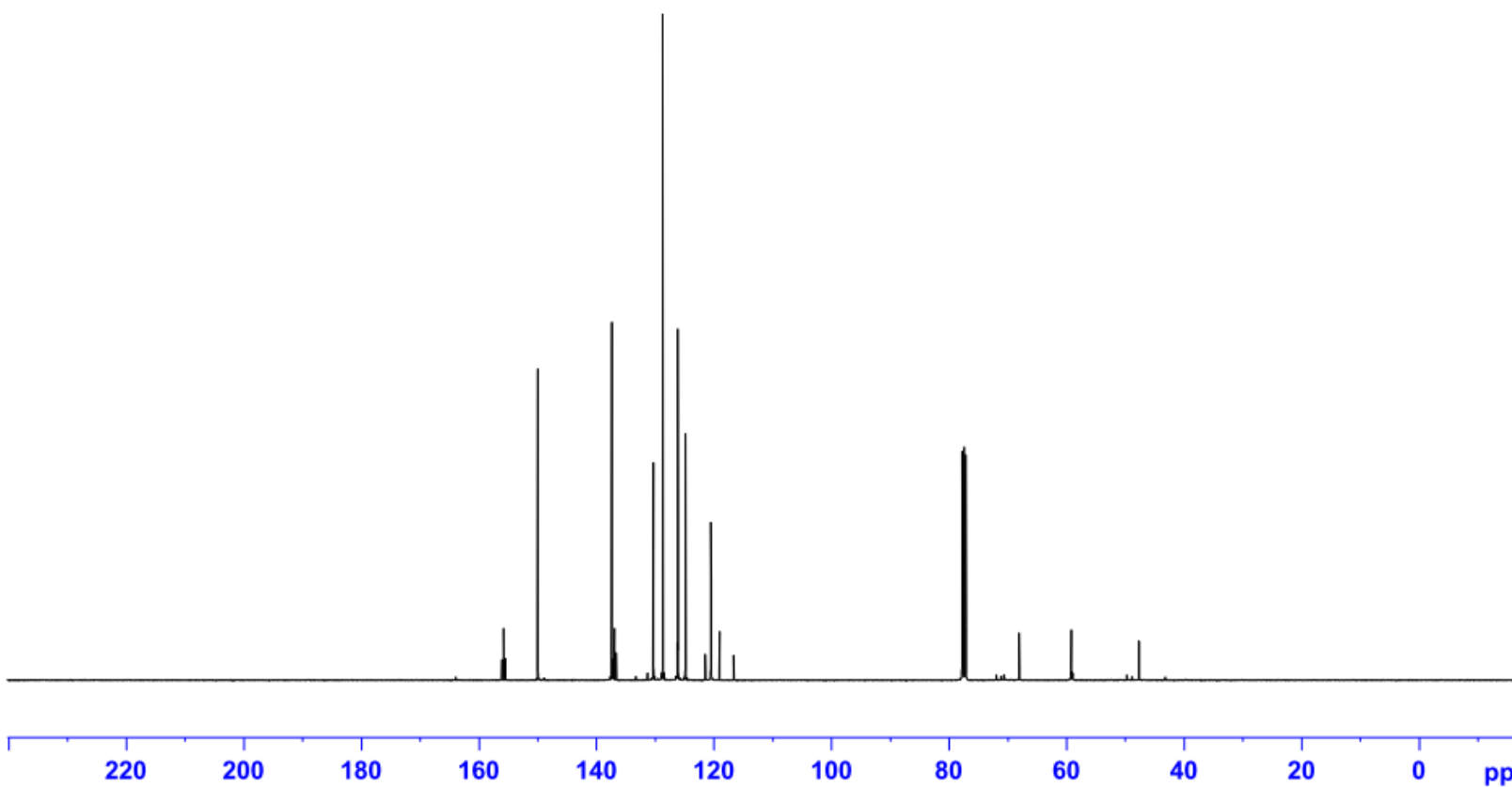
Figure 45. ^{19}F NMR of 2-(difluoro(phenyl)methyl)pyridine(**35**) in CDCl$_3$, 22°C.
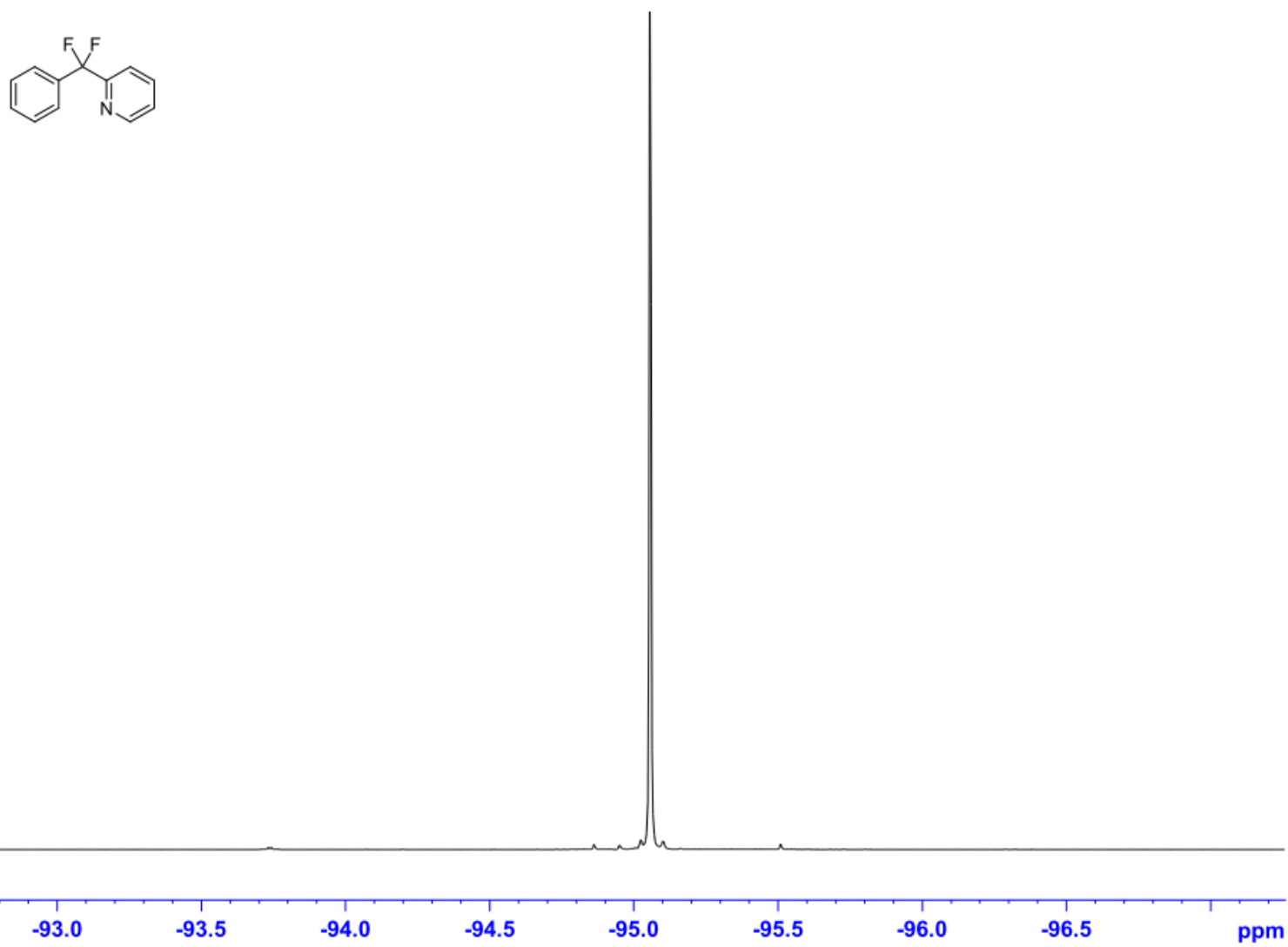
Studies of C-H(Sp^3) functionalization

Isolation of Isomerized 8-methylquinolylpalladium(IV) Hydroxo Di-2-pyridylketone Complexes (10BF$_4$) along withAddition of LiX (X= Br and Cl)
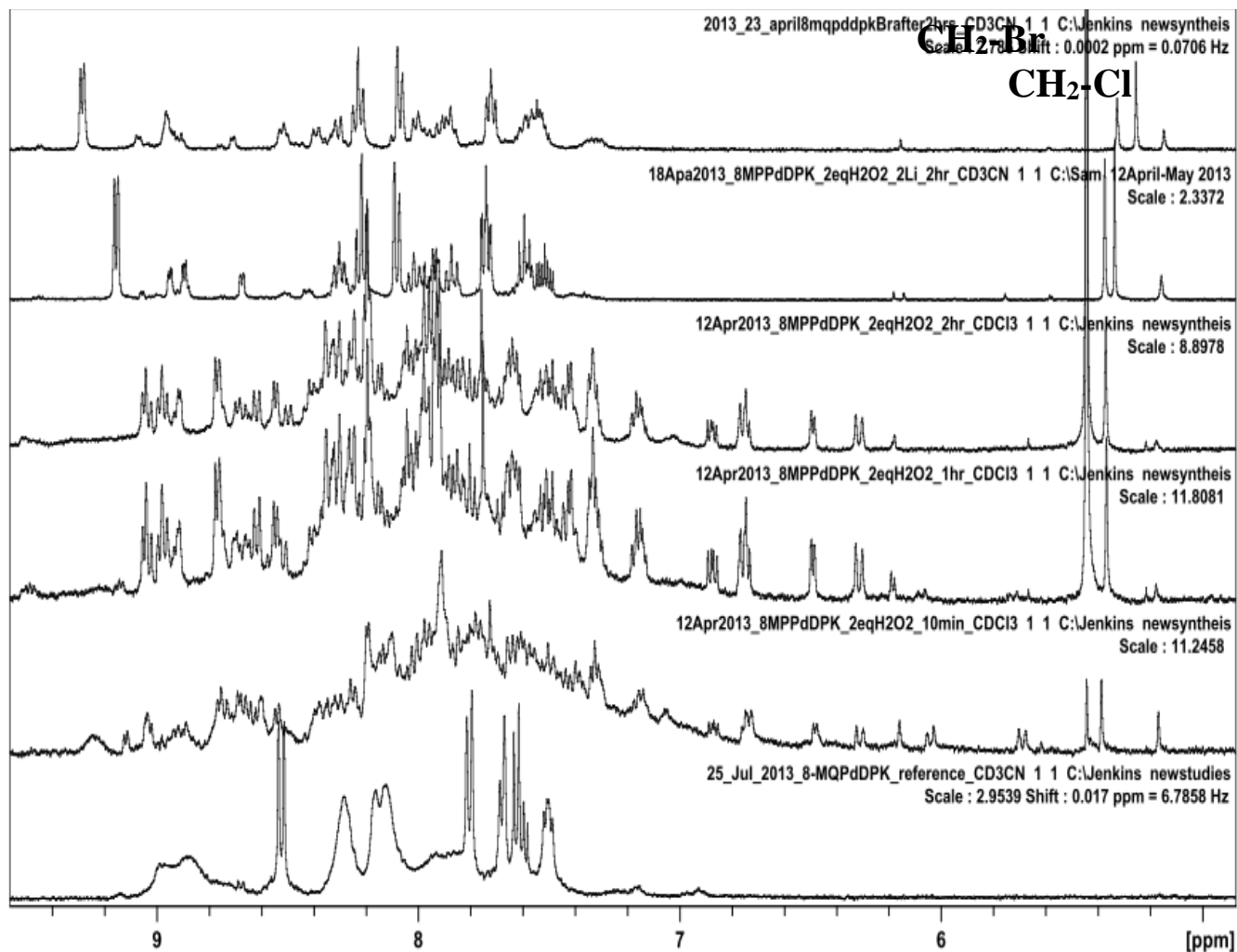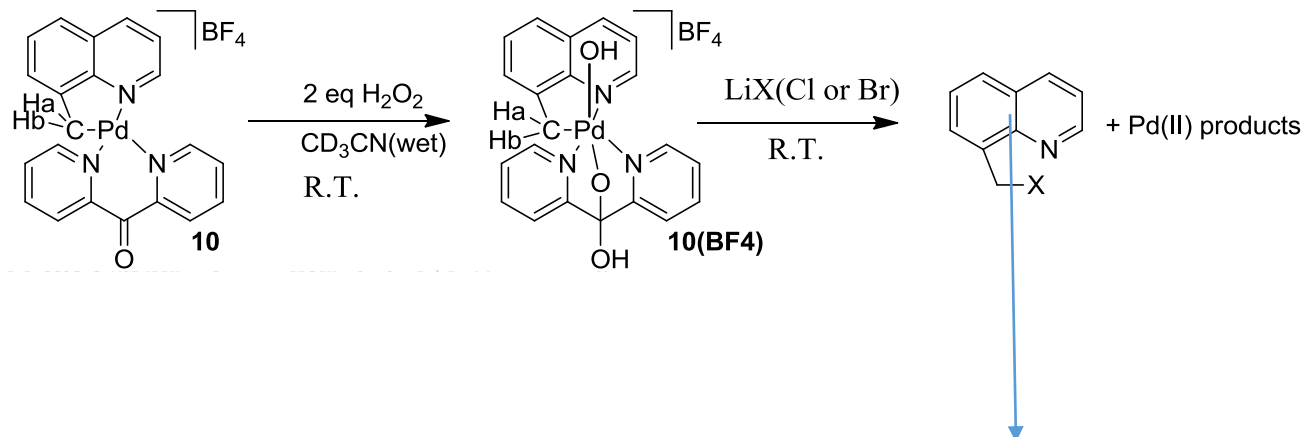
Isolation of Isomerized 8-methylquinolylpalladium(IV) Chloro Di-2-pyridylketone Complexes (10BF₄) using N-Chlorosuccinimide(NCS)
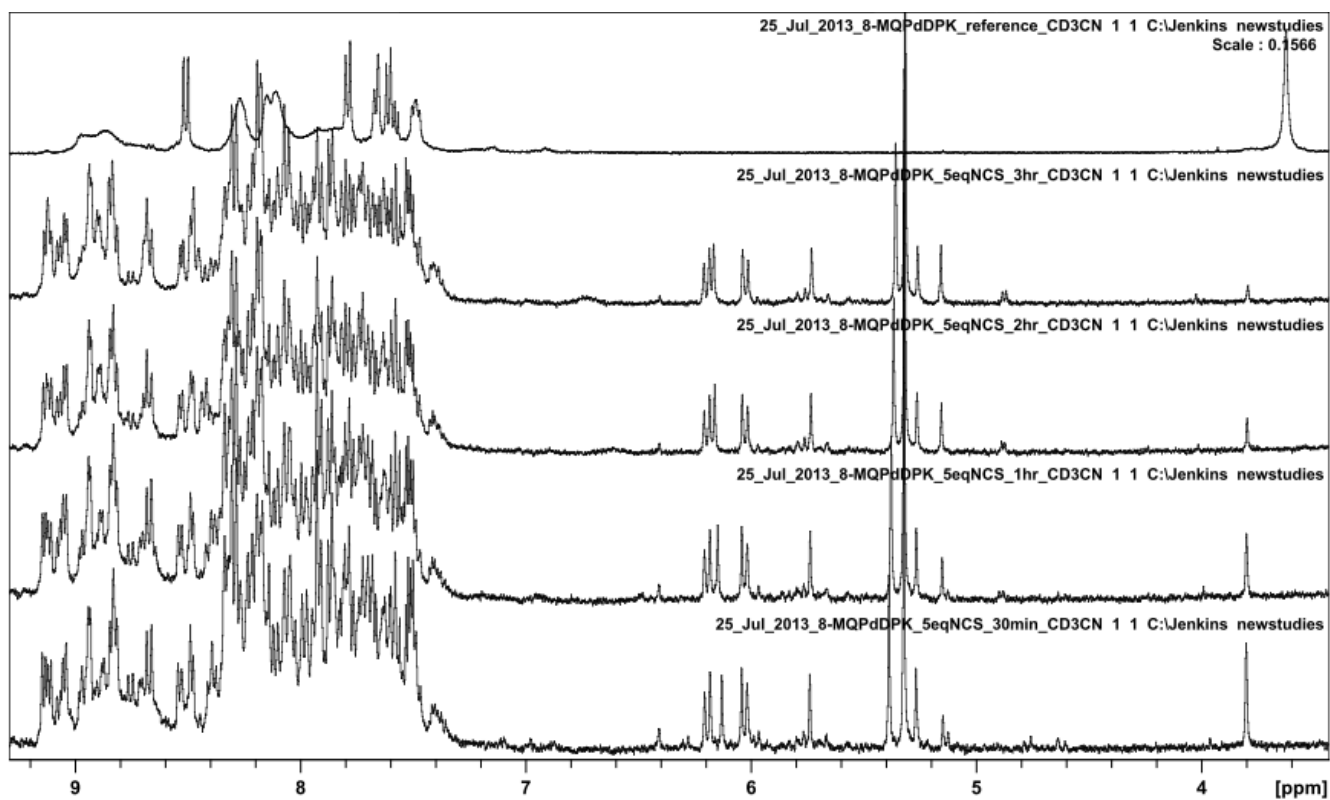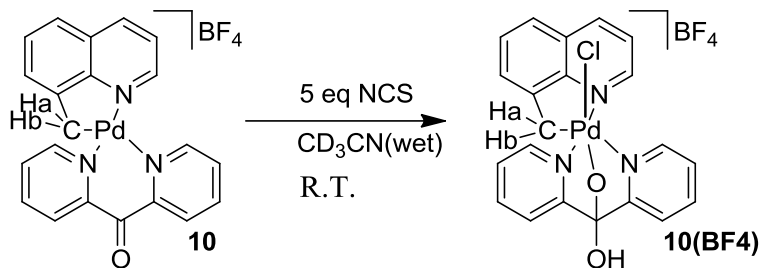
Isolation of Isomerized 8-methylquinolylpalladium(IV) Bromo Di-2-pyridylketone Complexes (10BF₄) using N-Bromosuccinimide(NBS)
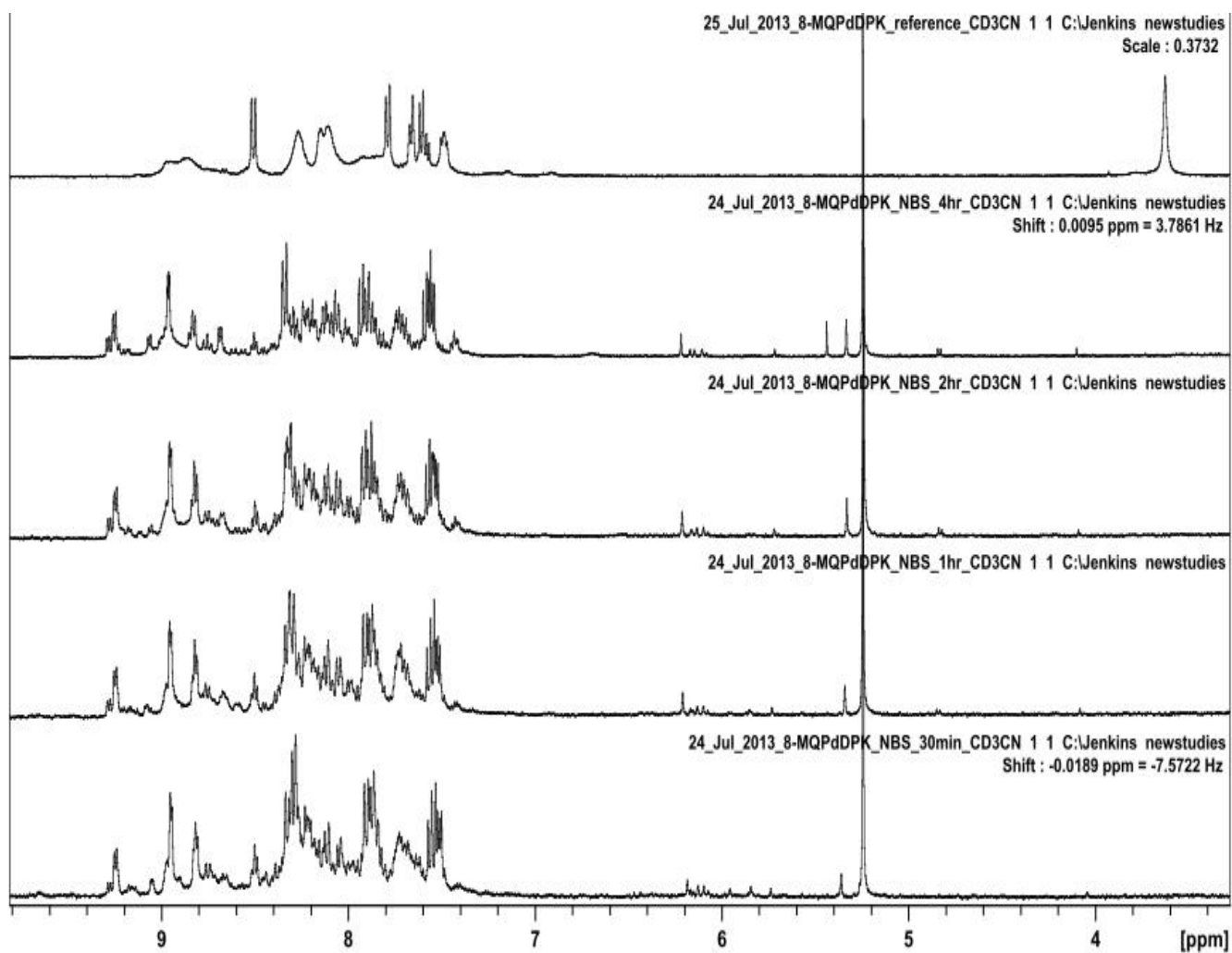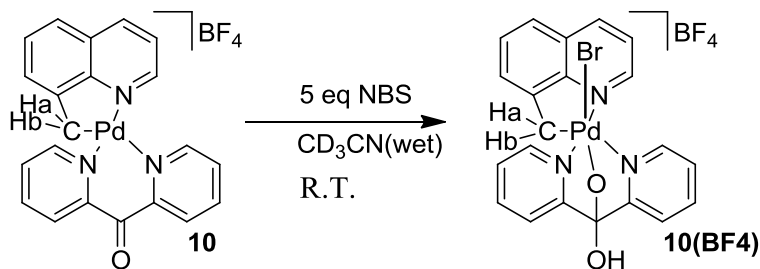
Isolation and Kinetic Analysis of 4-amino-2-*tert*-butylpyridyl Palladium(IV) Hydroxo Di-(2-pyridyl) Ketone Complex (18)
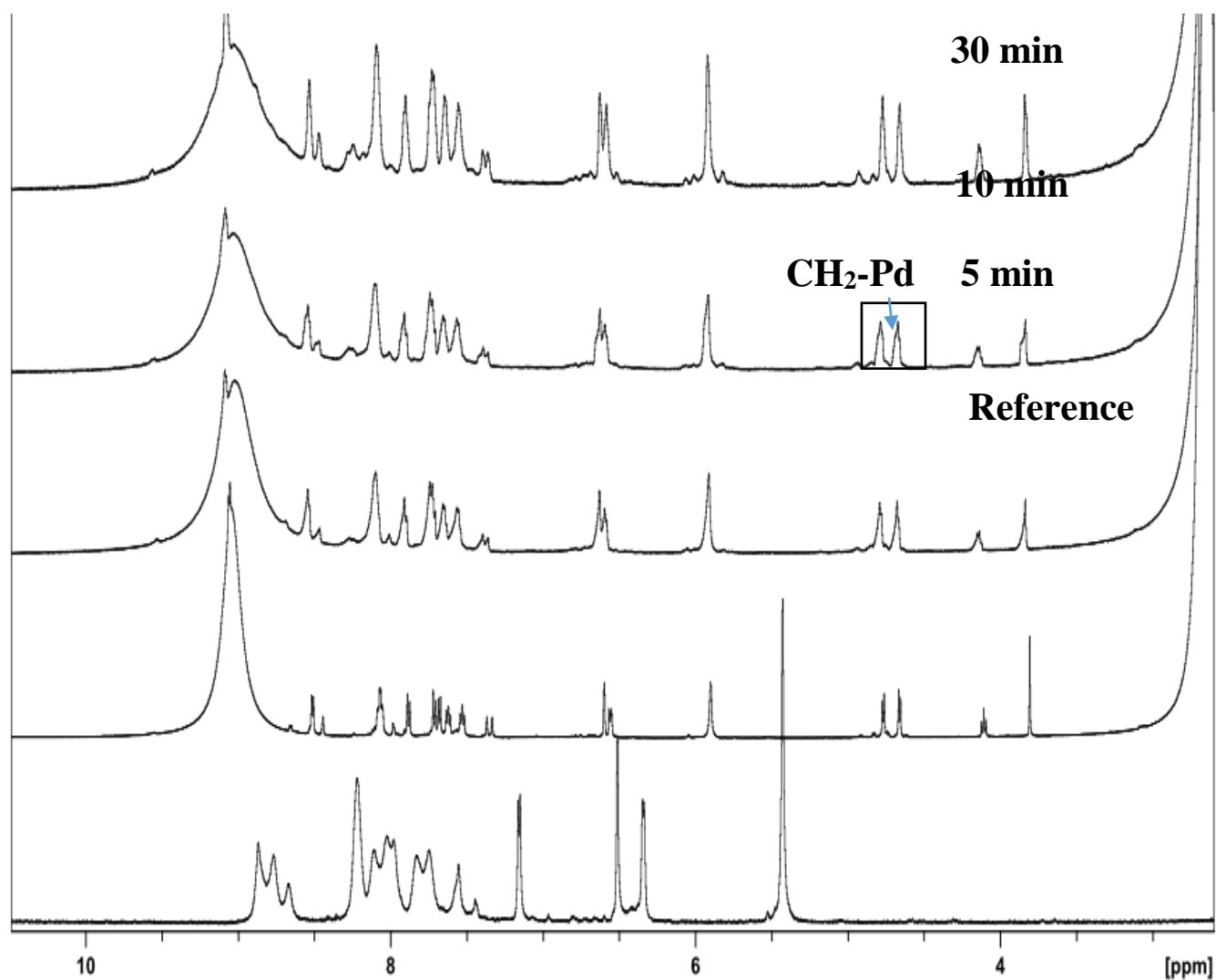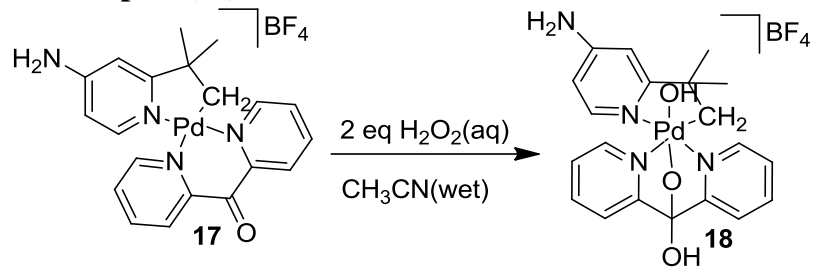
NOE Analysis of 4-amino-2-*tert*-butylpyridyl Palladium(IV) Hydroxo Di-(2-pyridyl) Ketone Complex (18)
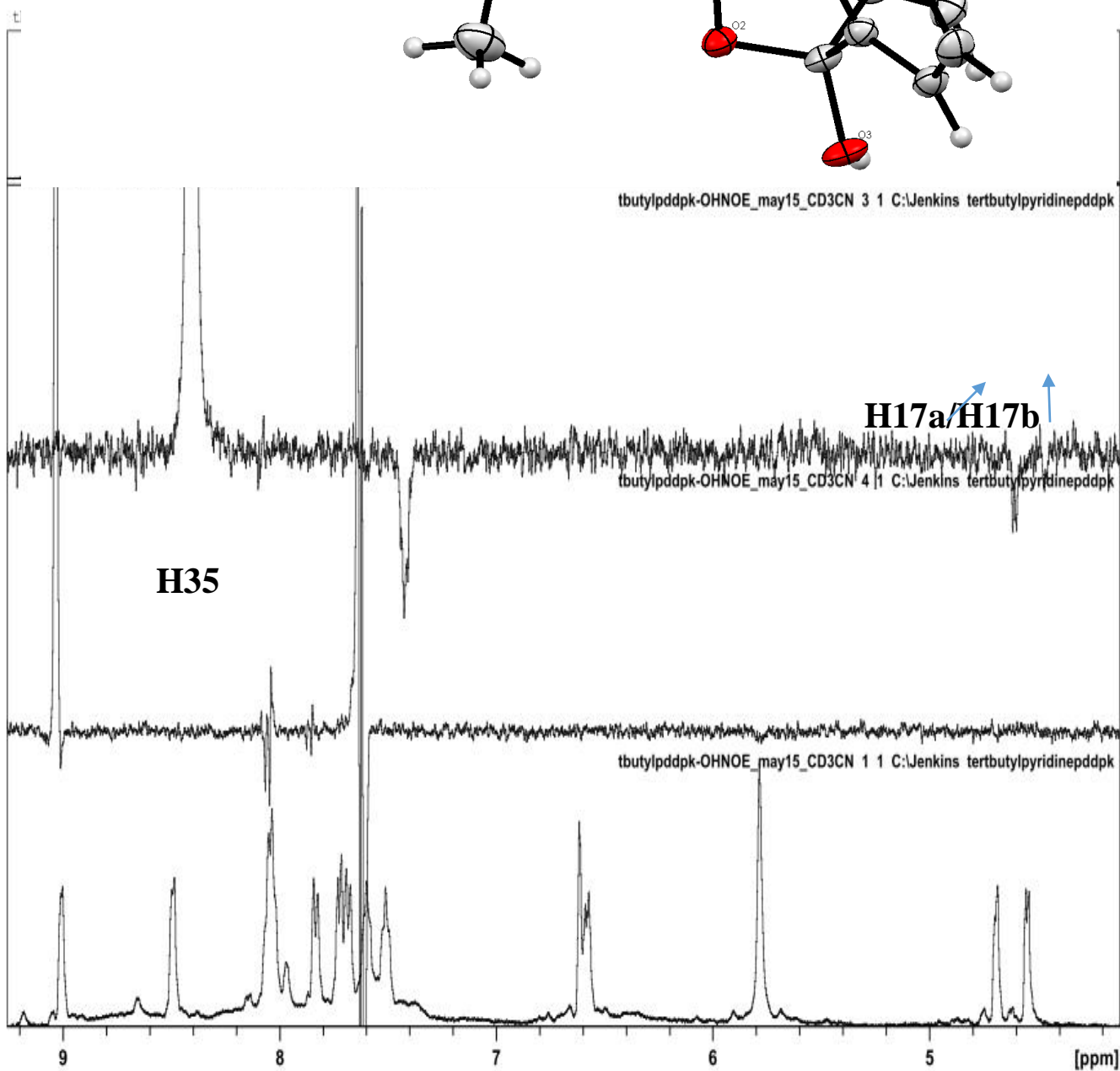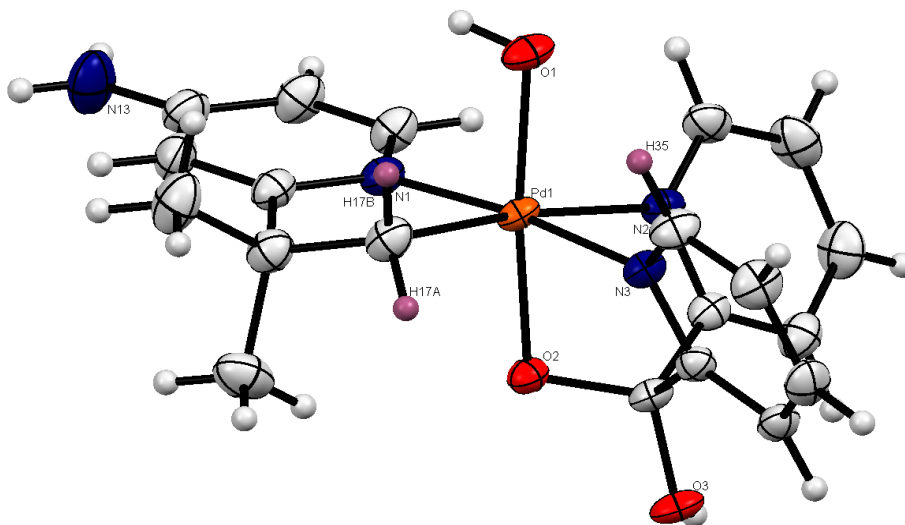
X-ray Crystal Structure Data and Procedures
8-methylquinolyl Palladium(II) Di-2-pyridylketone Complex (10)
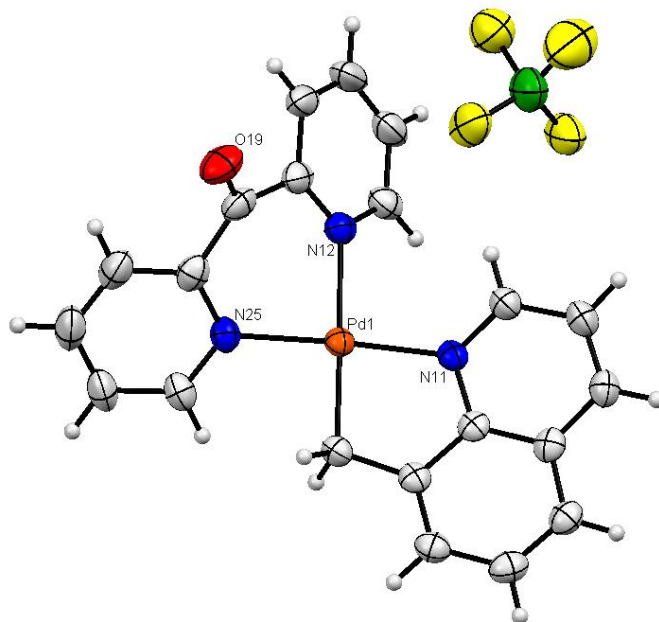
X-ray quality crystals of **10(BF₄)** were obtained by slow diffusion of benzene into a solution of **10(BF₄)** in dichloromethane at 25°C. A colorless prism-like specimen of $C_{21.50}H_{17}BClF_4N_3OPd$, approximate dimensions 0.14 mm × 0.16 mm × 0.25 mm, was used for the X-ray crystallographic analysis. The X-ray intensity data were measured on a Bruker APEX-II CCD system equipped with a graphite monochromator and a MoKα sealed tube ($\lambda = 0.71073$ Å). Data collection temperature was 150 K.

The total exposure time was 12.63 hours. The frames were integrated with the Bruker SAINT software package using a narrow-frame algorithm. The integration of the data using a monoclinic unit cell yielded a total of 26510 reflections to a maximum θ angle of 27.99° (0.76 Å resolution), of which 5058 were independent (average redundancy 5.241, completeness = 99.6%, R_{int} = 2.52%) and 4554 (90.04%) were greater than $2\sigma(F^2)$. The final cell constants of $a = 32.411(3)$ Å, $b = 7.9803(6)$ Å, $c = 22.0035(18)$ Å, β = 132.3370(10)°, $V = 4206.9(6)$ Å³, are based upon the refinement of the XYZ-centroids of 9943 reflections above 20 σ(I) with 5.008° < 2θ < 57.94°. Data were corrected for absorption effects using the multi-scan method (SADABS). The calculated minimum and maximum transmission coefficients (based on crystal size) are 0.7840 and 0.8660.

The structure was solved and refined using the Bruker SHELXTL Software Package, using the space group C2/c, with Z = 8 for the formula unit, $C_{21.50}H_{17}BClF_4N_3OPd$. The final anisotropic full-matrix least-squares refinement on F^2 with 493 variables converged at $R_1 = 4.21\%$, for the observed data and $wR_2 = 9.27\%$ for all data. The goodness-of-fit was 1.006. The largest peak in the final difference electron density synthesis was 1.239 e⁻/Å³ and the largest

hole was -0.679 e$^-$/Å^3 with an RMS deviation of 0.092 e$^-$/Å^3. On the basis of the final model, the calculated density was 1.775 g/cm^3 and F(000), 2232 e$^-$.

APEX2 Version 2010.11-3 (Bruker AXS Inc.)
SAINT Version 7.68A (Bruker AXS Inc., 2009)
SADABS Version 2008/1 (G. M. Sheldrick, Bruker AXS Inc.)
XPREP Version 2008/2 (G. M. Sheldrick, Bruker AXS Inc.)
XS Version 2008/1 (G. M. Sheldrick, *Acta Cryst.* (2008). A**64**, 112-122)
XL Version 2012/4 (G. M. Sheldrick, (2012) University of Gottingen, Germany)
Platon (A. L. Spek, *Acta Cryst.* (1990). A**46**, C-34)

Table 1. Sample and crystal data for UM2385.

Identification code	2385
Chemical formula	$C_{21.50}H_{17}BClF_4N_3OPd$
Formula weight	562.04
Temperature	150(2) K
Wavelength	0.71073 Å
Crystal size	$0.14 \times 0.16 \times 0.25$ mm
Crystal habit	colorless prism
Crystal system	monoclinic
Space group	C2/c
Unit cell dimensions	a = 32.411(3) Å α = 90°
	b = 7.9803(6) Å β = 132.3370(10)°
	c = 22.0035(18) Å γ = 90°
Volume	4206.9(6) Å^3
Z	8
Density (calculated)	1.775 Mg/cm^3
Absorption coefficient	1.065 mm^{-1}
F(000)	2232

Table 2. Data collection and structure refinement for UM2385.

Diffractometer	Bruker APEX-II CCD
Radiation source	sealed tube, MoKα
Theta range for data collection	1.85 to 27.99°

Index ranges	$-42 \leq h \leq 42$, $-10 \leq k \leq 10$, $-28 \leq l \leq 28$
Reflections collected	26510
Independent reflections	5058 [R(int) = 0.0252]
Coverage of independent reflections	99.6%
Absorption correction	multi-scan
Max. and min. transmission	0.8660 and 0.7840
Structure solution technique	direct methods
Structure solution program	ShelXS-97 (Sheldrick, 2008)
Refinement method	Full-matrix least-squares on F^2
Refinement program	ShelXL-2012 (Sheldrick, 2012)
Function minimized	$\Sigma\, w(F_o^2 - F_c^2)^2$
Data / restraints / parameters	5058 / 733 / 493
Goodness-of-fit on F^2	1.006
Δ/σ_{max}	0.001
Final R indices	4554 data; I>2σ(I) $R_1 = 0.0421$, $wR_2 = 0.0905$
	all data $R_1 = 0.0465$, $wR_2 = 0.0927$
Weighting scheme	$w=1/[\sigma^2(F_o^2)+(0.0100P)^2+37.0000P]$, $P=(F_o^2+2F_c^2)/3$
Largest diff. peak and hole	1.239 and -0.679 e$\mathring{A}^{-3}$
R.M.S. deviation from mean	0.092 e$\mathring{A}^{-3}$

4-amino-2-*tert*-butylpyridyl Palladium(II) Di-(2-pyridyl) Ketone Complex (17)
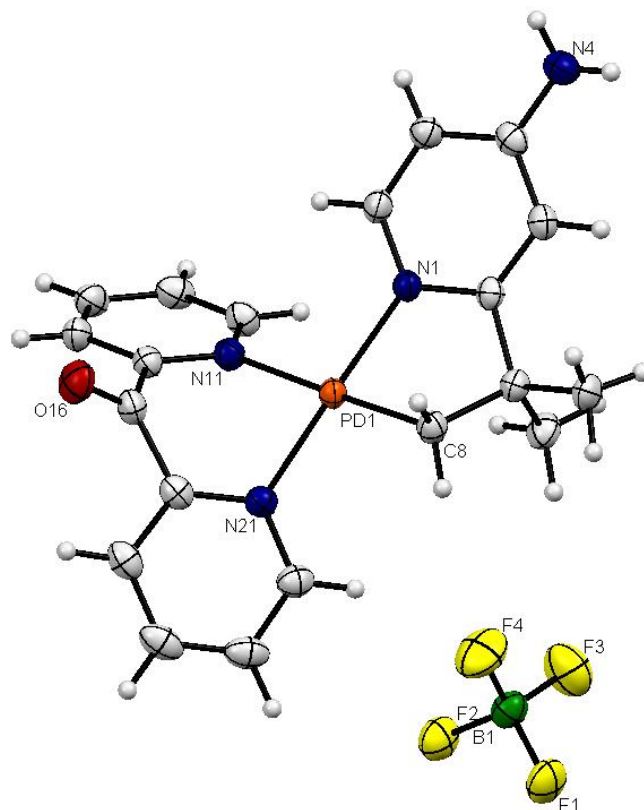
X-ray quality crystals of **17(BF₄)** were obtained by slow diffusion of benzene into a solution of **17(BF₄)** in dichloromethane at 25˚C. A yellow prism-like specimen of $C_{20}H_{21}BF_4N_4OPd$, approximate dimensions 0.15 mm × 0.20 mm × 0.26 mm, was used for the X-ray crystallographic analysis. The X-ray intensity data were measured on a Bruker APEX-II CCD system equipped with a graphite monochromator and a MoKα sealed tube (λ = 0.71073 Å). Data collection temperature was 150 K.

The total exposure time was 16.83 hours. The frames were integrated with the Bruker SAINT software package using a narrow-frame algorithm. The integration of the data using an orthorhombic unit cell yielded a total of 31099 reflections to a maximum θ angle of 30.00° (0.71 Å resolution), of which 6116 were independent (average redundancy 5.085, completeness = 100.0%, R_{int} = 1.90%) and 6017 (98.38%) were greater than $2\sigma(F^2)$. The final cell constants of a = 13.2641(8) Å, b = 17.5052(10) Å, c = 17.9840(11) Å, V = 4175.7(4) Å³, are based upon the refinement of the XYZ-centroids of 9960 reflections above 20 σ(I) with 4.469° < 2θ < 64.42°. Data were corrected for absorption effects using the multi-scan method (SADABS). The calculated minimum and maximum transmission coefficients (based on crystal size) are 0.8010 and 0.8680.

The structure was solved and refined using the Bruker SHELXTL Software Package, using the space group C222₁, with Z = 8 for the formula unit, $C_{20}H_{21}BF_4N_4OPd$. The final anisotropic full-matrix least-squares refinement on F^2 with 315 variables converged at R_1 = 1.96%, for the observed data and wR_2 =4.85% for all data. The goodness-of-fit was 1.000. The largest peak in the final difference electron density synthesis was 0.880 e⁻/Å³ and the largest hole was -0.253 e⁻

/Å^3 with an RMS deviation of 0.060 e$^-$/Å^3. On the basis of the final model, the calculated density was 1.675 g/cm^3 and F(000), 2112 e$^-$.

APEX2 Version 2010.11-3 (Bruker AXS Inc.)
SAINT Version 7.68A (Bruker AXS Inc., 2009)
SADABS Version 2008/1 (G. M. Sheldrick, Bruker AXS Inc.)
XPREP Version 2008/2 (G. M. Sheldrick, Bruker AXS Inc.)
XS Version 2008/1 (G. M. Sheldrick, *Acta Cryst.* (2008). A**64**, 112-122)
XL Version 2012/4 (G. M. Sheldrick, (2012) University of Gottingen, Germany)
Platon (A. L. Spek, *Acta Cryst.* (1990). A**46**, C-34)

Table 1. Sample and crystal data for UM2421.

Identification code	2421
Chemical formula	$C_{20}H_{21}BF_4N_4OPd$
Formula weight	526.62
Temperature	150(2) K
Wavelength	0.71073 Å
Crystal size	$0.15 \times 0.20 \times 0.26$ mm
Crystal habit	yellow prism
Crystal system	orthorhombic
Space group	$C222_1$
Unit cell dimensions	a = 13.2641(8) Å $\alpha = 90°$
	b = 17.5052(10) Å $\beta = 90°$
	c = 17.9840(11) Å $\gamma = 90°$
Volume	4175.7(4) Å^3
Z	8
Density (calculated)	1.675 Mg/cm^3
Absorption coefficient	0.944 mm^{-1}
F(000)	2112

Table 2. Data collection and structure refinement for UM2421.

Diffractometer	Bruker APEX-II CCD
Radiation source	sealed tube, MoKα
Theta range for data collection	1.93 to 30.00°
Index ranges	$-18 \leq h \leq 18$, $-24 \leq k \leq 23$, $-24 \leq l \leq 25$

Reflections collected	31099
Independent reflections	6116 [R(int) = 0.0190]
Coverage of independent reflections	100.0%
Absorption correction	multi-scan
Max. and min. transmission	0.8680 and 0.8010
Structure solution technique	direct methods
Structure solution program	ShelXS-97 (Sheldrick, 2008)
Refinement method	Full-matrix least-squares on F^2
Refinement program	ShelXL-2012 (Sheldrick, 2012)
Function minimized	$\Sigma \, w(F_o^2 - F_c^2)^2$
Data / restraints / parameters	6116 / 0 / 315
Goodness-of-fit on F^2	1.000
Δ/σ_{max}	0.002
Final R indices	6017 data; I>2σ(I) $\quad$ $R_1 = 0.0196$, $wR_2 = 0.0482$
	all data $\quad$ $R_1 = 0.0202$, $wR_2 = 0.0485$
Weighting scheme	$w=1/[\sigma^2(F_o^2)+(0.0250P)^2+3.8900P]$, $P=(F_o^2+2F_c^2)/3$
Absolute structure parameter	-0.0(0)
Largest diff. peak and hole	0.880 and -0.253 eÅ^{-3}
R.M.S. deviation from mean	0.060 eÅ^{-3}

Benzo[*h*]quinolinyl Palladium(II) Di-(2-pyridyl) Ketone Complex (8)
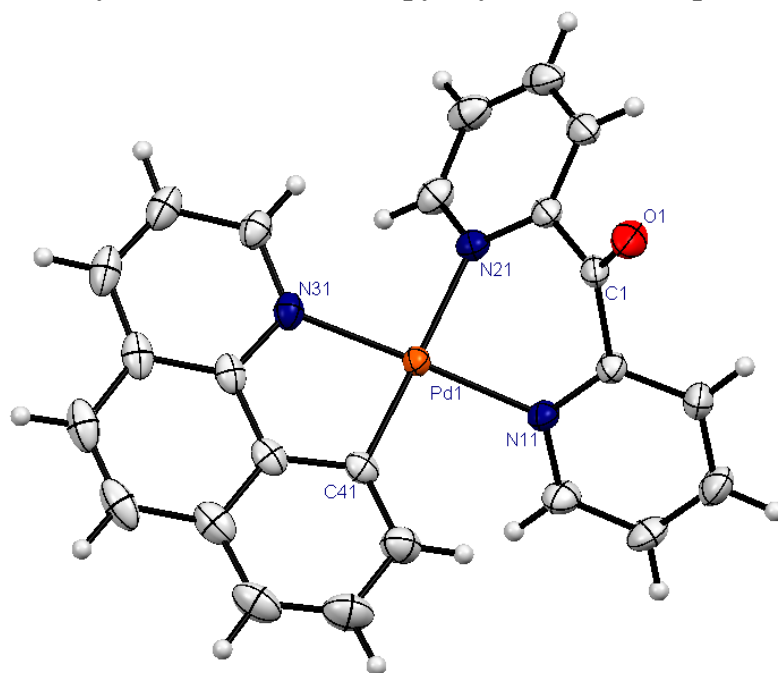
X-ray quality crystals of **8(BF₄)** were obtained by slow diffusion of benzene into a solution of **8(BF₄)** in dichloromethane at 25˚C. A colorless plate-like specimen of $C_{24.50}H_{17}BClF_4N_3OPd$, approximate dimensions 0.05 mm $\times$ 0.13 mm $\times$ 0.29 mm, was used for the X-ray crystallographic analysis. The X-ray intensity data were measured on a Bruker APEX-II CCD system equipped with a graphite monochromator and a MoKα sealed tube (λ = 0.71073 Å). Data collection temperature was 150 K.

The total exposure time was 15.15 hours. The frames were integrated with the Bruker SAINT software package using a narrow-frame algorithm. The integration of the data using a triclinic unit cell yielded a total of 17420 reflections to a maximum θ angle of 29.99° (0.71 Å resolution), of which 6665 were independent (average redundancy 2.614, completeness = 99.3%, R_{int} = 1.91%) and 6097 (91.48%) were greater than $2\sigma(F^2)$. The final cell constants of a = 7.8643(10) Å, b = 12.3147(16) Å, c = 12.7958(17) Å, α = 94.450(2)°, β = 100.497(2)°, γ = 107.175(2)°, V = 1152.7(3) Å^3, are based upon the refinement of the XYZ-centroids of 9824 reflections above 20 σ(I) with 4.440° < 2θ < 61.98°. Data were corrected for absorption effects using the multi-scan method (SADABS). The calculated minimum and maximum transmission coefficients (based on crystal size) are 0.8500 and 0.9520.

The structure was solved and refined using the Bruker SHELXTL Software Package, using the space group P-1, with Z = 2 for the formula unit, $C_{24.50}H_{17}BClF_4N_3OPd$. The final anisotropic full-matrix least-squares refinement on F^2 with 409 variables converged at R_1 = 2.66%, for the observed data and wR_2 =5.56% for all data. The goodness-of-fit was 1.000. The largest peak in the final difference electron density synthesis was 0.494 e$^-$/Å^3 and the largest hole was -0.566 e$^-$/Å^3 with an RMS deviation of 0.067 e$^-$/Å^3. On the basis of the final model, the calculated density was 1.723 g/cm^3 and F(000), 594 e$^-$.

APEX2 Version 2010.11-3 (Bruker AXS Inc.)
SAINT Version 7.68A (Bruker AXS Inc., 2009)
SADABS Version 2008/1 (G. M. Sheldrick, Bruker AXS Inc.)
XPREP Version 2008/2 (G. M. Sheldrick, Bruker AXS Inc.)
XS Version 2008/1 (G. M. Sheldrick, *Acta Cryst.* (2008). A**64**, 112-122)
XL Version 2012/4 (G. M. Sheldrick, (2012) University of Gottingen, Germany)
Platon (A. L. Spek, *Acta Cryst.* (1990). A**46**, C-34)


Table 1. Sample and crystal data for UM2383.

Identification code	2383
Chemical formula	$C_{24.50}H_{17}BClF_4N_3OPd$
Formula weight	598.07
Temperature	150(2) K
Wavelength	0.71073 Å
Crystal size	$0.05 \times 0.13 \times 0.29$ mm
Crystal habit	colorless plate
Crystal system	triclinic
Space group	P-1
Unit cell dimensions	a = 7.8643(10) Å $\quad \alpha = 94.450(2)°$
	b = 12.3147(16) Å $\quad \beta = 100.497(2)°$
	c = 12.7958(17) Å $\quad \gamma = 107.175(2)°$
Volume	1152.7(3) $Å^3$
Z	2
Density (calculated)	1.723 Mg/cm^3
Absorption coefficient	0.978 mm^{-1}
F(000)	594

Table 2. Data collection and structure refinement for UM2383.

Diffractometer	Bruker APEX-II CCD
Radiation source	sealed tube, MoKα
Theta range for data collection	2.22 to 29.99°
Index ranges	$-11 \le h \le 10$, $-17 \le k \le 17$, $-17 \le l \le 17$
Reflections collected	17420
Independent	6665 [R(int) = 0.0191]

reflections	
Coverage of independent reflections	99.3%
Absorption correction	multi-scan
Max. and min. transmission	0.9520 and 0.8500
Structure solution technique	direct methods
Structure solution program	ShelXS-97 (Sheldrick, 2008)
Refinement method	Full-matrix least-squares on F^2
Refinement program	ShelXL-2012 (Sheldrick, 2012)
Function minimized	$\Sigma\ w(F_o^2 - F_c^2)^2$
Data / restraints / parameters	6665 / 91 / 409
Goodness-of-fit on F^2	1.000
Δ/σ_{max}	0.002
Final R indices	6097 data; $I>2\sigma(I)$ $R_1 = 0.0266$, $wR_2 = 0.0538$
	all data $R_1 = 0.0310$, $wR_2 = 0.0556$
Weighting scheme	$w=1/[\sigma^2(F_o^2)+(0.0100P)^2+1.3720P]$, $P=(F_o^2+2F_c^2)/3$
Largest diff. peak and hole	0.494 and -0.566 eÅ^{-3}
R.M.S. deviation from mean	0.067 eÅ^{-3}

Oxapalladacycle of Benzo[*h*]quinolinyl Palladium(II) Di-(2-pyridyl) Complex (25)
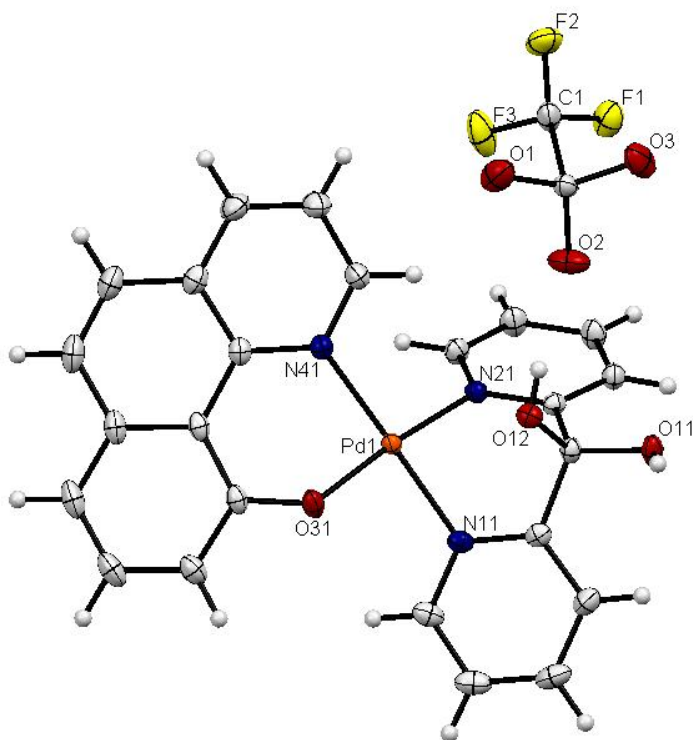
X-ray quality crystals of **25(CF₃SO₃)** were obtained by a solution of **25(CF₃SO₃)** in acetonitrile at -15˚C. A yellow-orange plate-like specimen of $C_{25}H_{18}F_3N_3O_6PdS$, approximate dimensions 0.04 mm × 0.35 mm × 0.50 mm, was used for the X-ray crystallographic analysis. The X-ray intensity data were measured on a Bruker APEX-II CCD system equipped with a graphite monochromator and a MoKα sealed tube (λ = 0.71073 Å). Data collection temperature was 150 K.

The total exposure time was 16.83 hours. The frames were integrated with the Bruker SAINT software package using a narrow-frame algorithm. The integration of the data using a triclinic unit cell yielded a total of 31241 reflections to a maximum θ angle of 30.00° (0.71 Å resolution), of which 6888 were independent (average redundancy 4.536, completeness = 99.2%, $R_{int} = 2.19\%$) and 6662 (96.72%) were greater than $2\sigma(F^2)$. The final cell constants of $a = 8.8520(5)$ Å, $b = 11.4778(7)$ Å, $c = 12.8395(8)$ Å, $\alpha = 69.5780(9)°$, $\beta = 77.1473(9)°$, $\gamma = 88.8129(9)°$, $V = 1189.58(12)$ Å^3, are based upon the refinement of the XYZ-centroids of 3926 reflections above 20 σ(I) with 5.187° < 2θ < 64.59°. Data were corrected for absorption effects using the multi-scan method (SADABS). The calculated minimum and maximum transmission coefficients (based on crystal size) are 0.6980 and 0.9630.

The structure was solved and refined using the Bruker SHELXTL Software Package, using the space group P-1, with Z = 2 for the formula unit, $C_{25}H_{18}F_3N_3O_6PdS$. The final anisotropic full-matrix least-squares refinement on F^2 with 377 variables converged at $R_1 = 2.09\%$, for the observed data and $wR_2 = 5.13\%$ for all data. The goodness-of-fit was 0.999.

The largest peak in the final difference electron density synthesis was 0.505 e⁻/Å³ and the largest hole was -0.373 e⁻/Å³ with an RMS deviation of 0.068 e⁻/Å³. On the basis of the final model, the calculated density was 1.820 g/cm³ and F(000), 652 e⁻.

APEX2 Version 2010.11-3 (Bruker AXS Inc.)
SAINT Version 7.68A (Bruker AXS Inc., 2009)
SADABS Version 2008/1 (G. M. Sheldrick, Bruker AXS Inc.)
XPREP Version 2008/2 (G. M. Sheldrick, Bruker AXS Inc.)
XS Version 2008/1 (G. M. Sheldrick, *Acta Cryst.* (2008). A**64**, 112-122)
XL Version 2012/4 (G. M. Sheldrick, (2012) University of Gottingen, Germany)
Platon (A. L. Spek, *Acta Cryst.* (1990). A**46**, C-34)

Table 1. Sample and crystal data for UM2416.

Identification code	2416
Chemical formula	$C_{25}H_{18}F_3N_3O_6PdS$
Formula weight	651.88
Temperature	150(2) K
Wavelength	0.71073 Å
Crystal size	$0.04 \times 0.35 \times 0.50$ mm
Crystal habit	yellow-orange plate
Crystal system	triclinic
Space group	P-1
Unit cell dimensions	a = 8.8520(5) Å α = 69.5780(9)°
	b = 11.4778(7) Å β = 77.1473(9)°
	c = 12.8395(8) Å γ = 88.8129(9)°
Volume	1189.58(12) Å³
Z	2
Density (calculated)	1.820 Mg/cm³
Absorption coefficient	0.941 mm⁻¹
F(000)	652

Table 2. Data collection and structure refinement for UM2416.

Diffractometer	Bruker APEX-II CCD
Radiation source	sealed tube, MoKα
Theta range for data collection	1.90 to 30.00°

Reflections collected	31241
Independent reflections	6888 [R(int) = 0.0219]
Coverage of independent reflections	99.2%
Absorption correction	multi-scan
Max. and min. transmission	0.9630 and 0.6980
Structure solution technique	direct methods
Structure solution program	ShelXS-97 (Sheldrick, 2008)
Refinement method	Full-matrix least-squares on F^2
Refinement program	ShelXL-2012 (Sheldrick, 2012)
Function minimized	$\Sigma\ w(F_o^2 - F_c^2)^2$
Data / restraints / parameters	6888 / 0 / 377
Goodness-of-fit on F^2	0.999
Δ/σ_{max}	0.001
Final R indices	6662 data; $I>2\sigma(I)$ — $R_1 = 0.0209$, $wR_2 = 0.0509$
	all data — $R_1 = 0.0218$, $wR_2 = 0.0513$
Weighting scheme	$w=1/[\sigma^2(F_o^2)+(0.0100P)^2+1.1770P]$, $P=(F_o^2+2F_c^2)/3$
Largest diff. peak and hole	0.505 and -0.373 eÅ^{-3}
R.M.S. deviation from mean	0.068 eÅ^{-3}

Homocoupling of Benzo[*h*]quinoline(28)
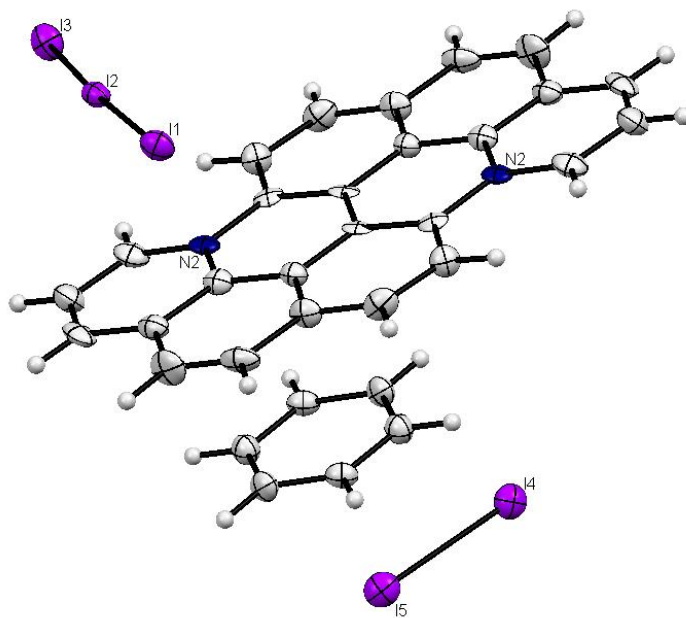
X-ray quality crystals of **28(I₃)₂** were obtained by slow diffusion of benzene into a solution of **28(I₃)₂** in acetonitrile(wet) at 25 °C. A purple needle-like specimen of $C_{32}H_{20}I_{10}N_2$, approximate dimensions 0.01 mm × 0.12 mm × 0.45 mm, was used for the X-ray crystallographic analysis. The X-ray intensity data were measured on a Bruker APEX-II CCD system equipped with a graphite monochromator and a MoKα sealed tube (λ = 0.71073 Å). Data collection temperature was 149 K.

The total exposure time was 16.83 hours. The frames were integrated with the Bruker SAINT software package using a narrow-frame algorithm. The integration of the data using a triclinic unit cell yielded a total of 13751 reflections to a maximum θ angle of 30.00° (0.71 Å resolution), of which 5538 were independent (average redundancy 2.483, completeness = 98.7%, R_{int} = 2.22%) and 4845 (87.49%) were greater than $2\sigma(F^2)$. The final cell constants of a = 7.7684(6) Å, b = 11.7365(10) Å, c = 12.3827(10) Å, α = 110.9607(11)°, β = 104.4288(11)°, γ = 102.3549(12)°, V = 961.96(14) Å^3, are based upon the refinement of the XYZ-centroids of 8911 reflections above 20 σ(I) with 5.637° < 2θ < 62.13°. Data were corrected for absorption effects using the multi-scan method (SADABS). The calculated minimum and maximum transmission coefficients (based on crystal size) are 0.5550 and 0.8860.

The structure was solved and refined using the Bruker SHELXTL Software Package, using the space group P-1, with Z = 1 for the formula unit, $C_{32}H_{20}I_{10}N_2$. The final anisotropic full-matrix least-squares refinement on F^2 with 209 variables converged at R_1 = 2.07%, for the observed data and wR_2 = 4.59% for all data. The goodness-of-fit was 1.000. The largest peak in the final difference electron density synthesis was 0.838 e⁻/Å^3 and the largest hole was -0.775 e⁻

/Å^3 with an RMS deviation of 0.133 e$^-$/Å^3. On the basis of the final model, the calculated density was 2.937 g/cm^3 and F(000), 756 e$^-$.

APEX2 Version 2010.11-3 (Bruker AXS Inc.)
SAINT Version 7.68A (Bruker AXS Inc., 2009)
SADABS Version 2008/1 (G. M. Sheldrick, Bruker AXS Inc.)
XPREP Version 2008/2 (G. M. Sheldrick, Bruker AXS Inc.)
XS Version 2008/1 (G. M. Sheldrick, *Acta Cryst.* (2008). A**64**, 112-122)
XL Version 2012/4 (G. M. Sheldrick, (2012) University of Gottingen, Germany)
Platon (A. L. Spek, *Acta Cryst.* (1990). A**46**, C-34)

Table 1. Sample and crystal data for UM2361.

Identification code	2361
Chemical formula	$C_{32}H_{20}I_{10}N_2$
Formula weight	1701.50
Temperature	149(2) K
Wavelength	0.71073 Å
Crystal size	$0.01 \times 0.12 \times 0.45$ mm
Crystal habit	purple needle
Crystal system	triclinic
Space group	P-1
Unit cell dimensions	a = 7.7684(6) Å α = 110.9607(11)°
	b = 11.7365(10) Å β = 104.4288(11)°
	c = 12.3827(10) Å γ = 102.3549(12)°
Volume	961.96(14) Å^3
Z	1
Density (calculated)	2.937 Mg/cm^3
Absorption coefficient	8.079 mm^{-1}
F(000)	756

Table 2. Data collection and structure refinement for UM2361.

Diffractometer	Bruker APEX-II CCD
Radiation source	sealed tube, MoKα
Theta range for data collection	2.05 to 30.00°
Index ranges	-10 ≤ h ≤ 10, -16 ≤ k ≤ 16, -17 ≤ l ≤ 17

Reflections collected	13751
Independent reflections	5538 [R(int) = 0.0222]
Coverage of independent reflections	98.7%
Absorption correction	multi-scan
Max. and min. transmission	0.8860 and 0.5550
Structure solution technique	direct methods
Structure solution program	ShelXS-97 (Sheldrick, 2008)
Refinement method	Full-matrix least-squares on F^2
Refinement program	ShelXL-2012 (Sheldrick, 2012)
Function minimized	$\Sigma\ w(F_o^2 - F_c^2)^2$
Data / restraints / parameters	5538 / 0 / 209
Goodness-of-fit on F^2	1.000
Δ/σ_{max}	0.002
Final R indices	4845 data; $I>2\sigma(I)$ $R_1 = 0.0207$, $wR_2 = 0.0438$
	all data $R_1 = 0.0259$, $wR_2 = 0.0459$
Weighting scheme	$w=1/[\sigma^2(F_o^2)+(0.0100P)^2+1.3920P]$, $P=(F_o^2+2F_c^2)/3$
Largest diff. peak and hole	0.838 and -0.775 eÅ^{-3}
R.M.S. deviation from mean	0.133 eÅ^{-3}

4-amino-2-*tert*-butylpyridyl Palladium(IV) Hydroxo Di-(2-pyridyl) Ketone Complex (18)
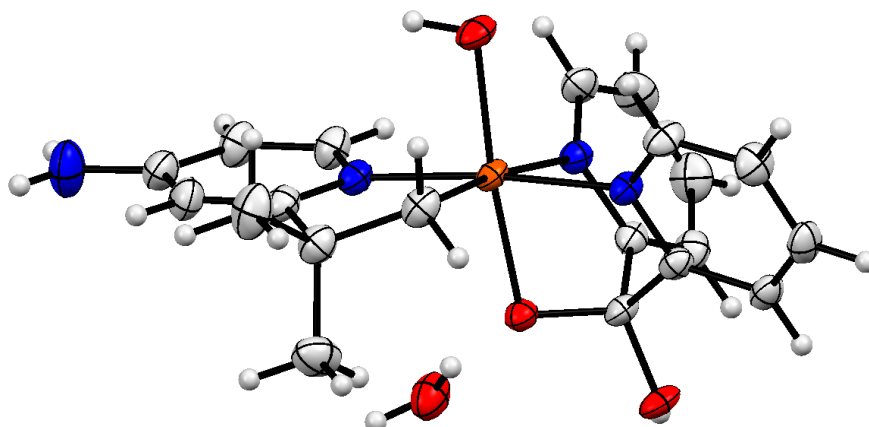
X-ray quality crystals of **18(BF₄)** were obtained by a solution of **18(BF₄)** in acetonitrile at -15˚C. A colorless needle-like specimen of $C_{22}H_{28}BF_4N_5O_4Pd$, approximate dimensions 0.03 mm × 0.03 mm × 0.35 mm, was used for the X-ray crystallographic analysis. The X-ray intensity data were measured on a Bruker APEX-II CCD system equipped with a graphite monochromator and a MoKα sealed tube (λ = 0.71073 Å). Data collection temperature was 150 K.

The total exposure time was 60.60 hours. The frames were integrated with the Bruker SAINT software package using a narrow-frame algorithm. The integration of the data using a triclinic unit cell yielded a total of 13697 reflections to a maximum θ angle of 26.00° (0.81 Å resolution), of which 5000 were independent (average redundancy 2.739, completeness = 99.9%, R_{int} = 3.45%) and 4345 (86.90%) were greater than $2\sigma(F^2)$. The final cell constants of a = 7.3490(8) Å, b = 12.1778(13) Å, c = 14.4432(16) Å, α = 81.9859(18)°, β = 85.7508(18)°, γ = 84.1390(18)°, V = 1270.9(2) Å³, are based upon the refinement of the XYZ-centroids of 4895 reflections above 20 σ(I) with 4.714° < 2θ < 54.11°. The calculated minimum and maximum transmission coefficients (based on crystal size) are 0.8340 and 0.9800.

The structure was solved and refined using the Bruker SHELXTL Software Package, using the space group P-1, with Z = 2 for the formula unit, $C_{22}H_{28}BF_4N_5O_4Pd$. The final anisotropic full-matrix least-squares refinement on F^2 with 425 variables converged at R_1 = 3.76%, for the observed data and wR_2 =8.14% for all data. The goodness-of-fit was 1.000. The largest peak in the final difference electron density synthesis was 0.811 e⁻/Å³ and the largest hole was -0.834 e⁻/Å³ with an RMS deviation of 0.090 e⁻/Å³. On the basis of the final model, the calculated density was 1.619 g/cm³ and F(000), 628 e⁻.

APEX2 Version 2010.11-3 (Bruker AXS Inc.)
SAINT Version 7.68A (Bruker AXS Inc., 2009)
SADABS Version 2008/1 (G. M. Sheldrick, Bruker AXS Inc.)

XPREP Version 2008/2 (G. M. Sheldrick, Bruker AXS Inc.)
XS Version 2008/1 (G. M. Sheldrick, *Acta Cryst.* (2008). A**64**, 112-122)
XL Version 2012/4 (G. M. Sheldrick, (2012) University of Gottingen, Germany)
Platon (A. L. Spek, *Acta Cryst.* (1990). A**46**, C-34)


Table 1. Sample and crystal data for UM2433.

Identification code	2433
Chemical formula	$C_{22}H_{28}BF_4N_5O_4Pd$
Formula weight	619.70
Temperature	150(2) K
Wavelength	0.71073 Å
Crystal size	$0.03 \times 0.03 \times 0.35$ mm
Crystal habit	colorless needle
Crystal system	triclinic
Space group	P-1
Unit cell dimensions	a = 7.3490(8) Å α = 81.9859(18)°
	b = 12.1778(13) Å β = 85.7508(18)°
	c = 14.4432(16) Å γ = 84.1390(18)°
Volume	1270.9(2) Å^3
Z	2
Density (calculated)	1.619 Mg/cm^3
Absorption coefficient	0.798 mm^{-1}
F(000)	628

Table 2. Data collection and structure refinement for UM2433.

Diffractometer	Bruker APEX-II CCD
Radiation source	sealed tube, MoKα
Theta range for data collection	2.07 to 26.00°
Index ranges	-8 ≤ h ≤ 9, -14 ≤ k ≤ 15, -17 ≤ l ≤ 17
Reflections collected	13697
Independent reflections	5000 [R(int) = 0.0345]
Coverage of independent	99.9%

reflections	
Absorption correction	multi-scan
Max. and min. transmission	0.9800 and 0.8340
Structure solution technique	direct methods
Structure solution program	ShelXS-97 (Sheldrick, 2008)
Refinement method	Full-matrix least-squares on F^2
Refinement program	ShelXL-2012 (Sheldrick, 2012)
Function minimized	$\Sigma\ w(F_o^2 - F_c^2)^2$
Data / restraints / parameters	5000 / 676 / 425
Goodness-of-fit on F^2	1.000
Final R indices	4345 data; I>2σ(I) $R_1 = 0.0376$, $wR_2 = 0.0767$
	all data $R_1 = 0.0478$, $wR_2 = 0.0814$
Weighting scheme	$w=1/[\sigma^2(F_o^2)+(0.0100P)^2+4.3250P]$, $P=(F_o^2+2F_c^2)/3$
Largest diff. peak and hole	0.811 and -0.834 eÅ^{-3}
R.M.S. deviation from mean	0.090 eÅ^{-3}

Benzo[*h*]quinolinyl Palladium(IV) Hydroxo Di-(2-pyridyl) Ketone Complex (24)
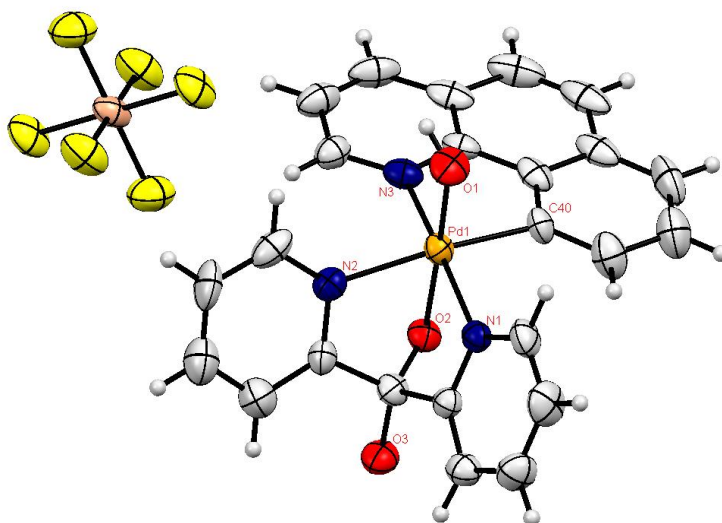
X-ray quality crystals of **24(PF$_6$)** were obtained by a solution of **24(PF$_6$)** in acetonitrile at -15˚C. A light orange-yellow prism-like specimen of C$_{48}$H$_{40}$F$_6$N$_6$O$_8$Pd$_2$Si, approximate dimensions 0.03 mm × 0.05 mm × 0.17 mm, was used for the X-ray crystallographic analysis. The X-ray intensity data were measured on a Bruker APEX-II CCD system equipped with a graphite monochromator and a MoKα sealed tube (λ = 0.71073 Å). Data collection temperature was 220 K.

The total exposure time was 43.87 hours. The frames were integrated with the Bruker SAINT software package using a narrow-frame algorithm. The integration of the data using a monoclinic unit cell yielded a total of 19462 reflections to a maximum θ angle of 25.00° (0.84 Å resolution), of which 3977 were independent (average redundancy 4.894, completeness = 99.9%, R$_{int}$ = 8.50%) and 2891 (72.69%) were greater than 2σ(F^2). The final cell constants of a = 7.2363(18) Å, b = 14.945(4) Å, c = 21.604(6) Å, β = 104.936(4)°, V = 2257.5(10) Å^3, are based upon the refinement of the XYZ-centroids of 2573 reflections above 20 σ(I) with 4.760° < 2θ < 42.04°. The calculated minimum and maximum transmission coefficients (based on crystal size) are 0.8270 and 0.9730.

The structure was solved and refined using the Bruker SHELXTL Software Package, using the space group P2$_1$/c, with Z = 2 for the formula unit, C$_{48}$H$_{40}$F$_6$N$_6$O$_8$Pd$_2$Si. The final anisotropic full-matrix least-squares refinement on F^2 with 357 variables converged at R$_1$ = 5.70%, for the observed data and wR$_2$ =11.52% for all data. The goodness-of-fit was 1.167. The largest peak in the final difference electron density synthesis was 1.799 e$^-$/Å^3 and the largest hole was -0.901 e$^-$

/Å^3 with an RMS deviation of 0.115 e$^-$/Å^3. On the basis of the final model, the calculated density was 1.742 g/cm^3 and F(000), 1188 e$^-$.

APEX2 Version 2010.11-3 (Bruker AXS Inc.)
SAINT Version 7.68A (Bruker AXS Inc., 2009)
SADABS Version 2008/1 (G. M. Sheldrick, Bruker AXS Inc.)
XPREP Version 2008/2 (G. M. Sheldrick, Bruker AXS Inc.)
XS Version 2008/1 (G. M. Sheldrick, *Acta Cryst.* (2008). A**64**, 112-122)
XL Version 2012/4 (G. M. Sheldrick, (2012) University of Gottingen, Germany)
Platon (A. L. Spek, *Acta Cryst.* (1990). A**46**, C-34)

## Table 1. Sample and crystal data for UM2445.

Identification code	2445
Chemical formula	$C_{48}H_{40}F_6N_6O_8Pd_2Si$
Formula weight	1183.75
Temperature	220(2) K
Wavelength	0.71073 Å
Crystal size	$0.03 \times 0.05 \times 0.17$ mm
Crystal habit	light orange-yellow prism
Crystal system	monoclinic
Space group	P2$_1$/c
Unit cell dimensions	a = 7.2363(18) Å $\alpha = 90°$
	b = 14.945(4) Å $\beta = 104.936(4)°$
	c = 21.604(6) Å $\gamma = 90°$
Volume	2257.5(10) Å^3
Z	2
Density (calculated)	1.742 Mg/cm^3
Absorption coefficient	0.912 mm^{-1}
F(000)	1188

Table 2. Data collection and structure refinement for UM2445.

Diffractometer	Bruker APEX-II CCD
Radiation source	sealed tube, MoKα
Theta range for data collection	2.38 to 25.00°
Index ranges	$-8 \leq h \leq 8, -17 \leq k \leq 17, -25 \leq l \leq 25$

Reflections collected	19462
Independent reflections	3977 [R(int) = 0.0850]
Coverage of independent reflections	99.9%
Absorption correction	multi-scan
Max. and min. transmission	0.9730 and 0.8270
Structure solution technique	direct methods
Structure solution program	ShelXS-97 (Sheldrick, 2008)
Refinement method	Full-matrix least-squares on F^2
Refinement program	ShelXL-2012 (Sheldrick, 2012)
Function minimized	$\Sigma\ w(F_o^2 - F_c^2)^2$
Data / restraints / parameters	3977 / 55 / 357
Goodness-of-fit on F^2	1.167
Δ/σ_{max}	0.001
Final R indices	2891 data; $I>2\sigma(I)$ — $R_1 = 0.0570$, $wR_2 = 0.1066$
	all data — $R_1 = 0.0882$, $wR_2 = 0.1152$
Weighting scheme	$w=1/[\sigma^2(F_o^2)+(0.0100P)^2+9.9500P]$, $P=(F_o^2+2F_c^2)/3$
Largest diff. peak and hole	1.799 and -0.901 eÅ^{-3}
R.M.S. deviation from mean	0.115 eÅ^{-3}

4-amino-2-*tert*-butylpyridine Palladium(IV) Fluoro Di-(2-pyridyl) Ketone Complex (19)
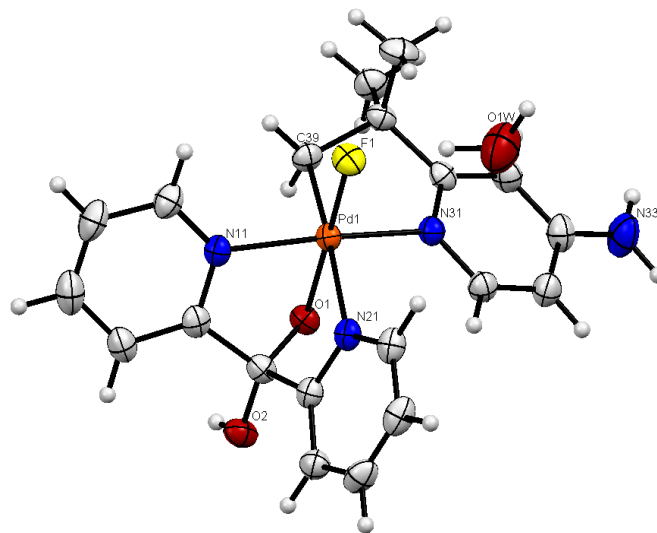
X-ray quality crystals of **19(BF₄)** were obtained by a solution of **19(BF₄)** in acetonitrile at -15˚C. A orange prism-like specimen of $C_{22}H_{27}BF_5N_5O_3Pd$, approximate dimensions 0.05 mm × 0.13 mm × 0.20 mm, was used for the X-ray crystallographic analysis. The X-ray intensity data were measured on a Bruker APEX-II CCD system equipped with a graphite monochromator and a MoKα sealed tube ($\lambda = 0.71073$ Å). Data collection temperature was 200 K.

The total exposure time was 14.14 hours. The frames were integrated with the Bruker SAINT software package using a narrow-frame algorithm. The integration of the data using a monoclinic unit cell yielded a total of 34231 reflections to a maximum θ angle of 27.50° (0.77 Å resolution), of which 5824 were independent (average redundancy 5.878, completeness = 100.0%, $R_{int} = 3.78\%$) and 4721 (81.06%) were greater than $2\sigma(F^2)$. The final cell constants of $a = 10.8409(14)$ Å, $b = 10.6222(14)$ Å, $c = 22.067(3)$ Å, $\beta = 92.9151(19)°$, $V = 2537.8(6)$ Å³, are based upon the refinement of the XYZ-centroids of 8487 reflections above 20 σ(I) with 5.372° < 2θ < 57.53°. The calculated minimum and maximum transmission coefficients (based on crystal size) are 0.8800 and 0.9610.

The structure was solved and refined using the Bruker SHELXTL Software Package, using the space group P2₁/n, with Z = 4 for the formula unit, $C_{22}H_{27}BF_5N_5O_3Pd$. The final anisotropic full-matrix least-squares refinement on F^2 with 378 variables converged at $R_1 = 3.29\%$, for the observed data and $wR_2 = 7.33\%$ for all data. The goodness-of-fit was 1.000. The largest peak in the final difference electron density synthesis was 0.856 e⁻/Å³ and the largest hole was -0.594 e⁻/Å³ with an RMS deviation of 0.075 e⁻/Å³. On the basis of the final model, the calculated density was 1.627 g/cm³ and F(000), 1256 e⁻.

Most H atoms were positioned from geometric considerations and refined as riding on the attached atom with optimized CH₃ group orientation and U_{iso} constrained to be 20% larger than U_{eqv} of the attached atom (50% larger for CH₃ groups). However H atoms in OH (O2), NH₂ (N33), H₂O (O1w) and coordinating Pd CH₂ (C39) groups were located from difference

Fourier map and freely refined with N-H in NH_2 group and O-H in water molecule restrained to be similar.
BF_4 ion is disordered in two alternative orientations (both make H bonds with OH group and water molecule) in a ratio 0.841(3):0.159(3). Geometry and atomic displacement parameters for ion in 2nd orientation were restrained to be tetrahedral and similar to ion in major orientation.

APEX2 Version 2010.11-3 (Bruker AXS Inc.)
SAINT Version 7.68A (Bruker AXS Inc., 2009)
SADABS Version 2008/1 (G. M. Sheldrick, Bruker AXS Inc.)
XPREP Version 2008/2 (G. M. Sheldrick, Bruker AXS Inc.)
XS Version 2008/1 (G. M. Sheldrick, *Acta Cryst.* (2008). A**64**, 112-122)
XL Version 2012/4 (G. M. Sheldrick, (2012) University of Gottingen, Germany)
Platon (A. L. Spek, *Acta Cryst.* (1990). A**46**, C-34)

Table 1. Sample and crystal data for UM2453.

Identification code	2453
Chemical formula	$C_{22}H_{27}BF_5N_5O_3Pd$
Formula weight	621.69
Temperature	200(2) K
Wavelength	0.71073 Å
Crystal size	$0.05 \times 0.13 \times 0.20$ mm
Crystal habit	orange prism
Crystal system	monoclinic
Space group	$P2_1/n$
Unit cell dimensions	a = 10.8409(14) Å $\alpha = 90°$
	b = 10.6222(14) Å $\beta = 92.9151(19)°$
	c = 22.067(3) Å $\gamma = 90°$
Volume	2537.8(6) Å^3
Z	4
Density (calculated)	1.627 Mg/cm^3
Absorption coefficient	0.802 mm^{-1}
F(000)	1256

Table 2. Data collection and structure refinement for UM2453.

Diffractometer	Bruker APEX-II CCD
Radiation source	sealed tube, MoKα

Theta range for data collection	1.85 to 27.50°
Index ranges	$-14 \leq h \leq 14$, $-13 \leq k \leq 13$, $-28 \leq l \leq 28$
Reflections collected	34231
Independent reflections	5824 [R(int) = 0.0378]
Coverage of independent reflections	100.0%
Absorption correction	multi-scan
Max. and min. transmission	0.9610 and 0.8800
Structure solution technique	direct methods
Structure solution program	ShelXS-97 (Sheldrick, 2008)
Refinement method	Full-matrix least-squares on F^2
Refinement program	ShelXL-2012 (Sheldrick, 2012)
Function minimized	$\Sigma \, w(F_o^2 - F_c^2)^2$
Data / restraints / parameters	5824 / 23 / 378
Goodness-of-fit on F^2	1.000
Δ/σ_{max}	0.001
Final R indices	4721 data; I>2σ(I) $R_1 = 0.0329$, $wR_2 = 0.0663$
	all data $R_1 = 0.0462$, $wR_2 = 0.0733$
Weighting scheme	$w=1/[\sigma^2(F_o^2)+(0.0200P)^2+4.7750P]$, $P=(F_o^2+2F_c^2)/3$
Largest diff. peak and hole	0.856 and -0.594 eÅ^{-3}
R.M.S. deviation from mean	0.075 eÅ^{-3}

Synthesis of (*E*)-1,2-bis(5-bromo-2-(1-bromo-2-methylpropan-2-yl)pyridin-4-yl)diazene (23)
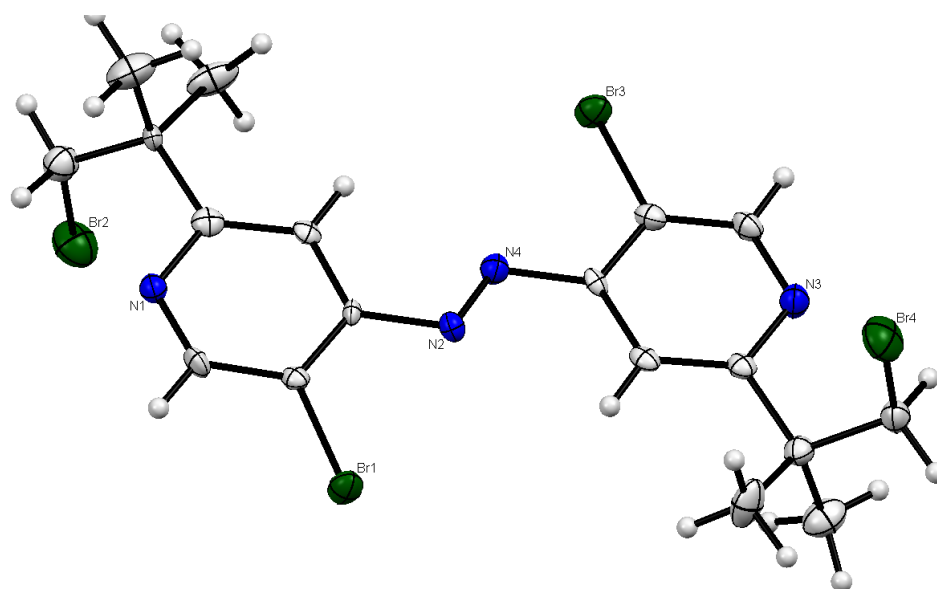
The total exposure time was 15.87 hours. The frames were integrated with the Bruker SAINT software package using a narrow-frame algorithm. The integration of the data using an orthorhombic unit cell yielded a total of 18354 reflections to a maximum θ angle of 26.00° (0.81 Å resolution), of which 4139 were independent (average redundancy 4.434, completeness = 99.9%, R_{int} = 4.53%) and 3778 (91.28%) were greater than 2σ(F^2). The final cell constants of a = 10.4072(10) Å, b = 11.0979(11) Å, c = 18.1569(18) Å, V = 2097.1(4) Å^3, are based upon the refinement of the XYZ-centroids of 5235 reflections above 20 σ(I) with 4.486° < 2θ < 53.21°. The calculated minimum and maximum transmission coefficients (based on crystal size) are 0.3930 and 0.5410.

The structure was solved and refined using the Bruker SHELXTL Software Package, using the space group Pca2$_1$, with Z = 4 for the formula unit, $C_{18}H_{20}Br_4N_4$. The final anisotropic full-matrix least-squares refinement on F^2 with 240 variables converged at R_1 = 3.96%, for the observed data and wR_2 = 8.74% for all data. The goodness-of-fit was 1.017. The largest peak in the final difference electron density synthesis was 1.805 e$^-$/Å^3 and the largest hole was -0.621 e$^-$/Å^3 with an RMS deviation of 0.120 e$^-$/Å^3. On the basis of the final model, the calculated density was 1.938 g/cm^3 and F(000), 1184 e$^-$.

APEX2 Version 2010.11-3 (Bruker AXS Inc.)
SAINT Version 7.68A (Bruker AXS Inc., 2009)
SADABS Version 2008/1 (G. M. Sheldrick, Bruker AXS Inc.)
XPREP Version 2008/2 (G. M. Sheldrick, Bruker AXS Inc.)

XS Version 2008/1 (G. M. Sheldrick, *Acta Cryst.* (2008). A**64**, 112-122)
XL Version 2012/4 (G. M. Sheldrick, (2012) University of Gottingen, Germany)
Platon (A. L. Spek, *Acta Cryst.* (1990). A**46**, C-34)

Table 1. Sample and crystal data for UM2459.

Identification code	2459
Chemical formula	$C_{18}H_{20}Br_4N_4$
Formula weight	612.02
Temperature	150(2) K
Wavelength	0.71073 Å
Crystal size	$0.08 \times 0.10 \times 0.12$ mm
Crystal habit	orange prism
Crystal system	orthorhombic
Space group	$Pca2_1$
Unit cell dimensions	a = 10.4072(10) Å $\alpha = 90°$
	b = 11.0979(11) Å $\beta = 90°$
	c = 18.1569(18) Å $\gamma = 90°$
Volume	2097.1(4) Å^3
Z	4
Density (calculated)	1.938 Mg/cm^3
Absorption coefficient	7.686 mm^{-1}
F(000)	1184

Table 2. Data collection and structure refinement for UM2459.

Diffractometer	Bruker APEX-II CCD
Radiation source	sealed tube, MoKα
Theta range for data collection	2.24 to 26.00°
Index ranges	$-12 \leq h \leq 12, -13 \leq k \leq 13, -22 \leq l \leq 22$
Reflections collected	18354
Independent reflections	4139 [R(int) = 0.0453]
Coverage of independent reflections	99.9%

Absorption correction	multi-scan	
Max. and min. transmission	0.5410 and 0.3930	
Structure solution technique	direct methods	
Structure solution program	ShelXS-97 (Sheldrick, 2008)	
Refinement method	Full-matrix least-squares on F^2	
Refinement program	ShelXL-2012 (Sheldrick, 2012)	
Function minimized	$\Sigma\ w(F_o^2 - F_c^2)^2$	
Data / restraints / parameters	4139 / 1 / 240	
Goodness-of-fit on F^2	1.017	
Final R indices	3778 data; I>2σ(I)	$R_1 = 0.0396$, w$R_2 = 0.0849$
	all data	$R_1 = 0.0455$, w$R_2 = 0.0874$
Weighting scheme	w=1/[$\sigma^2(F_o^2)$+(0.0200P)^2+15.0000P] , P=(F_o^2+2F_c^2)/3	
Absolute structure parameter	0.3(0)	
Largest diff. peak and hole	1.805 and -0.621 e$\mathring{A}^{-3}$	

References

1. Lyons, T. W.; Sanford, M. S. *Chem. Rev.* **2010**, *110*, 1147.

2. Ackermann, L. *Chem. Rev.* **2011**, *111*, 1315.

3. Yamaguchi, J.; Yamaguchi, A. D.; Itami, K. *Angew. Chem., Int. Ed.* **2012**, *51*, 8960.

4. Neufeldt, S. R.; Sanford, M. S. *Acc. Chem. Res.* **2012**, *45*, 936.

5. Vedernikov, A. N. *Acc. Chem. Res.* **2012**, *45*, 803.

6. Doyle, M. P.; Golberg, K. I. *Acc. Chem. Res.* 2012 , *45*, 777.

7. Sanhueza, I. A.; Wagner, A. M.; Sanford, M. S.; Schoenebeck, F. *Chem. Sci.* **2013**, *4*, 2767.

8. Maleckis, A.; Kampf, J. W.; Sanford, M. S. *J. Am. Chem. Soc.* **2013**, *135*, 6618.

9. Engle, K. M.; Mei, T.-S., Wang, X.; Yu, J. Q. *Angew. Chem., Int. Ed.* **2011**, *50*, 1478.

10. Furuya, T.; Ritter, T. *J. Am. Chem. Soc.* **2008**, *130*, 10060

11. Hull, K. L.; Anani, W. Q.; Sanford, M. S. *J Am. Chem. Soc.* **2006**, *128*, 7134.

12. Ball, N.; Sanford, M. S. *J. Am. Chem. Soc.* **2009**, *131*, 3796.

13. Ritter, T.; Kamlet, A.; Furuya, T. *Nature* **2011**, *473*, 470.

14. Furuya, T.; Benitez, D.; Ekaterina, T.; Strom, A. E.; Pingping, T.; Goddard, W. A.; Ritter, T. *J. Am. Chem. Soc.* **2010**, *132*, 3793.

15. Gouverneur, V.; Hollingworth C. *Chem. Commun*. **2012**, *48*, 2929.

16. Pilon, M. C.; Grushin, V. V. *Organometallics* **1998**, *17*, 1774.

17. Grushin, V. V. *Acc. Chem. Res.* **2010**, *43*, 160.

18. Grushin, V. V. *Chem. Eur. J.* **2002**, *8*, 1006.

19. Maimone, T. J.; Milner, P. J.; Kinzel, T.; Zhang, Y.; Takase, M. K.; Buchwald, S. L. *J. Am. Chem. Soc.* **2011**, *133*, 18106.

20. Noel, T.;Maimone, T. J.; Buchwald, S. L. *Angew. Chem., Int. Ed.* **2011**, *50*, 8900.

21. Watson, D. A.; Su, M.; Teverovskiy, G.; Zhang, Y.; Garcia-Fortanet,J.; Kinzel, T.; Buchwald, S. L. *Science* **2009**, *321*, 1661.

22. Topczewski, J. J.; Tewson, T. J.; Nguyen, H. M. *J. Am. Chem. Soc.* **2011**, *133*, 19318.

23. Katcher, M. H.; Sha, A.; Doyle, A. G. *J. Am. Chem. Soc.* **2011**, *133*, 15902.

24. Hollingworth, C.; Hazari, A.; Hopkinson,M. N.; Tredwell, M.; Benedetto, E.; Huiban, M.; Gee, A. D.;Brown, J. M.; Gouverneur, V. *Angew. Chem., Int. Ed.* **2011**, *50*, 2613.

25. Katcher, M. H.; Doyle, A. G. *J. Am. Chem. Soc.* **2010**, *132*, 17402.

26. Casitas, A.; Canta, M.; Sola, M.; Costas, M.; Ribas, X. *J. Am. Chem. Soc*. **2011**, *133*, 19386.

27. Tang, P.; Furuya, T.; Ritter, T. *J. Am. Chem. Soc.* **2010**, *132*, 12150.

28. Hull, K. L.; Anani, W. Q.; Sanford, M. S. *J. Am. Chem. Soc.* **2006**,*128*, 7134.

29. Chan, C. S. L.; Wasa, M.; Wang, X.; Yu, J. Q. *Angew. Chem., Int. Ed.* **2011**, *50*, 9081.

30. Wang, X.; Mei, T. S.; Yu, J. Q. *J. Am. Chem. Soc.* **2009**, *131*, 7520.

31. McMurtrey, K. B.; Racowski, J. M.; Sanford, M. S. *Org. Lett.* **2012**, *14*, 4094.

32. Racowski, J. M.; Gary, B. G.; Sanford, M. S. *Angew. Chem., Int. Ed.* **2012**, *51*, 3414.

33. Stahl, S. S.; Labinger, J. A.; Bercaw, J. E. *Angew. Chem., Int. Ed.* **1998**, *37*, 2181.

34. Noyori, R. *Chem. Commun*. **2005**, 1807.

35. Stahl, S. S. *Science* **2005**, *309*, 1824.

36. Stahl, S. S. *Angew. Chem., Int. Ed.* **2004**, *43*, 3400.

37. Oloo, W.; Zavalij, P. Y.; Zhang, J.; Khaskin, E.; Vedernikov, A. N. *J. Am. Chem. Soc.* **2010**, *132*, 14400.

38. Giri, R.; Liang, J.; Lei, J. G.; Li, J. J.; Wang, D.-H.; Chen, X.; Naggar, I. C.; Guo, C.; Foxman, B. M.; Yu, J. Q. *Angew. Chem., Int. Ed.* **2005**, *44*, 7420.

39. Shabashov, D.; Daugulis, O. *J. Am. Chem. Soc.* **2010**, *132*, 3965.

40. Vicente, J.; Chicote, M.T.; Lagunas, M.C.; Jones, P.G.; Bembenek, E.; *Organometallics* **1994**, *13*, 1243.

41. (a) Vicente, J.; Arcas, A.; Hernandez, J. F.; Bautista, D. *Angew. Chem., Int. Ed.* **2011**, *50*, 6896-6899. (b) Vicente, J.; Arcas, A.; Hernandez, J. F.; Bautista, D. *Inorg. Chem.* **2011**, *50*, 5339.

42. Vicente, J.; Arcas, A.; Hernandez, J. F.; Bautista, D. *Chem. Commun.* **2010**, *46*, 7253.

43. Kaspi, A. W.; Vigalok, A. *Topics in Organometallic Chemistry* **2010**, *31*, 19.

44. (a)Zhang, J.; Khaskin, E.; Anderson, N.P. ; Zavalij, P.Y.; Vedernikov, A.N. *Chem. Commun.* **2008**, *31*, 3625. (b)Wang, D.; Zavalij, P. Y.; Vedernikov, A. N. *Organometallics* **2013**, ASAP.

45. Jones, W. D. *Inorg. Chem.* **2005**, *44*, 4475.

46. Dong, C. G.; Hu, Q. S. *Angew. Chem., Int.Ed.* **2006**, *45*, 2289.

47. Campeau, L.C.; Schipper, D. J.; Fagnou, K. *J. Am. Chem. Soc.* **2008**, 130, 3266.

48. Ren, H.; Knochel, P. *Angew. Chem., Int. Ed.* **2006**, 45, 3462.

49. Dyker, G. *Angew. Chem., Int. Ed.* **1992**, *31*, 1023.

50. Ishii, Y.; Chatani, N.; Kakiuchi, F.; Murai, S. *Organometallics* **1997**, *16*, 3615.

51. Jun, C. H.; Hwang, D. C.; Na,S.-J. *Chem. Commun.* **1998**, 1405.

52. DeBoef, B.; Pastine, S. J.;Sames, D. *J. Am. Chem. Soc.* **2004**, *126*, 6556.

53. Tsuchikama, K.;Kasagawa, M.; Endo, K.; Shibata, T. *Org. Lett*. **2009**, *11*, 1821.

54. Dyker, G. *Angew. Chem., Int. Ed.* **1994**, 33, 103.

55. Barder, T. E.;Walker, S. D.; Martinelli, J. R.; Buchwald, S. L. *J. Am. Chem. Soc.* **2005**, *127*, 4685.

56. Chaumontet, M.; Piccardi, R.; Audic, N.; Hitce,J.; Peglion, J.-L.; Clot, E.; Baudoin, O. *J. Am. Chem. Soc.* **2008**, *130*, 15157.

57. Chaumontet, M.; Piccardi, R.; Baudoin, O. *Angew. Chem., Int. Ed*. **2009**, *48*, 179.

58. Lafrance, M.; Gorelsky, S. I.; Fagnou, K. *J. Am. Chem. Soc.* **2007**, *129*, 14570.

59. Lie´gault, B.; Fagnou, K. *Organometallics* **2008**, *27*, 4841.

60. Giri, R.; Maugel, N.; Li, J.-J.;Wang, D.-H.; Breazzano, S. P.; Saunders, L. B.; Yu, J. Q. *J. Am.Chem. Soc.* **2007**, *129*, 3510.

61. Wang, D.-H.; Wasa, M.; Giri, R.;Yu, J.-Q. *J. Am. Chem. Soc.* **2008**, *130*, 7190.

62. Wang, X.; Hu, Y.; Bonacorsi, S.; Hong, Y.; Burrell, R.; Yu J. Q. *J. Am. Chem. Soc.* **2013**, *135,* 10326.

63. Giri, R.; Lan, Y.; Liu, P.; Houk, K. N.; Yu, J.Q. *J. Am. Chem. Soc.* **2012**, *134, 14118*.

64. Stowers, K. J.; Kubota, A.; Sanford, M. S. *Chem. Sci.* **2012**, *3*, 3192.

65. Zhang, J.; Khaskin, E.; Anderson, N.P.; Zavalij, P.Y.; Vedernikov, A.N. *Chem. Commun.* **2008**, *31*, 3625.

66. Furuya, T.; Ritter, T. *J. Am. Chem. Soc.* **2008**, *130*, 10060.

67. Barlaam, B.; Bird, G. T.; Lambert-van der Brempt, C.; Campbell, D.; Foster, S. J.; Maciewicz, R. *Journal of Medicinal Chemistry* **1999**, *42*, 4890.

68. Dwyer, A. N.; Grossel, M. C.; Horton, P. N. *Supramol. Chem.* **2004**, *16*, 405.

69. Pfeiffer, W. D. *Science of Synthesis* **2007**, *35*, 139.

70. McMurtrey, K. B.; Racowski, J. M.; Sanford, M. S. *Org. Lett.* **2012**, *14*, 4094.

71. Pokhrela, L.; Kimb, Y.; Nguyena, T. D.; Priora, A. M.; Lua, J.; Changb, K.; Huaa, D. H. *Org. Lett.* **2012**, *22*, 3480.

72. Shipman, M.; Meyers, A. I. *J. Org. Chem.* **1991**, *56*, 7098.

73. Zhang, X.; Yu, M.; Yao, J.; Zhang, Y. *Synlett.* **2012**, *23*, 463.

74. Chang, Y.; Lee, H.; Bae, C. *Org. Synth.* **2010**, *87*, 245.